

**Ploidy-dependent effect of prolonged photoperiod  
on mode of reproduction and photosynthesis  
in the *Ranunculus auricomus* complex (Ranunculaceae)**

Dissertation

For the award of degree

**“Doctor rerum naturalium“**

at the Georg-August-Universität Göttingen

Within the doctoral program Biology

of the Georg-August University School of Science (GAUSS)

Submitted by

**Fuad Bahrul Ulum**

From Indonesia

Göttingen, 2021

## **Thesis committee**

Prof. Dr. Elvira Hörandl  
Department of Systematics, Biodiversity and Evolution of Plants  
Albrecht-von-Haller Institute for Plant Sciences  
University of Goettingen, Germany

Prof. Dr. Hermann Behling  
Department of Palynology and Climate Dynamic  
Albrecht-von-Haller Institute for Plant Sciences  
University of Goettingen, Germany

## **Members of the Examination Board**

1<sup>st</sup> Reviewer Prof. Dr. Elvira Hörandl  
Department of Systematics, Biodiversity and Evolution of Plants  
Albrecht-von-Haller Institute for Plant Sciences  
University of Goettingen, Germany

2<sup>nd</sup> Reviewer Prof. Dr. Hermann Behling  
Department of Palynology and Climate Dynamic  
Albrecht-von-Haller Institute for Plant Sciences  
University of Goettingen, Germany

## **Further members of the Examination Board**

PD Dr. Franz Hadacek  
Dept. of Plant Biochemistry  
University of Goettingen, Germany

Jun.-Prof. Dr. Jan de Vries  
Institute for Microbiology and Genetics  
Department of Applied Bioinformatics  
University of Goettingen, Germany

Prof. Dr. Stefan Scheu  
J.F. Blumenbach Institute of Zoology and Anthropology  
University of Goettingen, Germany

Prof. Dr. Holger Kreft  
Department of Biodiversity, Macroecology & Conservation Biogeography Group  
Faculty of Forest Sciences and Forest Ecology  
University of Goettingen, Germany

Date of the oral examination: 12 July 2021

## Table of content

Thesis committee .....	i
Table of content .....	ii
List of Tables .....	iv
List of Figures .....	v
Summary .....	vi
Chapter 1: Introduction.....	1
1.1 Polyploidy .....	1
1.2 Photoperiod .....	2
1.3 Mode of reproduction .....	3
1.4 The <i>Ranunculus auricomus</i> complex .....	5
1.5 Aims of the thesis.....	6
Chapter 2: Ploidy-dependent effects of light stress on the mode of reproduction in the <i>Ranunculus auricomus</i> complex (Ranunculaceae).....	7
2.1 Abstract .....	7
2.2 Introduction .....	8
2.3 Materials and Methods.....	10
2.4 Results.....	14
2.5 Discussion .....	20
2.6 Conclusions .....	24
Chapter 3: Ploidy-dependent effects of prolonged photoperiod on photosynthesis performance of the <i>Ranunculus auricomus</i> complex (Ranunculaceae).....	40
3.1 Simple Summary .....	40
3.2 Abstract .....	40
3.3 Introduction .....	41
3.4 Material and Methods .....	44
3.5 Results.....	47
3.6 Discussion .....	56
3.7 Conclusion .....	62

Chapter 4: Discussion .....	83
4.1 Mode of ovule formation.....	83
4.2 Mode of seed formation .....	85
4.3 Photoprotective mechanisms .....	86
References .....	89
List of Publications .....	101
Thesis declarations .....	101
Acknowledgment.....	102
Curriculum vitae.....	103

## List of Tables

Table 2.1 P-values for the two way ANOVAs to determine the interaction effect of stress treatment and ploidy level on the proportion of sexual ovules. ....	16
Table 2.2 Observed reproductive pathways of three cytotypes of the <i>R. auricomus</i> complex. ....	19
Table 3.1 Summary statistics and P- values of Wilcoxon-Mann-Whitney-Test for determination effects of prolonged photoperiod on relative electron transport rate .....	52
Table 3.2 P-values of Kruskal-Wallis-Tests for determination of significant differences of relative electron transport rate, induction curve parameters, and specific energy fluxes parameters of JIP-test.....	53
Table 3.3 Summary statistic and P- values of Wilcoxon-Mann-Whitney-Test for determination of effects of prolonged photoperiod on induction curves parameters between treatments ...	55
Table 3.4 Summary statistics and P- values of Wilcoxon-Mann-Whitney-Test for determination of effects of prolonged photoperiod on specific energy fluxes parameters of JIP-test between treatments.....	59

## List of Figures

Figure 2.1 Megasporogenesis of <i>R. variabilis</i> plants. ....	15
Figure 2.2 Proportions of sexual ovules in the <i>R. auricomus</i> complex.....	15
Figure 2.3 Proportions of well-developed seeds in the <i>R. auricomus</i> complex .....	17
Figure 2.4 Proportions of sexual seeds in the <i>R. auricomus</i> complex.....	18
Figure 3.1 Photosynthesis performance of <i>Ranunculus auricomus</i> complex .....	49
Figure 3.2 Effect photoperiod on the relative electron transport rate, induction curves, and fast fluorescence transient curves (OJIP) .....	50
Figure 3.3 Photoperiod effect on relative electron transport rate .....	51
Figure 3.4 Photoperiod effect on induction curve parameters.....	54
Figure 3.5 Photoperiod effect on specific energy fluxes parameters of JIP-test.....	57

## Summary

Polyploidy, whole-genome duplication, enhances stress-tolerance to drastic environmental compared to their diploid progenitor by enabling more extensive adaptation as advantages of gene and genome duplication. Polyploidy acts as drivers of evolution and speciation in plants. Polyploidy in angiosperms is an influential factor to trigger apomixis, the reproduction of asexual seeds. Apomixis is usually facultative, which means that both sexual and apomictic seeds can be formed by the same plant. Environmental abiotic stress, e.g., light stress, can change the frequency of apomixis. Photoperiod stress in plants influences flowering, photosynthesis, growth, metabolite profiles, and production of reactive oxygen species (ROS). The light stress creates photodamage due to the inhibition of photosystem II (PSII) repair and alternation in the photosynthetic redox signaling pathways. Apomeiosis, the production of unreduced embryo sacs, versus meiotic development is influenced by ROS scavenging. The excess of ROS in reproductive tissue generates oxidative stress. In the archespor, oxidative stress might lead to DNA double-strand breaks (DSBs) and induction of meiosis as a DNA repair mechanism. Stress-adapted plants are able to maintain the metabolic network in ROS scavenging, including compatible solutes, antioxidants, and stress-responsive proteins. In polyploid plants, the higher stress tolerance reduces oxidative stress. Hence, in facultative apomictic polyploids, lowered stress levels could result in a decrease in proportions of meiotic ovules and favor apomeiotic development. The main aims of this research were to explore with prolonged photoperiods whether polyploidy alters proportions of sexual ovule and sexual seed formation under light stress conditions and to observed the extent of stress effect on photosynthesis in the leaves that appear together with the flower buds. I used three facultative apomictic, pseudogamous cytotypes of the *Ranunculus auricomus* complex (diploid, tetraploid, and hexaploid). Stress treatments were applied by extended light periods (16.5 h) and control (10 h) in climate growth chambers. Proportions of apomeiotic vs. meiotic development in the ovule were evaluated with clearing methods, and the mode of seed formation was examined by single seed flow cytometric seed screening (ssFCSS). I further studied pollen stainability to understand the effects of pollen quality on seed formation. In basal leaves, I analyzed the effect of extended photoperiod on photosynthesis efficiency as a proxy of stress conditions. The flower buds are covered by green sepals as photosynthetic tissue, and hence we expect the same photosynthetic performance and stress effects as in the basal leaves. Photosynthesis performance was measured by applying an extensive analysis of chlorophyll a fluorescence to record the parameters: PSII maximum efficiency ( $\phi$ PSII), the maximum quantum efficiency of PSII photochemistry (QY\_max), relative electron transport rate (rETR), fluorescence induction curve (IC) of non-photochemical quenching (NPQ), and fast fluorescence transient curve (OJIP curve). Results revealed that under

extended photoperiod, all cytotypes produced significantly more sexual ovules than in the controls, with the strongest effects on diploids. The stress treatment affected neither the frequency of seed set nor the proportion of sexual seeds nor pollen quality. Prolonged photoperiod did not enhance the photosynthesis efficiency ( $QY_{max}$  and  $\phi_{PSII}$ ) of three cytotypes of *R. auricomus*. Among cytotypes, diploids were the most sensitive to the extended photoperiod compared to polyploids as indicated by the alternation of non-photochemical quenching parameters ( $NPQ$ ,  $q_E$ ,  $NPQ_E$ , and  $q_N$ ), specific energy flux parameters ( $ABS/RC$ ,  $DI_o/RC$ , and  $TR_o/RC$ ), and performance index on absorption basis ( $PI_{Abs}$ ). In tetraploids, the fraction of light excess was quenched into photochemistry ( $qP$ ), but another fraction exceeded the capacity of photon trapping ( $TR_o/RC$ ), hence dissipated as non-photochemical quenching ( $qL$ ). The hexaploids presented a variation of photosynthesis performance among two clones which might relate to different habitats. These findings confirm our hypothesis that megasporogenesis is triggered by light stress treatments. Comparisons of cytotypes support the hypothesis that ovule development in polyploid plants is less sensitive to prolonged photoperiods and responds to a lesser extent with sexual ovule formation. Polyploids may better buffer environmental stress, which releases the potential for aposporous ovule development from somatic cells, and may facilitate the establishment of apomictic seed formation. The photosynthesis performance of *R. auricomus* relates to the mode of ovule formation, as diploids showed the highest sensitivity to prolonged photoperiod concomitant to the highest proportions of sexual ovules, followed by tetraploids. Hexaploids, however, exhibited a very large variance in the proportions of sexual ovules, which we also observed here in photosynthesis performance. I suppose that this variation is mostly referable to two different ecotypes.



## Chapter 1: Introduction

### 1.1 Polyploidy

Polyploidy, the presence of more than two complete sets of chromosomes, is regarded as an extensive feature of chromosome evolution in many eukaryote taxa (Ramsey and Schemske, 1998; Soltis and Soltis, 1999; Comai, 2005; Otto, 2007; Van de Peer et al., 2020). In angiosperms, more than 30 % have one ancient polyploidization event in their history (Masterson, 1994; Landis et al., 2018; Van de Peer et al., 2020). Polyploids arise through hybridization of two species with associated genome doubling (allopolyploidy) or genome doubling in a single species (autopolyploidy) (Grant, 1981; Soltis and Soltis, 2000; Comai, 2005; Landis et al., 2018). Polyploidy provides at least three advantages, i.e., heterosis or hybrid vigor that display polyploids is more vigorous than diploids; gene redundancy protects polyploids from the deleterious effect of mutations; and asexual reproduction facilitates reproduction in the absence of sexual mates. In other words, polyploidy also inhibits several disadvantages, e.g., disruption effect of nuclear and cell enlargement, presence of aneuploidy, and epigenetic instability (Comai, 2005).

In a stable environment, organisms perform slow optimization over time and polyploid individuals may be less competitive to their diploid progenitors, but in a changing environment, polyploids show a better mechanism for more extensive change (Van de Peer et al., 2020). Several studies reported the better adaptive potential of polyploids than diploids to extreme conditions as consequence of higher genetic variation and buffering effect of their duplicate genes in short-term adaptation (Van de Peer et al., 2009; Van de Peer et al., 2017; Doyle and Coate, 2019) and in long-term adaptation (Van de Peer et al., 2020). Polyploid plants are considered to be a common mode of speciation with expanded ecological niches (Baniaga et al., 2020; Van de Peer et al., 2020) and greater colonizing ability over latitudinal and longitudinal gradients (Brochmann et al., 2004; Schinkel et al., 2016; Rice et al., 2019). Polyploids exhibit improvement such as adaptivity to abiotic stress, e.g. drought (del Pozo and Ramirez-Parra, 2014; Martínez et al., 2018), cold (Klatt et al., 2018), heat (Godfree et al., 2017), salt (Chao et al., 2013), and light (Coate et al., 2013), biotic-stress tolerance e.g., against pathogen (Keane et al., 2014; Hannweg et al., 2016; Hias et al., 2017), against competitors (Wu et al., 2019; Harms et al., 2020), in mutualistic interaction photosynthesis efficiency (Anneberg and Segraves, 2019; Acuña-Rodríguez et al., 2020), metabolite alternation (Iannicelli et al., 2020), and reactive oxygen species (ROS) scavenging (Deng et al., 2012; Wei et al., 2019). Polyploidy also influences plant reproduction and fitness, especially apomixis, i.e., the asexual reproduction via seed (Asker and Jerling, 1992). The

establishment of apomixis correlated to the polyploidy has been presented in several studies (Quarin, 1986; Zappacosta et al., 2014; Delgado et al., 2016).

## 1.2 Photoperiod

Photoperiod is the total amount of daily light and darkness exposure to organisms, naturally promoted by the tilt of the earth's axis (Jackson, 2009). In a plant, photoperiod alternation influences light signal in the leaves, circadian rhythm synchronization, bud set, flowering, and vegetative development (Jeong and Clark, 2005; Jackson, 2009), photosynthesis (Bauerle et al., 2012; Kinoshita et al., 2020), growth (Wu et al., 2004), metabolite (Sulpice et al., 2014; de Castro et al., 2019), and mode of reproduction (Saran and de Wet, 1976; Quarin, 1986; Klatt et al., 2016). Based on the plants preference to the daily light period, Major (1980) and Thomas and Vince-Prue (1984) in (Mungoma, 1988) classified plants into three categories:

1. Short-day plants: flowering occurs only in shorter day-lengths than the critical day-length.
2. Long-day plants: flowering is initiated only in day-lengths that exceed the critical day-length.
3. Day-neutral plans: flowering is not affected by day-length.

Among plant structure, the green leaf is the most affected organ by photoperiod stress (Wu et al., 2004) which is associated with the photosynthesis function (Bauerle et al., 2012). Prolongation of the light period induces photoperiod stress and causes damage in photosystem II and resulting photoinhibition (Roerber et al., 2021). Photoperiod stress leads to the accumulation of oxidative stress during the dark period of following extended daylight. On the next day, the stress reduced the photosynthesis performance (Abuelsoud et al., 2020). The enhancement of ROS later turns to block the synthesis of PSII protein in chloroplast (Takahashi and Murata, 2008). Photosynthesis organisms regulate photoprotection mechanisms to avoid net photoinhibition by the movement of leaves and chloroplasts, screening photo radiation, ROS scavenging, dissipation light energy into heat ( $qE$ ), cyclic electron flow (CEF) around photosystem I (PSI), and photorespiratory pathway (Takahashi and Badger, 2011).

### 1.2.1 Stress effect on photosynthesis performance

Chlorophyll within leaf exists as pigment-protein complexes in PSII, PSI, and within the light-harvesting complexes (LHC) associated with each of these reaction centers (Murchie and Lawson, 2013). During photosynthesis, light energy is absorbed by a light-harvesting complex of PSII and induces a photochemical process in which an electron is transferred from the reaction center chlorophyll, P680, to the primary quinone acceptor of PSII,  $Q_A$ . However, some

absorbed light energy can be lost from PSII as chlorophyll fluorescence or dissipated into heat. These three fates of absorbed light are in direct competition for excitation energy. If the rate of one direction increases the rate of the other two will decrease (Kautsky and Hirsch, 1931; Maxwell and Johnson, 2000; Baker, 2008). Chlorophyll a fluorescence analysis is widely used method for measurement of photosynthesis performance and represents the plant response to the environmental stress (Krause and Weis, 1991; Maxwell and Johnson, 2000; Müller et al., 2001; Strasser et al., 2004; Ralph and Gademann, 2005; Baker, 2008; Roháček et al., 2008; Murchie and Lawson, 2013; Stirbet et al., 2018). Thus the yield of chlorophyll fluorescence emission gives information about the quantum efficiency of photochemistry and heat dissipation (Murchie and Lawson, 2013). Based on the Chl a fluorescence, we can extract several parameters, i.e., PSII maximum efficiency ( $\phi$ PSII), the maximum quantum efficiency of PSII photochemistry (QY\_max), relative electron transport rate (rETR), fluorescence induction curve (IC) of non-photochemical quenching (NPQ), and fast fluorescence transient curve (OJIP curve). QY\_max gives a robust indicator of the maximum quantum efficiency of PSII photochemistry, and the value of the non-stressed plant is remarkably consistent at ca 0.83 (Björkman and Demmig, 1987).  $\phi$ PSII gives the proportion of absorbed light that is actually used in PSII. Any decrease in this parameter is reflecting an increase in NPQ. The NPQ estimates heat dissipation and can be separated into higher energy state quenching  $q_E$ , quenching caused by state transitions ( $q_T$ ) which refer to the migration of peripheral LHCII from PSII to PSI, and photoinhibition quenching ( $q_I$ ) that important in high light level and refers to any sustained quenching (Murchie and Lawson, 2013). The OJIP curve shows polyphasic rise as a proxy for the QY\_max. Several performance indices from JIP test provide measures of efficiencies of specific electron transport reaction in the thylakoid membrane and can be used to quantify the stress tolerance of the plant (Stirbet et al., 2018).

### 1.3 Mode of reproduction

Reproduction in eukaryotes is the original process of “recapitulation of ontogeny”. The reproduction begins with the formation of a zygote that involves syngamy (sexual reproduction) or development from an egg cell without syngamy (asexual reproduction) (Mogie, 1992). These modes of reproduction provide distinct advantages in the natural population. Sexual reproduction in plants serves genetic and phenotypic variation for better adaptation to environmental changes and the breeding of new varieties. In contrast, asexual reproduction yields clonal offspring that are genetically identical to the mother plant, thus fixing complex genotypes (Schmidt et al., 2015). In flowering plants, sexual reproduction is the most common mode of reproduction (Koltunow, 1993; Tucker and Koltunow, 2009), but asexual reproduction via seed (apomixis) (Asker and Jerling, 1992) nevertheless is widespread in 293 genera (Hojsgaard et al., 2014b).

Sexual reproduction in angiosperm is initiated by double fertilization involving the fusion of reducing male and female gametes in the ovule and producing embryo and endosperm as the organ of seeds. In contrast, apomixis evolved seed formation by the development of functional female gamete without meiosis (apomeiosis), developing embryo without fertilization (parthenogenesis), and a functional endosperm. In terms of timing of development, apomixis is divided into gametophytic apomixis and sporophytic apomixis. The gametophytic apomixis is initiated early in gametophyte development during ovule development, but sporophytic apomixis develops at the later development of ovules or usually occurs in mature ovules (Koltunow, 1993). In gametophytic apomixis, diplospory is developed via restitution of meiosis, whereas apospory is developed from a non-meiotic cell of the nucellus. Both diplospory and apospory result in an embryo sac with an unreduced embryo and several unreduced polar nuclei (Nogler, 1984a; Asker and Jerling, 1992; Carman, 1997; Hojsgaard and Hörandl, 2019). In sporophytic apomixis, adventitious embryony is initiated directly from somatic cells in ovules tissues that do not belong to megagametophyte structure (Nogler, 1984b; Asker and Jerling, 1992; Koltunow, 1993). The seed formation of apomictic plants requires fertilization of polar nuclei (pseudogamy) or without fertilization (autonomously), and pseudogamy is usually combine with facultative apomixis (Hojsgaard and Hörandl, 2019).

### 1.3.1 Stress effect on mode of reproduction

Apomixis is expressed facultatively in most plants. The coexistence of sexuality and apomixis makes some degree of sexuality in apomixis plants possible. The formation of apomictic seeds alone as obligate apomixis is very rare (Asker and Jerling, 1992). In facultative apomixis, the level of viable asexual seed formation can vary considerably between individuals (Bicknell and Koltunow, 2004). Environmental factors play an important role in controlling reproduction and fitness trade-offs (Quarin, 1999; Šarhanová et al., 2012; Schinkel et al., 2016). Since plants are sessile organisms, they are expose to unfavorable abiotic conditions such as severe drought, temperature, alkaline, light, nutrients (Shah et al., 2016). Increasing of sexuality of facultative apomixis after stress had been reported, e.g. in *Eragrostis* (Selva et al., 2020), *Paspalum* (Quarin, 1986; Delgado et al., 2016; Karunarathne et al., 2020), *Boechera* (Aliyu et al., 2010; Mateo de Arias, 2015; Gao, 2018; Carman et al., 2019), and in *Ranunculus* (Klatt et al., 2016; Klatt et al., 2018). Nevertheless, the mechanisms of how the stress alters the proportion of sexual and asexual seed formation are still not so well understood.

Environmental stress alters the accumulation of ROS, which triggers oxidative stress, and enhances the frequency of homologous recombination during meiosis (De Storme and Geelen, 2014). In germline precursor cells of diploid plants, mild oxidative stress may increase the level of DNA double-strand breaks (DSBs) as an initiator of meiosis (Hörandl and Hadacek,

2013), while strong stress causes oxidative damage and abortion of gametophyte (De Storme and Geelen, 2014). In polyploids, however, a better stress tolerance might reduce the stimulus of meiosis, hence the asexual pathway to the apomictic seed formation as a surrogate of the sexual reproduction (Hörandl and Hadacek, 2013).

#### 1.4 The *Ranunculus auricomus* complex

The *Ranunculus auricomus* complex is a Eurasian predominantly apomixis group that comprises ca. 800 polyploid apomictic species and four diploid sexual species (Hörandl, 1998). In central Europe, These species grow at a broad range of habitats from riverside area to forest margin and semi-dry anthropogenic meadow (Paun et al., 2006; Hörandl et al., 2009; Hodač et al., 2014; Hojsgaard et al., 2014a). *R. auricomus* is well-established a model system for studying reproduction modes and the mechanism that trigger evolution of sex and apomixis compared due to the higher frequency of facultative apomixis (Nogler, 1984b; Hörandl and Tensch, 2009; Aliyu et al., 2010; Hojsgaard et al., 2014a; Klatt et al., 2016). Our model system of *R. auricomus* complex comprises three cytotypes (diploid, tetraploid, and hexaploid) that closely related and genetically similar to sexual progenitor species and autopolyploid hybrid that originated from three species (*R. cassubicifolius* W. Koch, *R. carpaticola* Soó and *R. notabilis notabilis* Hörandl & Guterm) (Paun et al., 2006; Hodač et al., 2014; Barke et al., 2018; Barke et al., 2020). Recently, Karbstein et al. (2020) proposed a taxonomic revision uniting the two former taxa under *R. cassubicifolius*, but for simplicity, I keep the original names.

The natural diploid apomictic in *R. auricomus* was not known; therefore, I use diploid plants of F2 synthetic hybrids crosses of the sexual taxa *R. carpaticola* x *R. notabilis* (Barke et al., 2018; Barke et al., 2020) in this study. The tetraploid of *R. variabilis* plants are putative natural allopolyploids of the *R. carpaticola/cassubicifolius* lineage and *R. notabilis* lineage that occurs sympatrically with the parental species (Hodač et al., 2014). Tetraploids were grown from seeds of plants that were originally collected near Schönau, Mühlkreis, Austria (48°22'46.00"N 14°44'46.00"E, wet meadow) by L. Hodač and K. Spitzer (LH002, GOET). The hexaploids of *R. carpaticola* x *cassubicifolius* were grown from seeds of natural hybrids of *R. carpaticola* x *R. cassubicifolius* (original clone 29 from a forest margin and clone 35 from a meadow (Hörandl et al., 2009; Klatt et al., 2016). The hexaploids were previously studied for light stress effect on reproductive mode and metabolite alternation in the climatic chamber (Klatt et al., 2016). In the study, hexaploids were grown under a controlled environment that has been optimized following the original habitat of the provenance of *R. auricomus* complex in forest margin or understory habitats in Slovakia (Paun et al., 2006). I assume that three cytotypes of *R. auricomus* complex are pre-adapted to the same natural light condition since their

progenitors and the natural hybrids cover the similar geographical area and altitudinal zone (Hörandl et al., 2009).

## 1.5 Aims of the thesis

This thesis aims to shed light on the effect of photoperiod stress on the mode of reproduction and photosynthesis performance and whether polyploidy alters stress response. Based on the model system of the facultative apomictic *R. auricomus* complex, I applied a comprehensive analysis to test how stress regulation differs between three cytotypes on the reproductive development within three-component gametophytic apomixis: 1) apomeiosis (formation of unreduced embryo sacs); 2) parthenogenesis (embryo development without fertilization of egg cell); 3) functional endosperm development with male genome contribution from the pollen (pseudogamously) or independent from pollen (autonomously), the treatments effect on pollen quality as the pollen-dependent character of the seed formation, and photoprotective mechanisms of the photosynthetic organ that support the reproductive tissue.

**Chapter 2-** The main objectives of this chapter were to assess the stress expression between the treatments on (1) the alternation of apomeiosis to meiosis; (2) the pollen quality; (3) the mode of seed formation; and (4) seed set and to evaluate the sign of buffer stress in polyploids. In this chapter, I also presented the plant's clonality and the relation among cytotypes based on the genotyping with simple sequence repeater (SSR).

**Chapter 3-** The main objective of chapter 3 was to examine the photoprotective mechanism of three cytotypes based on their alternation in chlorophyll a fluorescence measurement and to combine the result of photoperiod stress on photosynthesis performance with the alternation of ovule formation.

## **Chapter 2: Ploidy-dependent effects of light stress on the mode of reproduction in the *Ranunculus auricomus* complex (Ranunculaceae)**

Fuad Bahrul Ulum, Camila Castro, Elvira Hörandl

Published in *Frontiers in Plant Science* 11 (2020): 104

DOI:10.3389/fpls.2020.00104

### **2.1 Abstract**

Polyploidy in angiosperms is an influential factor to trigger apomixis, the reproduction of asexual seeds. Apomixis is usually facultative, which means that both sexual and apomictic seeds can be formed by the same plant. Environmental abiotic stress, e.g. light stress, can change the frequency of apomixis. Previous work suggested effects of stress treatments on meiosis and megasporogenesis. We hypothesized that polyploidy would alter the stress response and hence reproductive phenotypes of different cytotypes. The main aims of this research were to explore with prolonged photoperiods, whether polyploidy alters proportions of sexual ovule and sexual seed formation under light stress conditions. We used three facultative apomictic, pseudogamous cytotypes of the *Ranunculus auricomus* complex (diploid, tetraploid, and hexaploid). Stress treatments were applied by extended light periods (16.5 h) and control (10 h) in climate growth chambers. Proportions of apomeiotic vs. meiotic development in the ovule were evaluated with clearing methods, and mode of seed formation was examined by single seed flow cytometric seed screening (ssFCSS). We further studied pollen stainability to understand effects of pollen quality on seed formation. Results revealed that under extended photoperiod, all cytotypes produced significantly more sexual ovules than in the control, with strongest effects on diploids. The stress treatment affected neither the frequency of seed set nor the proportion of sexual seeds nor pollen quality. Successful seed formation appears to be dependent on balanced maternal: paternal genome contributions. Diploid cytotypes had mostly sexual seed formation, while polyploid cytotypes formed predominantly apomictic seeds. Pollen quality was in hexaploids better than in diploid and tetraploids. These findings confirm our hypothesis that megasporogenesis is triggered by light stress treatments. Comparisons of cytotypes support the hypothesis that ovule development in polyploid plants is less sensitive to prolonged photoperiods and responds to a lesser extent with sexual ovule formation. Polyploids may better buffer environmental stress, which releases the potential for aposporous ovule development from somatic cells, and may facilitate the establishment of apomictic seed formation.

Keywords: apomixis, ssFCSS, light stress, meiosis, pollen, polyploidy, *Ranunculus*, seed formation

## 2.2 Introduction

Polyploidy is a heritable trait of obtaining more than two sets of chromosomes in the nuclei (Comai, 2005). A polyploid arises either from intraspecific genome duplication (autopolyploidy) or the merging of the genome of distinct species through hybridization and subsequent genome duplication (allopolyploidy) (Grant, 1981). Polyploidy is quite common in flowering plants, estimated to occur in more than 50 % of species (Soltis et al., 2015) and is considered as a major factor in plant evolution (Soltis et al., 2014). Even though polyploidy is potentially obstructed by several disadvantages, e.g., disruption effects of structural enlargement of nuclei, side effects of aneuploidy, and epigenetic mutation, it also provides advantages such as heterosis, gene redundancy, and novel gene combinations. Heterosis favors polyploids that are more vigorous than their diploid progenitors, while gene redundancy protects polyploids from the deleterious effect of mutation (Comai, 2005).

Polyploidisation, with higher DNA content, increases the cell size and promotes diversity of the genome, transcriptome, and metabolome. These improvements imply a greater resistance to environmental change (Schoenfelder and Fox, 2015). Several studies reported a better adaptivity of polyploid plants to abiotic stress conditions, such as salt (Chao et al., 2013), drought (del Pozo and Ramirez-Parra, 2014; Martínez et al., 2018), drought and heat stress (Godfree et al., 2017), cold (Klatt et al., 2018), and light (Coate et al., 2012). The better stress response and adaptation of polyploids to abiotic conditions are probably under epigenetic control (del Pozo and Ramirez-Parra, 2014). Polyploidy changes the methylation profile under stressful environments, as reported, e.g. for *Brassica napus* after drought (Jiang et al., 2019).

Notably, stress conditions can also influence mode of reproduction, especially apomixis, the asexual reproduction via seed (Nogler, 1984a). Apomixis is widespread in angiosperms (Hojsgaard et al., 2014b) and occurs most frequently in polyploid cytotypes, but occasionally also in diploids (Grant, 1981; Carman, 1997; Hojsgaard and Hörandl, 2019). Gametophytic apomixis, the form of interest here, involves formation of an unreduced embryo sac from an unreduced megaspore via meiotic restitution of the megaspore mother cell (diplospory) or from a somatic cell of the nucellus tissue (apospory) (Asker and Jerling, 1992; Koltunow and Grossniklaus, 2003). Functional seed development through gametophytic apomixis involves three components: (1) apomeiosis (formation of unreduced embryo sac); (2) parthenogenesis (embryo development without fertilization of egg cell); and (3) functional endosperm development with male genome contributions from the pollen (pseudogamously) or independent from pollen (autonomously) (Nogler, 1984a). Male development is usually meiotic, but microsporogenesis is often disturbed, and hence final pollen quality is often strongly reduced (Asker and Jerling, 1992; Izmailow, 1996; Horandl et al., 1997; Mráz et al.,



2009). Apomixis is heritable (Ozias-Akins and van Dijk, 2007), and under genetic and epigenetic control (Grimanelli, 2012; Hand and Koltunow, 2014). Natural apomixis is frequently facultative, which means that the plant produces sexual and asexual seeds within one generation, often within the same flower or inflorescence (Bicknell et al., 2003; Aliyu et al., 2010; Cosendai and Hörandl, 2010; Hojsgaard et al., 2013; Schinkel et al., 2016).

Alternation of frequencies of asexual vs. sexual reproduction was observed under abiotic stress conditions, e.g., temperature, drought stress, salt stress, and photoperiod in many different genera (Evans and Knox, 1969; Saran and de Wet, 1976; Quarin, 1986; Gounaris et al., 1991; Klatt et al., 2016; Rodrigo et al., 2017; Klatt et al., 2018). Such a condition-dependent sex is also known from other asexual eukaryotes (Ram and Hadany, 2016). Abiotic stress leads to the accumulation of ROS (Reactive oxygen species) in plant tissues, which triggers oxidative damage, but also can initiate various epigenetic, genetic and hormonal signaling pathways for plant development (Halliwell, 2006; Foyer and Noctor, 2009; Huang et al., 2019). In the germline precursor cells, oxidative stress may increase the level of DNA double-strand breaks (DSBs) as initiator of meiosis. Here meiosis could act as DNA repair system (Hörandl and Hadacek, 2013). The above-mentioned studies on condition-dependent sex in plants support this hypothesis. In polyploids, however, an improved tolerance of stress conditions might decrease the stimulus for meiosis, and consequently trigger the alternative asexual development (Hörandl and Hadacek, 2013). However, a putative differential response of cytotypes to stress conditions with respect to mode of reproduction was so far not investigated.

We use here as a model system three cytotypes of the *Ranunculus auricomus* complex, a Eurasian polyploid complex with facultative, aposporous and pseudogamous apomixis (Nogler, 1984b; Hojsgaard et al., 2014a). In Central Europe, the *R. auricomus* complex comprises three closely related and genetically similar sexual progenitor species, and polyploid apomictic hybrids of these taxa (Hörandl et al., 2009; Hodač et al., 2014). One of the hexaploid hybrids (*R. carpaticola* x *cassubicifolius*) with facultative apomixis (Hojsgaard et al., 2014a) was used previously for testing the response to light stress. This previous experiment using extended photoperiod enhanced sexual megaspore formation in these hexaploid *R. auricomus* clones concomitant with oxidative stress (Klatt et al., 2016). In our study, we test the hypothesis that with the light stress treatment, diploids would respond more intensively to stress conditions with higher frequencies of sexual development than higher ploidy levels. Here we extend the treatment of (Klatt et al., 2016) to diploid, lower polyploid (tetraploid), and the same hexaploid plants to observe effects on mode of reproduction in different ploidy levels. To simulate the effect of extended photoperiod on the components of gametophytic apomixis, we study here two developmental steps, namely ovule formation, and seed formation. Since

microsporogenesis is meiotic without an alternative asexual developmental pathway, we focus here on pollen quality as a possible factor for successful seed formation. The main aims of this research are to explore with light stress treatments whether ploidy level alters stress response with respect to mode of reproduction, and whether stress response correlates positively to sexual megaspore formation and/or proportions of sexual seed formation.

## **2.3 Materials and Methods**

### **2.3.1 Plant material**

We used for the extended photoperiod experiment facultative apomictic plants of the *Ranunculus auricomus* complex from three different cytotypes. These cytotypes are hybrids that originated from three Central European parental species (*R. cassubicifolius*, *R. carpaticola*, and *R. notabilis*). The diploid plants were synthetic F2 hybrids of *R. carpaticola* x *R. notabilis* and represent sister or sibling individuals from two parental lines; see details of crossing design in Barke et al. (2018). We used these plants because natural diploid apomicts are not known for the *R. auricomus* complex. The tetraploids were garden offspring of *Ranunculus variabilis*, which is a putative natural allopolyploid of the *R. carpaticola/cassubicifolius* lineage and the *R. notabilis* lineage, and occurs sympatrically with the parental species in Central Europe (Hodač et al., 2014). The hexaploids were garden offspring of *Ranunculus carpaticola* x *cassubicifolius*, the same plants as used by Klatt et al. (2016). Hence, all cytotypes are hybrids, and they share the genetic background of closely related parental species (Hörandl et al., 2009). Since the parental taxa and the natural hybrids occur all in the same geographical area and altitudinal zone (Hörandl et al., 2009), we can also assume that they are all pre-adapted to the same natural light conditions. The ploidy level of tetraploids was ascertained using flow cytometry following methods of (Klatt et al., 2016). A list of materials with an identity number and ploidy levels is given in the Appendix (Suppl. Table. 1). Plants were cultivated in the old botanical garden of the University of Goettingen from summer to winter for exposure to natural conditions, to stimulate the flower initiation.

### **2.3.2 Growth Chamber Setup**

The plants were moved into the climate growth chamber when sprouting at the beginning of the spring season. We run experiments for two years to get a more complete sampling. The first-year experiment was started from the first week of March 2017; the second year was started from first February 2018. A total of c. 25 plants from each cytotype were grown with 10-hour photoperiod (control) and 16 plus 0.5 hours photoperiod (stress treatment) following (Klatt et al., 2016). Temperature setup and relative humidity were kept stable at 18 °C and 60 % respectively. The light intensity was measured with a photometer (3415F Quantum Light

Meter, Spectrum Technologies, Inc, Plainfield, USA) as photoactive radiation (PAR) c. 250  $\mu\text{mol m}^{-2} \text{s}^{-1}$  (measured at shoot tips).

### 2.3.3 Plant Genotyping

Genotyping by Simple sequence repeats (SSRs) was applied to verify the plant's clonality and the relationships of cytotypes. We conducted SSRs only to tetraploid plants following methods by (Klatt et al., 2016). The SSR data for the other two cytotypes were derived from (Barke et al., 2018) for diploids and (Klatt et al., 2016) for hexaploids. Genomic DNA was performed by extracting dried leaf samples using Invisorb® Spin Plat Mini Kit (Qiagen, Hilden, Germany) according to the manufacturer's protocol. Multiplex Polymerase Chain reaction (PCR) was conducted at 25  $\mu\text{l}$  volumes, containing 1  $\mu\text{l}$  template DNA, 12.5 Roti®-Pol TaqS Master mix (Carl Roth GmbH + Co. KG, Karlsruhe, Germany), 1  $\mu\text{l}$  Forward Primer, 1  $\mu\text{l}$  Reverse Primer, 0.125  $\mu\text{l}$   $\text{MgCl}_2$ , 1  $\mu\text{l}$  CAG-Primer (FAM or HEX labeled). PCR reactions were run in a BIORAT™ Thermal Cycler. PRC machine setting was: 94 °C for 10 min, then 14 x (denaturation at 94 °C for 60 s, annealing at 62 °C+ 0.5 °C per cycle for 90 s, extension at 72 °C for 60 s), followed subsequently by 35 x (denaturation at 94 °C for 30 s, annealing at 55 °C for 30 s and extension at 72 °C for 30 s), last extension step at 72 °C for 60 s and final storage conditions at 4 °C. PCR samples were adjusted before 85  $\mu\text{l}$  formamide (HiDi) was added. This mixture was run in an automatic capillarity sequencer Genetic Analyzer 3130 (Applied Biosystems, Forster City, CA, USA) using Gene Scan 500 Rox (Applied Biosystems) as size standard after a denaturing pretreatment for 3 min at 92 °C. Scoring of the electropherograms was done using Genemarker V2.4.2 (SoftGenetics LLC, State College, PA, USA) and exported as a binary matrix presence/absence of alleles to characterize multilocus genotypes. We applied Neighbour-joining analysis based on Jaccard similarity index in FAMD to test the SSR profiles (Schlüter and Harris, 2006). Branch support values were derived from the majority consensus tree from 1000 bootstrap replicates. FigTree v1.4.2 (Rambaut, 2007) visualized the result.

### 2.3.4 Female development

Development of embryo sacs was already previously characterized within the *R. auricomus* complex on both apomictic and sexual species and is quite uniform (Nogler, 1984a; Hojsgaard et al., 2014a; Klatt et al., 2016; Barke et al., 2018): the megaspore mother cell differentiates near the micropyle and undergoes meiosis, resulting in a megaspore tetrad. In sexual development, only the chalazal megaspore develops further and produces after three mitotic divisions a typical 7-celled, 8-nucleate *Polygonum* type embryo sac (with three antipodals, a binucleate central cell, two synergids, and one egg cell). Apomictic development is characterized by enlargement of a somatic cell in the nucellus which emerges in parallel and

aside the megaspore tetrad, and continues embryo sac development into an unreduced *Polygonum* type embryo sac, whereas all megaspores abort. Embryological analysis of the female development was made at the end of sporogenesis and the beginning of gametogenesis, following Hojsgaard et al., (2014a) and Barke et al. (2018). *R. variabilis*, the only taxon that was analyzed for the first time here, did not show any deviations in timing or type of development. Flower buds were fixed at Formalin : acetic acid : ethanol : dH<sub>2</sub>O (2 : 1 : 10 : 3.5) (FAA) for 48 h, and stored in 75% ethanol (Hojsgaard et al., 2014a). The flower bud was treated by dehydrating in four steps of 30 min incubation in 1 ml of 70%, 95%, and 100% (two times). Then the flower buds were treated by clearing method in five steps of 30 min in 300 µl of upgrading series of methyl salicylate diluted in ethanol (25%, 50%, 70%, 85%, and 100%) (Young et al., 1979). The perianth of selected flower buds was removed, ovaries were dissected and mounted in methyl salicylate on glass slides. Female sporogenesis and early stages of sexual or aposporous gametophyte development were analysed with differential interface contrast (DIC) in a light transmission microscope (Leica DM5500B with DFC 450 Camera, LAS V41 software, Leica Microsystems, Wetzlar, Germany). The determination of sexual and asexual ovules was made by the absence or presence of aposporous initial cells (AIC), respectively (van Baarlen et al., 2002). We excluded ovules with unclear structure and aborted ones. We only considered the data from a plant that had a minimum of five observable ovules. Additional data from (Klatt et al., 2016) were added to increase the N value for the hexaploid cytotype.

### **2.3.5 Seed set**

After we collected the sample for embryological analysis, the remaining flowers were then manually pollinated to increase fertilization rates. In fruiting stages, we bagged a minimum of five peduncles with collective fruits with porous plastic bags to avoid seed loss. We harvested the mature collective fruits and evaluated the proportion of well-developed seeds (seed-set percentage) among ploidies per flower on individual according to Hörandl (2008). Well-developed seeds were stored at room temperature and were used for reproductive pathway analysis.

### **2.3.6 Reproductive pathway of seed formation**

The reproductive pathway was evaluated by single seed flow cytometric seed screening (ssFCSS) (Matzk et al., 2000). Two steel balls grounded a single seed (Ø 4 mm) in a 2 ml Eppendorf tube in a TissueLyzer II (Qiagen, Hilden, Germany; 30 Hz s<sup>-1</sup> for 7 s). Nuclear isolation and staining were attained in two steps using Otto buffers (Otto, 1990). In the first step, nuclear isolation, 200 µl Otto I buffer (0.1 M citric acid monohydrate, 0.5 % v/v Tween 20) was added and hand shaken with the ground material for 30 s. The solution was then

filtered (30 µm mesh, Celltrics® Münster, Germany) into plastic tubes (3.5 ml, 55 mm x 12 mm, Sarstedt, Nümbrecht, Germany). In the second step, staining, 800 µl otto II buffer (0.4 M Na<sub>2</sub>HPO<sub>2</sub>, ddH<sub>2</sub>O and charged with 3 ng/ml 4',6-diamidinophenyl-indole (Sigma-Aldrich, Munich, Germany)) was added to the filtrate, and the solution was measured directly in Flow cytometer (CyFlow® Ploidy Analyser (Sysmex Partec GmbH, Görlitz, Germany) in the Blue fluorescence (UV LED, gain 365). Histograms were analyzed using CyView™ V.1.6 software (Partec GmbH). The coefficients of variation were less than 8%. The ploidy levels of embryo and endosperm were determined, and peak indices (PI) (mean peak value of the embryo compared to the mean peak of endosperm) were assessed (Suppl. Fig. 5). For a *Polygonum* type embryo sac with two polar nuclei, the peak index for a sexual seed is c. 1.5, while for asexual seeds it can be 2.0, 2.5, or 3.0, depending on the contribution of pollen nuclei to endosperm formation. We observed the following developmental pathways: Sexual, pseudogamous apomixis, autonomous apomixis, and B<sub>III</sub>-hybrids (Hojsgaard and Hörandl, 2019). B<sub>III</sub>-hybrids arise from an unreduced embryo sac, whereby egg cell and polar nuclei were fertilized. The B<sub>III</sub>-hybrids were excluded for the determination of the proportion of sexual seeds since this mode of reproduction is intermediate between sexual and asexual seed formation.

### 2.3.7 Pollen stainability

Pollen stainability was determined on a minimum of 500 pollen grains per plant from all cytotypes in both chambers by using 10% Lugol's iodine (I<sub>2</sub>KI) solution, following methods by (Schinkel et al., 2017). The stainability of starch content was used as an indicator of viable pollen under a light microscope (LEICA DM5500B with DFC 450 C camera, LAS V41 software, Leica Microsystems, Wetzlar, Germany) at 400x magnification. The viable pollen grains were indicated by black-stained color, but brownish, reddish, and translucent (empty) pollen was counted as non-viable.

### 2.3.8 Statistical analyses

All data were tested for their normality distribution by Kolmogorov-Smirnov and Shapiro-Wilk test and for their homogeneity of variance with the Levene test. Female development, seed set, reproduction pathway of seed formation, and pollen viability were determined per flower as a percentage and subsequently averaged per plants. The percentage of data were arcsine transformed before statistical analysis. We tested the influence of treatment on mean sexual ovules and seed set among ploidies with General Linear Model (GLM) univariate (Two-way ANOVA) for completely randomized factorial design model, and means were compared according to the least significant difference (LSD) test at 0.05 probability level (p-value < 0.05). Tukey HSD was performed to the means of sexual ovules to determine the main factors.

Nonparametric Kruskal-Wallis and Mann-Whitney U-test were applied to test the influence of treatment on sexual seed formation per ploidy. Boxplots were plotted with untransformed percentage values and show the 25<sup>th</sup>, and 75<sup>th</sup> percentile ranges as a box, and the median as a black line: circles are outliers; asterisks are extreme values. All statistical analyses were performed with IBM SPSS Statistic 25 (IBM Deutschland GmbH).

## 2.4 Results

### 2.4.1 Female Development

The ovule development of all three cytotypes of the *R. auricomus* complex showed the same pattern of a typical *Polygonum* type embryo sac (Suppl. Figs. 1-4). We had observed 6,505 ovules (c. 18 ovules per flower bud) among cytotypes at megasporogenesis and early megagametogenesis. At this stage, sexual and asexual ovules can be discriminated (Suppl. Fig. 4). At the megasporogenesis stage, a meiotic division of a megaspore mother cell produced four cells, i.e. a megaspore tetrad. During the next step, three cells aborted, and only the chalazal cell remained as functional megaspore. At megagametogenesis stage, the functional megaspore enlarged with the presence of vacuoles and continued with three nuclear divisions, resulting in a total of eight nuclei. Development of sexual ovules was indicated by the absence of any aposporous initial cell (AIC) during megasporogenesis and early megagametogenesis. On the other hand, in asexual ovules, one or more AIC was observed directly near the megaspores at the chalazal pole or near to this area, but at a different optical layer (Figure 2.1).

### 2.4.2 Effects of ploidy, treatment, and combined effect of ploidy/treatment to the proportion of female development

Extended photoperiod enhanced the proportion of sexual ovules in all three cytotypes of the *R. auricomus* complex. The mean proportion of sexual ovules significantly increased from control treatment to stress treatment ( $80.37$  (mean)  $\pm 19.38$  (sd) % to  $99.26 \pm 1.26$  %; p-value < 0.001) in diploid, ( $57.90 \pm 8.79$  % to  $80.29 \pm 10.67$  %; p-value < 0.001) in tetraploids, and  $52.61 \pm 26.11$  % to  $70.36 \pm 20.04$  %; p-value = 0.006) in hexaploids (Figure 2.2). ANOVA revealed significant alterations by the main effect photoperiod (p-value < 0.001) and ploidy (p-value < 0.001), but not by the interrelationship between them (p-value = ns). Tukey HSD revealed significant differences in control treatment between diploids and hexaploids (p-value = 0.047) and in stress treatment between diploids and polyploids (p-value < 0.001) but there is neither a significant difference between tetraploids and hexaploids in the both treatments nor among diploids and tetraploid in the control treatment (p-value = ns) (Suppl. Table 3).

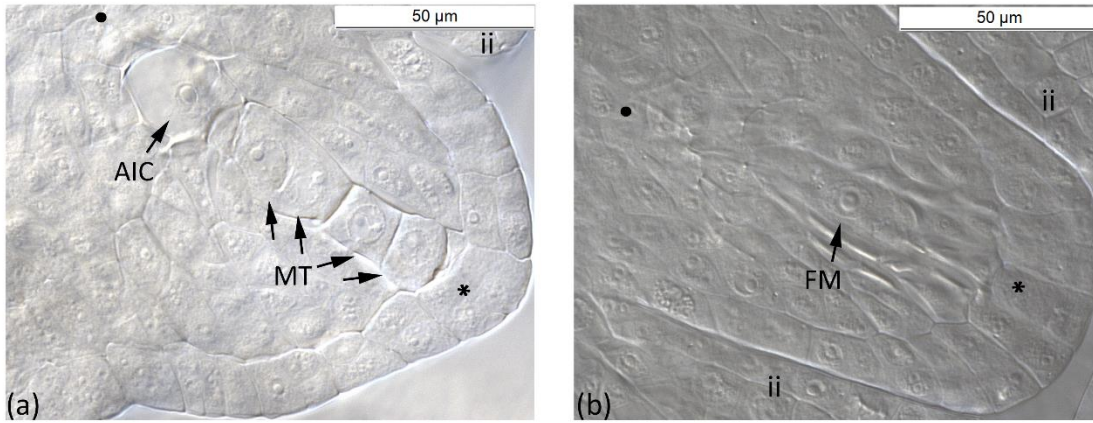


Figure 2.1 Megasporogenesis of *R. variabilis* plants. (a) Asexual ovule during megaspore formation. The germline with megasporocyte tetrad and one aposporous initial cell near the chalazal pole is shown. (b) Sexual ovule during functional megaspore formation. Only one cell near the chalazal pole survived and developed into a functional megaspore whereas the other three cells are aborted. Plant individual: **(a)** LH1406030B4-7 (Tetraploid); **(b)** LH1406030B4-19 (Tetraploid). AIC, Aposporous Initial Cell; FM, Functional Megaspore; ii, inner integument; MT, Megasporocyte Tetrad; SY, Synergid; ●, chalazal pole; \*, micropylar pole. Scale bar: 50  $\mu$ m.

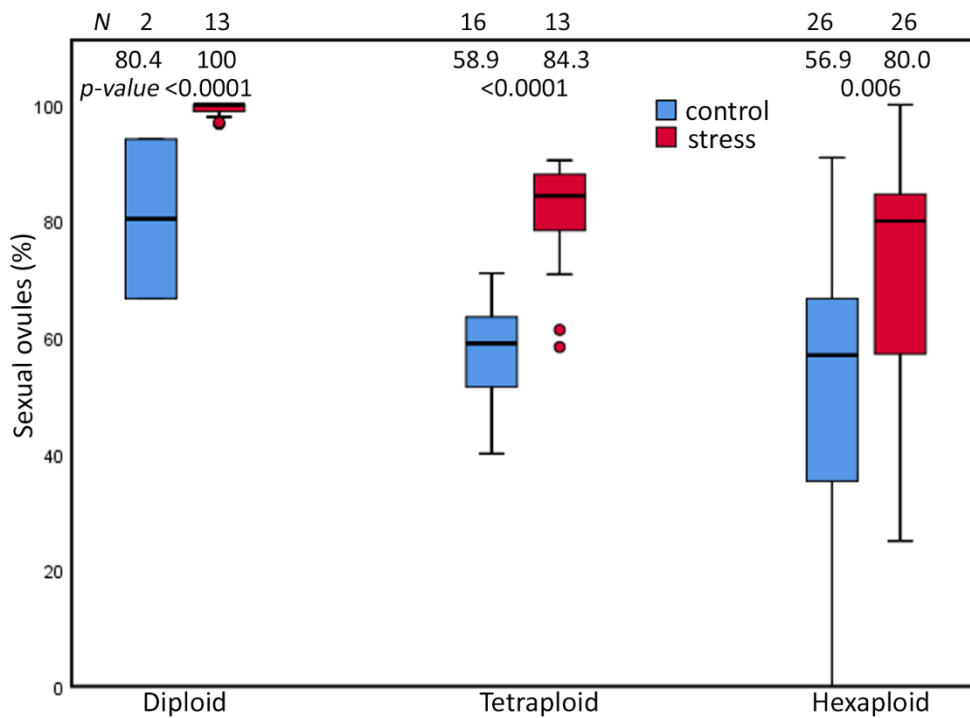


Figure 2.2 Proportions of sexual ovules in the *R. auricomus* complex plants grown in climatic chamber under prolonged photoperiod (stress) and shortened photoperiod (control). Mean values and statistical significance are given in figure. N = number of individuals. For the test statistics, see Suppl. Table 2.

Table 2.1 P-values for the two way ANOVAs to determine the interaction effect of stress treatment and ploidy level on the proportion of sexual ovules.

Source	Type III Sum of Squares	df	Mean Square	F	Sig.
Ploidy	1.769	2	0.885	14.091	0.001
Treatment	1.529	1	1.529	24.357	0.001
Ploidy x Treatment	0.132	2	0.066	1.053	0.353

a. R Squared = 0.574 (Adjusted R Squared = 0.551)

### 2.4.3 Seed set

Extended photoperiod did not influence the proportion of well-developed seeds among cytotypes of *R. auricomus* complex. Our investigation of 83 individuals revealed that no significant difference in seed set between plants grown in control and stress chamber (p-value = ns) (Figure 2.3). Diploid plants under stress treatment produced a higher mean but not significant different proportions of well-developed seeds (mean value = 50.22 %) compared to control treatments (mean value = 39.84 %; p-value = 0.300). Tetraploid plants under stress treatment produced a mean of 28.97 % compared to a mean of 31.09 % (p-value = 0.459) under control treatment. Hexaploid plants under stress treatment produced a mean of 43.04 % compared to a mean of 42.17 % (p-value = 0.880) under control treatment. A two-way ANOVA revealed only significant differences between the ploidies (p-value < 0.001), but neither a significant effect on treatment nor an interaction effect (p-value = ns) (Suppl. Table 4). Multiple comparison tests revealed that significant differences were observed between diploids and tetraploids (p-value < 0.001; Tukey HSD) and between tetraploids and hexaploids (p-value < 0.001; Tukey HSD) (Suppl. Table 5).

### 2.4.4 Reproductive pathways of seed formation

Extended photoperiod did not enhance the proportion of sexual seed over ploidies. The mean value of the proportion of sexual seeds was not significantly different between treatments among ploidies (p-value = ns, Mann-Whitney U-test) (Figure 2.4, Suppl. Table 6). Analysis of 1,468 seeds among ploidies indicated several reproductive pathways in the *R. auricomus* complex (Table 2.2). In diploid plants, the majority of seeds was formed sexually while in tetraploid and hexaploid plants, asexuality was the most frequent reproduction mode (Figure 2.4). In diploid sexual seeds, we observed the ratio of embryo to endosperm DNA content of 2C:3C, which is the indication of double fertilization between reduced egg cell with one sperm cell (1(m)+1(p)) and two polar nuclei with the other sperm cell (1(m)+1(m)+1(p)), producing a Peak Index (PI) of 1.5. A few apomictic seeds were observed (two with pseudogamous endosperm and one with autonomous endosperm) only in the stress treatment. The pseudogamous endosperm comes from the development of an unreduced embryo (2(m)) and fertilization of two polar nuclei with one or two reduced or unreduced sperm cells



( $2(m)+2(m)+1(p)$  or  $2(p)$ ), with ratios of embryo to endosperm of 2C:5C (PI = 2.5) and 2C:6C (PI = 3.0). Autonomous endosperm develops from an unreduced embryo ( $2(m)$ ) and unfertilized of two polar nuclei ( $2Cm+2Cm$ ) with the ratio of embryo to endosperm of 2C:4C (PI = 2.0), which is caused by the absence of paternal genome in seed development.

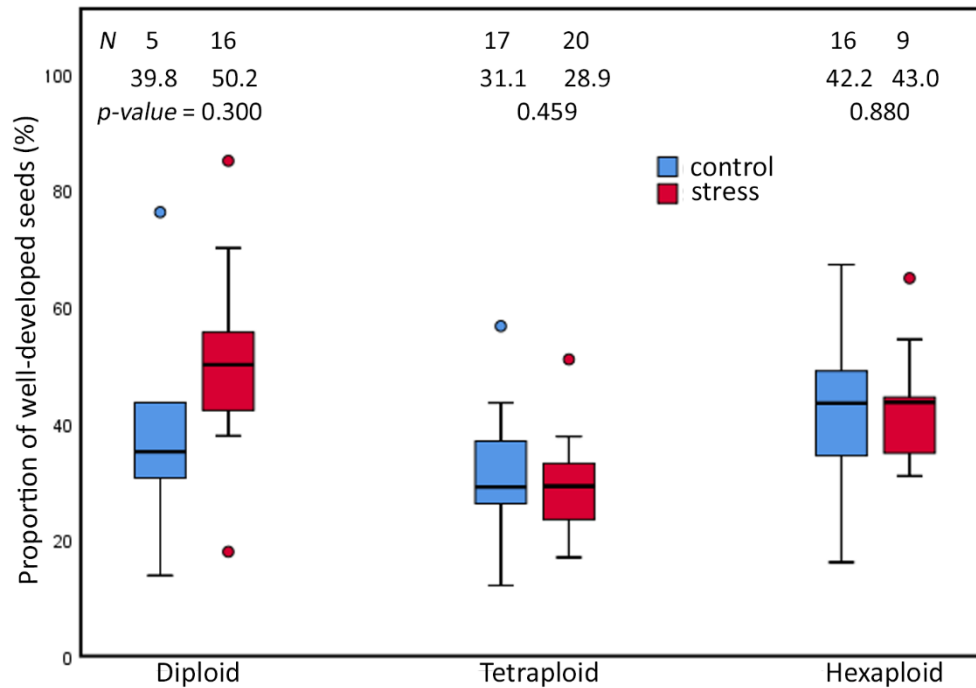


Figure 2.3 Proportions of well-developed seeds in the *R. auricomus* complex plants grown in climatic chambers under prolonged photoperiod (stress) and shortened photoperiod (control). Mean values and statistical significance are given in figure. N = number of individuals. For the test statistic, see Suppl. Table 2.

Tetraploid and hexaploid plants displayed more variation on the mode of seed reproduction. Sexual reproduction mode was present in 39 (6.2%) tetraploid seeds and 36 (7.5%) hexaploid seeds. Pseudogamous endosperm was the most frequent mode of seed formation and appeared in 543 (86.3%) tetraploid seeds and 433 (90.7%) hexaploid seeds. Generally, this mode of reproduction produced a PI value of 3.0. The less frequent forms of pseudogamous endosperm with a PI = 2.5 and PI = 4.0 originated from the contribution of one reduced sperm nucleus or two unreduced sperm nuclei. Autonomous endosperms (PI = 2.0) were the most infrequent mode of seed formation, in a total of four seeds (0.55%) from tetraploids and nine seeds (1.93%) from hexaploids. Another type of reproduction mode, i.e. partial apomixis with an unreduced egg cell fertilized by reduced pollen ( $B_{III}$ -hybrid), was more frequent in tetraploid plants (45 seeds or 12.43%) compared with only one case in hexaploid plants (Table 2.2).

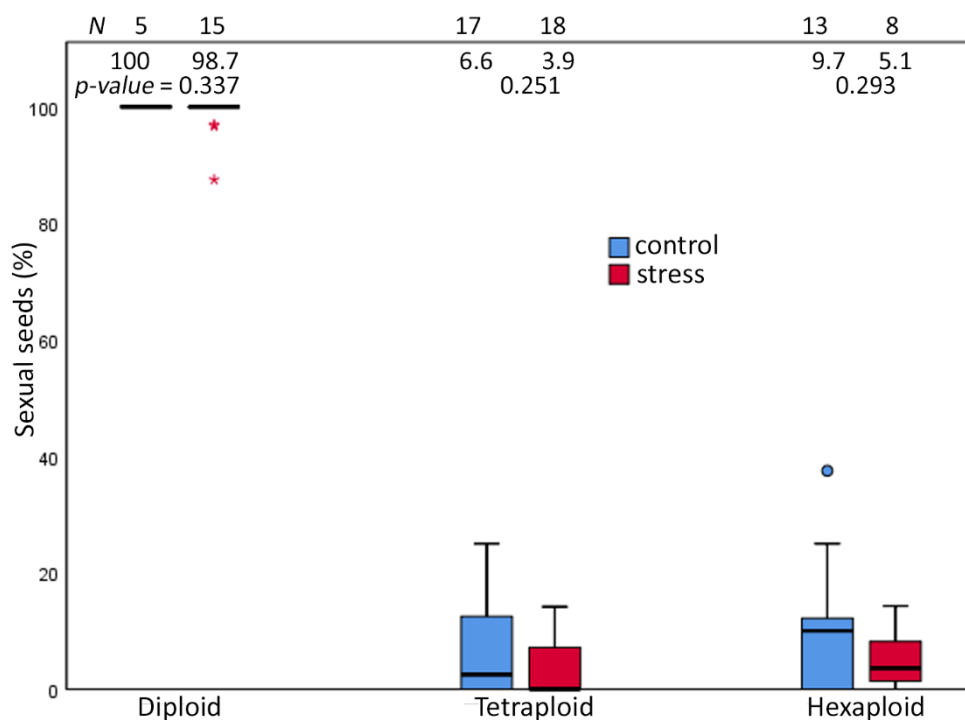


Figure 2.4 Proportions of sexual seeds in the *R. auricomus* complex plants grown in climatic chambers under prolonged photoperiod (stress) and shortened photoperiod (control). Mean values and statistical significance are given in figure. N = number of individuals. For the test statistic, see Suppl. Table 2.

Table 2.2 Observed reproductive pathways of three cytotypes of the *R. auricomus* complex. Cx reflects ploidy based on DNA content : m. maternal genome contribution; p. paternal genome contribution. PI, peak index.

Ploidy	Reproduction mode	Genome contribution to embryo/endosperm			Sperm nuclei contribution to endosperm	PI	Number of observations (ssFCSS)	
		Embryo (Cx)	Endosperm (Cx)	Em:End			Control	Stress
Diploid	Sexual	1(m)+1(p)	2(m)+1(p)	2C:3C	1	1.5	77	282
	Apomictic	2(m)	2(m)+2(m)†	2C:4C	0	2	0	1
		2(m)	4(m)+1(p)‡	2C:5C	1	2.5	0	1
		2(m)	4(m)+1(p)+ 1(p) or 4(m)+2(p)‡	2C:6C	2 or 1	3	0	1
Tetraploid	Sexual	2(m)+2(p)	4(m)+2(p)	4C:6C	1	1.5	19	20
	Apomictic	4(m)	4(m)+4(m)†	4C:8C	0	2	0	2
		4(m)	8(m)+2(p)‡	4C:10C	1	2.5	10	24
		4(m)	8(m)+2(p)+ 2(p) or 8(m)+4(p)‡	4C:12C	2 or 1	3	196	307
		4(m)	8(m)+4(p)+ 4(p)‡	4C:16C	2	4	2	4
	B <sub>III</sub> - hybrid	4(m)+2(p)	8(m)+2(p) +2(p)	6C:12C	2	2	22	3
		4(m)+2(p)	8(m)+2(p)	6C:10C	1	1.6	5	15
Hexaploid	Sexual	3(m)+3(p)	6(m)+3(p)	6C:9C	1	1.5	22	14
	Apomictic	6(m)	6(m)+6(m)†	6C:12C	0	2	5	2
		6(m)	12(m)+3(p) ‡	6C:15C	1	2.5	20	19
		6(m)	12(m)+3(p) +3(p) or 12(m)+6(p) ‡	6C:18C	2 or 1	3	246	142
		6(m)	12(m)+6(p) +6(p) ‡	6C:24C	2	4	3	3
	B <sub>III</sub> - hybrid	6(m)+3(p)	12(m)+3(p)+3(p) or 12(m)+6(p)	9C:18C	2 or 1	2	1	0

† Autonomous endosperm

‡ Pseudogamous endosperm, polar nuclei were fertilized by one reduced/unreduced or two reduced/unreduced sperm nuclei

### **2.4.5 Pollen stainability**

Extended photoperiod did not alter the proportion of viable pollen between treatments. The assessment through 34,348 pollen grains from 67 plants revealed no significant differences in pollen viability between plants of the same cytotype grown in both treatments (p-value = ns; see Suppl. Fig. 6). Hexaploids produced a higher mean proportion of viable pollen (mean value = 64.6% in control treatment and 60.7% in stress treatment) compared to diploids (49.9% in control treatment and 52.9% in stress treatment) and tetraploids (50.3% in control treatment and 52.4% in stress treatment). Multiple comparison tests among ploidies revealed that the only significant differences were observed between tetraploid and hexaploid plants (p-value < 0.001; Tukey HSD; Suppl. Table 7).

## **2.5 Discussion**

Mode of reproduction in the facultative apomictic plant is influenced by abiotic stress, e.g. by light (Knox, 1967; Saran and de Wet, 1976; Quarin, 1986; Klatt et al., 2016). However, these studies compared stress and control treatments only within the same cytotype. Under the same conditions, the degree of facultative apomixis is usually related to ploidy level (Delgado et al., 2016; Kaushal et al., 2018). In this study, we presented for the first time developmental patterns among three cytotypes of the *R. auricomus* complex under stress and control conditions. We tested the hypotheses that prolonged photoperiod enhances only the first component of apomixis, i.e., apomeiotic embryo sac development, with the expectation of a buffer effect of stress in polyploids. The other two apomixis components, i.e. parthenogenesis and endosperm development, were not affected by different photoperiods.

### **2.5.1 Effects of ploidy, treatment, and combined effect of ploidy/treatment to the proportion of female development**

Prolonged photoperiod enhanced the proportion of sexual ovules, with a greater effect on diploids but lesser effect on tetraploids and hexaploids. Enhancement on the proportion of sexual ovules after the same type of light stress had been reported before only in the hexaploid cytotype (Klatt et al., 2016). The hexaploids also formed a comparable proportion of sexual ovules under garden conditions (Hojsgaard et al., 2014b). The three cytotypes of the *R. auricomus* complex exhibited a similar mode of reproduction as the pairwise comparison of data revealed insignificant differences between ploidies in control treatments. The result of controls and also the high genetic similarity of the three cytotypes (Suppl. Fig. 7) make it unlikely that slightly different genetic backgrounds of the cytotypes had influenced the results of our experiments. The proportion of sexual ovules of the diploid cytotype grown in the garden, ranging from 45 % to 82 % (Barke et al., 2018), was still within the range of our data. These plants represent recently formed synthetic F2 hybrids (Barke et al., 2018) with lower

proportions of apospory than in the polyploids that already had established apomixis in the natural source populations. However, despite these more lineage-specific features, differential effects of treatments were observed in all three cytotypes in the early stages of development.

The prolonged photoperiod (16 plus 0.5 h) may have expanded the accumulation of ROS (Reactive oxygen species) in the reproductive tissue, as reported for the hexaploids based on analysis of secondary metabolite profiles (Klatt et al., 2016). Results support the hypothesis that the oxidative lesions might mobilize the meiotic DNA repair system in the megaspore mother cell and trigger meiosis and megasporogenesis (Hörandl and Hadacek, 2013). This stimulus might increase the proportion of functional megaspores as a cellular survival strategy for the germline (Rodrigo et al., 2017), as shown remarkably in our diploids. Differential genetic stress regulation of sexual and apomictic plants was also observed in seedlings of *Boechera*, and may be important for the bypass of the meiotic pathway (Shah et al., 2016).

In tetraploids and hexaploids, the oxidative stress of prolonged photoperiods might be different. This could be due to altered photosynthetic electron transport capacities (Coate et al., 2013), or to altered secondary metabolite profiles in polyploids and hybrids (Orians, 2000). We speculate that lowered oxidative stress in polyploids might not be severe enough to induce sufficient double strand breaks that would be essential for a correct processing of meiosis (Keeney et al., 2014). Consequently, meiosis and megasporogenesis might be disturbed. Failure of megasporogenesis might release aposporous initial cell (AIC) development. Cell-specific transcriptome studies on aposporous *Hieracium* subg. *Pilosella* suggested that contact and cross-talk between AICs and functional megaspores could be the trigger for mitotic development of the former and degeneration of the latter (Juranić et al., 2018). We suppose a similar interaction of AICs and megaspores in the *Ranunculus auricomus* complex as they always occur together in close neighborhood, and we observed the presence of AICs together with young (2-nucleate stage) meiotic embryo sacs but not at later stages (Suppl. Fig. 2 c-d and 4). The emergence of aposporous initials starts in the *Ranunculus auricomus* complex mostly at the end of megasporogenesis and is correlated to disturbance of megasporogenesis. The surviving aposporous cells grow faster than the meiotic cell and occupy the mode of megagametogenesis and seed development (Hojsgaard et al., 2014a; Barke et al., 2018). The stress only affects the megaspore but leaves apomeiosis as the surrogate for the sexual pathway (Hörandl and Hadacek, 2013). Alternatively, polyploids with more DNA content have more repair templates for the DSBs, and a higher dose of stress would be required to break the DNA (Schoenfelder and Fox, 2015). Here polyploidy might promote DNA damage tolerance under elevated stress as described (Schoenfelder and Fox, 2015) and buffers stress effects (Hörandl and Hadacek, 2013).

Environmental stress plays a role as an inhibition factor under an epigenetic mechanism that disturbs or interrupts the silencing signal of apomictic-conditioning (Rodrigo et al., 2017). At least in diploid *Ranunculus*, the treatment might strengthen a signal transduction pathway that promotes switching from apomeiosis to meiosis, as demonstrated in facultative *Boechea* after drought stress (Mateo de Arias, 2015; Gao, 2018; Carman et al., 2019). In polyploids, the whole duplication genome (WDG) provides the co-loss or co-retention condition, which maintains a constant set of miRNA for basic biological functions (Liu and Sun, 2019). Our data suggested that polyploids respond to the stress via homeostatic regulation in the frequency of apospory vs. megasporogenesis. The high variability of the proportions of sexual ovules among our genetically identical polyploids supports the findings of epigenetic and transcriptional control mechanisms as the background for the phenotypic expression of apospory (Schmidt et al., 2014). Our result supports the hypothesis that phenotypic features of apomixis in flowering plants are strongly affected by polyploidy (Delgado et al., 2016; Kaushal et al., 2018) and subjected to epigenetic control (Rodrigo et al., 2017).

### **2.5.2 Effects of ploidy, treatment, and combined effect of ploidy/treatment to the seed development and mode of reproduction**

The prolonged photoperiod affected neither the frequency of seed set, the proportion of sexual seeds, nor the pollen viability. *Ranunculus auricomus* complex plants generally lose a high seed proportion compared to rates of ovule formation due to their high seed abortion rate, exceeding one-half to two-third (Izmailow, 1996; Hörandl, 2008; Hörandl and Tensch, 2009; Klatt et al., 2016; Barke et al., 2018). This failure on seed formation arises at early stages and during the development of endosperm tissue (Barke et al., 2018). The diploid cytotype, which generally reproduces sexually, delivers a better seed set than the higher ploidy levels. In contrast, tetraploids and hexaploids, which are predominantly facultative apomictic, showed a reversed pattern, by increasing frequencies of asexual seeds.

Pollen quality is an external factor influencing the seed set of all cytotypes. The great variation in pollen quality, as observed here, is typical for apomictic plants (Asker and Jerling, 1992). The lower quality of tetraploid pollen was concomitant with a lower seed set of the tetraploids, while the better pollen quality in diploids and hexaploids corresponded to a higher seed set in these cytotypes. For seed formation, the contribution of a male gamete to fertilize the central nuclei is the major requirement for proper endosperm development (Vinkenoog et al., 2003). The diploids keep their sexual ovules growing into sexual seeds in both treatments, while the survival of three apomictic seeds in the stress treatment represented rare exceptions from seed abortion. Similar results have been reported from the garden experiment (Barke et al., 2018). Diploid plants are sensitive to genomic imprinting deviation in the endosperm (Hörandl

and Temsch, 2009; Barke et al., 2018), i.e. a 2:1 constant ratio for maternal (m) to paternal (p) genome contribution to endosperm (Spielman et al., 2003; Vinkenoog et al., 2003; Hörandl and Temsch, 2009; Barke et al., 2018). The occurrences of genome imbalance in pseudogamously (4m:1p and 4m:2p) and autonomously formed seed (4m:0p) suggested that endosperm imbalance inhibited apomictic seed formation in our diploid cytotype.

On the other hand, in polyploids, the development of sexual ovules aborted to a large extent and was replaced by aposporous initials that completed megagametogenesis. Apomictic seed formation in polyploids is mainly influenced by the competitive capacity of the unreduced embryo sac formation rather than by the light regime during megagametogenesis and seed development (Hojsgaard et al., 2013; Klatt et al., 2016; Hodač et al., 2019). The surviving aposporous initials continue to develop into aposporous embryo sacs, and seeds are formed mostly via parthenogenesis and pseudogamous apomixis. This mode of reproduction is indicated by the parthenogenetic embryo (an unreduced egg cell develops without male gamete fusion) and pseudogamous endosperm (two unreduced polar nuclei fuses with one or two male gametes). Parthenogenesis appears mostly in our asexual polyploid seeds as a significant factor promoting unreduced gametophytes against reduced one and seed formation (Hojsgaard and Hörandl, 2019). A significant number of B<sub>III</sub>-hybrids in tetraploids were formed through fertilization of unreduced egg cells as partial apomixis, as it was also occasionally observed in other FCSS studies (e.g. Schinkel et al., 2016; Barke et al., 2018; Klatt et al., 2018). This B<sub>III</sub>-hybrid had probably an extremely long period of egg cell receptivity in this cytotype as assumed in diploid *Ranunculus* (Barke et al., 2018). Additionally, pollen-independent seed development via autonomous apomixis was also a rare event in polyploids. Asexual seed formation via pseudogamy is predominant in most apomictic plants (Mogie, 1992) as observed in our polyploids. The most common developmental pathway, however, used both sperm nuclei, or the unreduced sperm nucleus, for fertilization of polar nuclei, and hence restored the optimal 2m:1p ratio in the endosperm; these pathways result in a peak index of 3.0 in flow cytometric seed screening and represent the major proportions of apomictic seeds in both tetraploids (92%) and hexaploids (88%), see data in Table 2.2. Unbalanced genome contributions were also observed. Even though the diploids are quite sensitive to genomic imprinting, the polyploids in *Ranunculus* are more relaxed as expected (Grimanelli et al., 2012; Quarin, 1999). The current theory suggests that epigenetic mutation in polyploids creates relaxation on genomic imprinting during endosperm development (Grimanelli et al., 1997; Quarin, 1999; Kaushal et al., 2018). This could be the reason of higher seed set in hexaploid than in tetraploid cytotypes, similar to in hexaploid *Potentilla puberula* that had higher seed set than the tetraploids (Dobeš et al., 2018). These findings suggest the presence of a buffer effect on genomic imprinting in polyploids.

Our results suggest that the light regime only affects the proportion of sexual ovules, but the effect does not continue on the mode of seed formation. This finding supports the oxidative stress initiation hypothesis (Hörandl and Hadacek, 2013) that light stress affects only female meiosis, but has no relevance to further development. Polyploids express predominantly apospory, probably by improved mechanisms to buffer the abiotic stress, and are able to establish apomictic seed formation. These findings are in line with the general observation that apomixis mostly occurs in polyploid plants, despite the fact that the pathway can occur in diploids as well, albeit in much lower frequencies. Hence, stress resistance of polyploids may indirectly facilitate the establishment of apomixis, but is not necessarily essential for its expression, as proposed by Hojsgaard and Hörandl (2019).

## 2.6 Conclusions

Three cytotypes of facultative *R. auricomus* complex express the alternation of proportions of asexual ovules into more sexual ovules after prolonged photoperiod. We hypothesize that light stress increases ROS formation that triggers oxidative stress. The oxidative stress might stimulate the meiotic DNA repair system in the megaspore mother cell and suppresses mitotic division, resulting in sexual ovules. The effect of prolonged photoperiod on megasporogenesis was most pronounced in diploids; the lower effect of light stress in polyploids is probably as a consequence of higher stress resistance. In polyploids, high rates of seed abortion left a lower proportion of sexual seeds, whereas in diploids the sexual pathway is still predominant. Seed formation is not influenced by environmental stress conditions, but rather depending on proper endosperm formation. Our findings shed light on the predominance of apomixis occurrence in polyploid plants.

**Data Availability Statement:** The raw data are deposited at the data repository of the University of Göttingen <https://data.goettingen-research-online.de/>, under doi [10.3389/fpls.2020.00104](https://doi.org/10.3389/fpls.2020.00104)

**Author Contributions:** FU and EH designed research. FU performed research, analyzed and interpreted data. CC contributed to FCSS and microsatellite analysis. FU wrote the manuscript with contributions of EH.

**Funding:** This project was funded by The German Research Fund DFG (DFG Hörandl Ho 4395 4-1) to EH and by the Indonesia endowment fund for education, grant no. PRJ-2369/LPDP.3/2016 to FU.

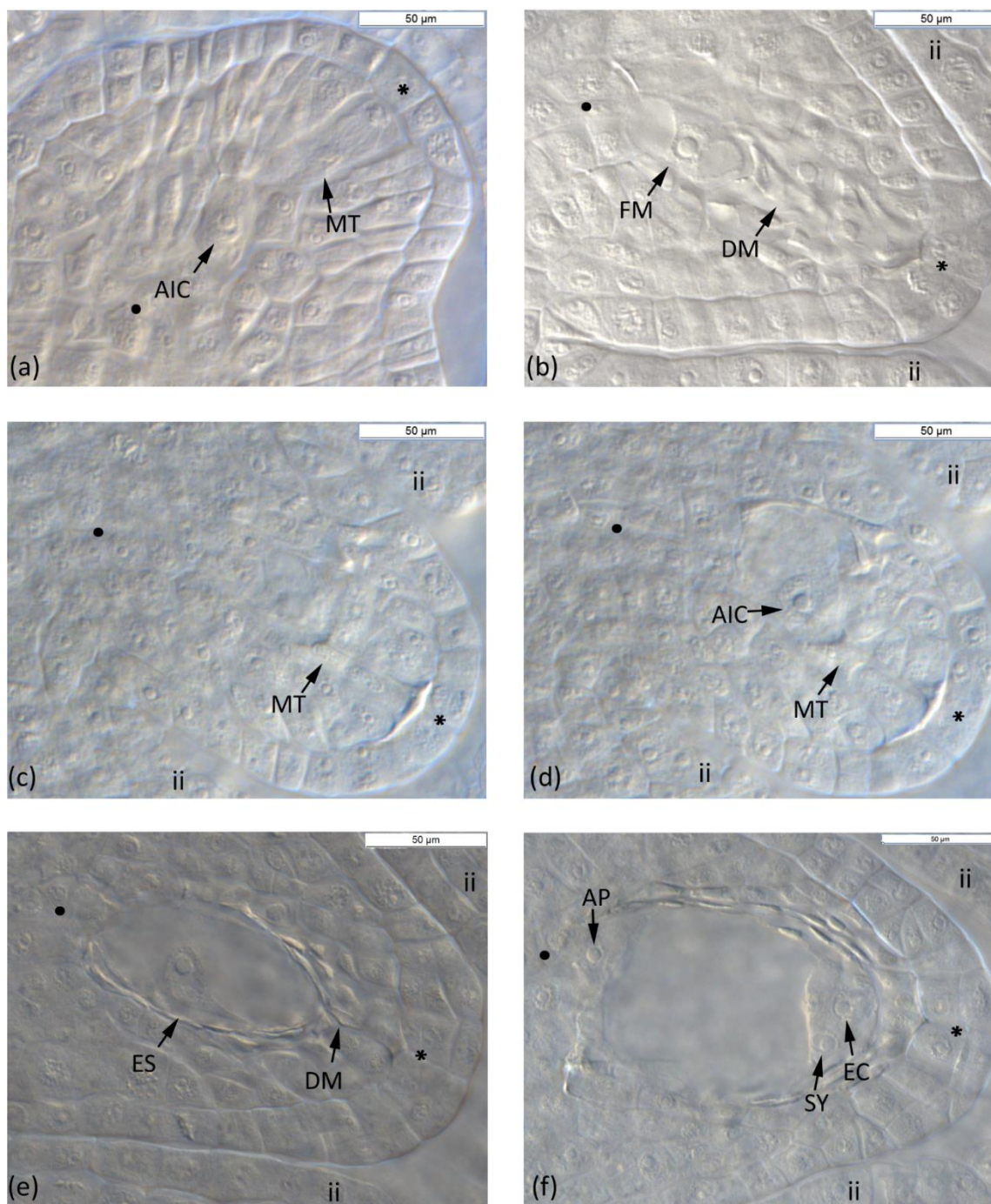


**Conflict of Interest:** The authors declare that the research was conducted in the absence of any commercial or financial relationships that could be construed as a potential conflict of interest.

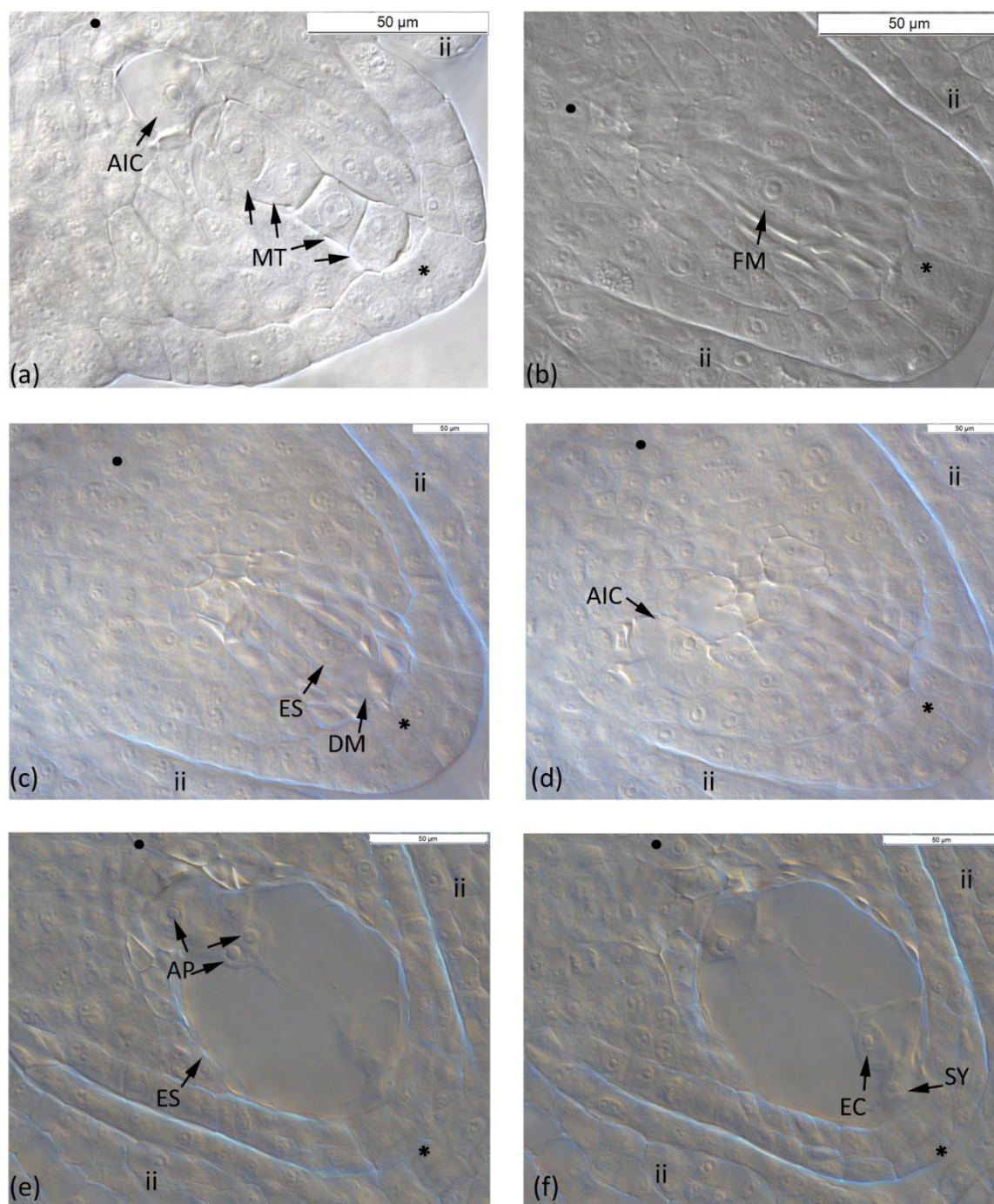
**Acknowledgments:** Silvia Friedrichs for nursing the plants; Birthe Barke for help with data interpretation; referees for valuable comments on the manuscript.

**Supplementary Material**

**Supplementary Figures**

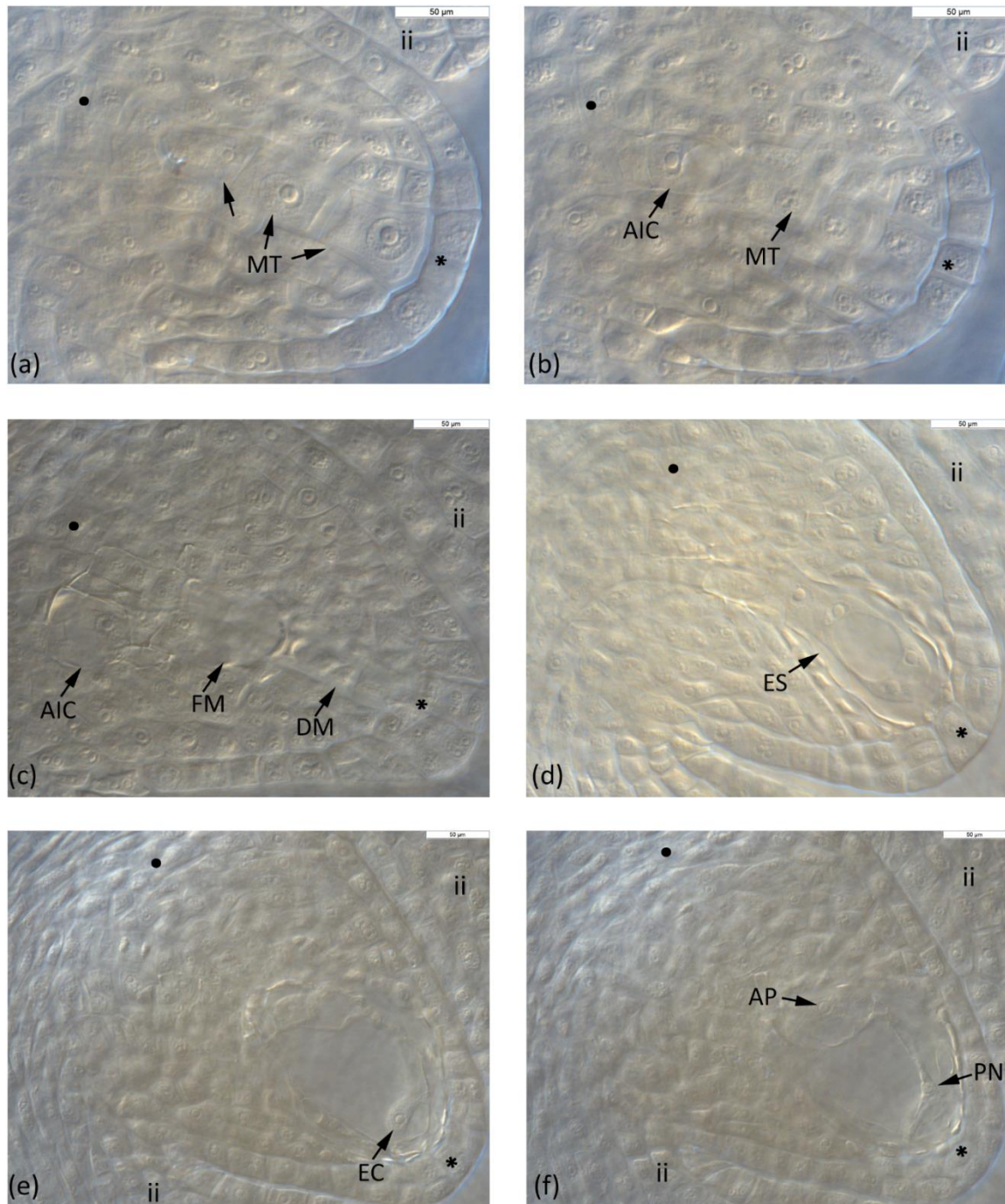


**Supplementary Figure 1.** Key reproductive stage of ovule development facultative apomictic diploid *R. carpaticola x notabilis*. **(a)** Asexual ovule with megaspores in meiotic division and an aposporous initial cell; **(b)** Sexual ovule with a functional megaspore enlarge within two vacuoles and three aborted megaspore at micropylar pole; **(c-d)** One asexual ovule in two different layers, with an aborted megaspore tetrad (c) and a big aposporous initial cell (d); **(e)** Sexual ovule with a young embryo sac at germline position (one nucleus visible and another in another optical layer); **(f)** Mature embryo sac with egg cell and synergids at micropylar pole and antipodal cells at chalazal pole. Plant individual: **(a)** F3xJ6/25; **(b)** F10XF7/01; **(c-d)** F3xJ6/19; **(e-f)** J6XF3/23 . AIC, Aposporous Initial Cell; AP, Antipodal Cells; DM, degenerated megaspores; EC, Egg Cell; ES, Embryo Sac; FM, Functional Megaspore; ii, inner integument; MT, Megaspore Tetrad; SY, Synergid●, chalazal pole; \*, micropylar pole. Scale bar: 50 µm.

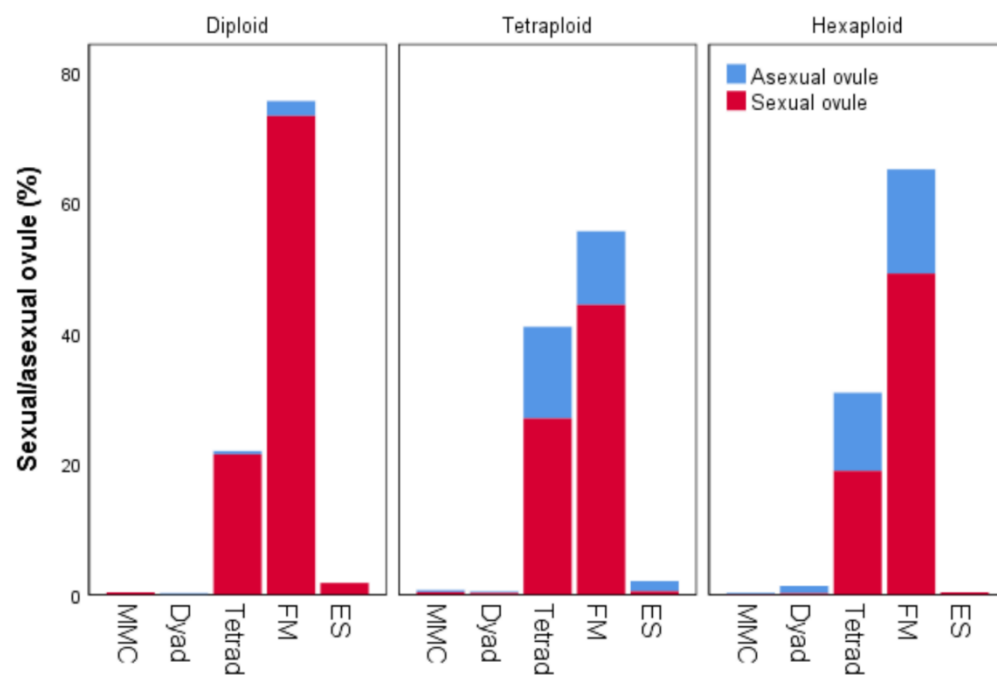


**Supplementary Figure 2.** Key reproductive stage of ovule development facultative apomictic tetraploid *Ranunculus variabilis*. **(a)** Asexual ovule with megaspore tetrads in alignment with an aposporous initial cell at chalazal pole; **(b)** Sexual ovule with an enlarged functional megaspore and degenerated meiotic products; **(c-d)** One asexual ovule in two different layers with a young (2-nucleate stage) meiotic embryo sac (c) and AIC (d); **(e-f)** One ovule in two different layers with a mature embryo sac with an egg cell and two synergids near to micropylar pole and three antipodal cells at chalazal pole. Plant individual: **(a)** LH1406030B4-7; **(b)** LH1406030B4-19; **(c-d)** LH1406030B5-08; **(e-f)** LH1406030B5-08. AIC, Aposporous Initial Cell; AP, Antipodal Cells; DM, degenerated megaspores; EC, Egg Cell; ES, Embryo Sac; FM, Functional Megaspore; ii, inner integument; MT, Megaspore Tetrad; SY, Synergid; ●, chalazal pole; \*, micropylar pole. Scale bar: 50 µm.

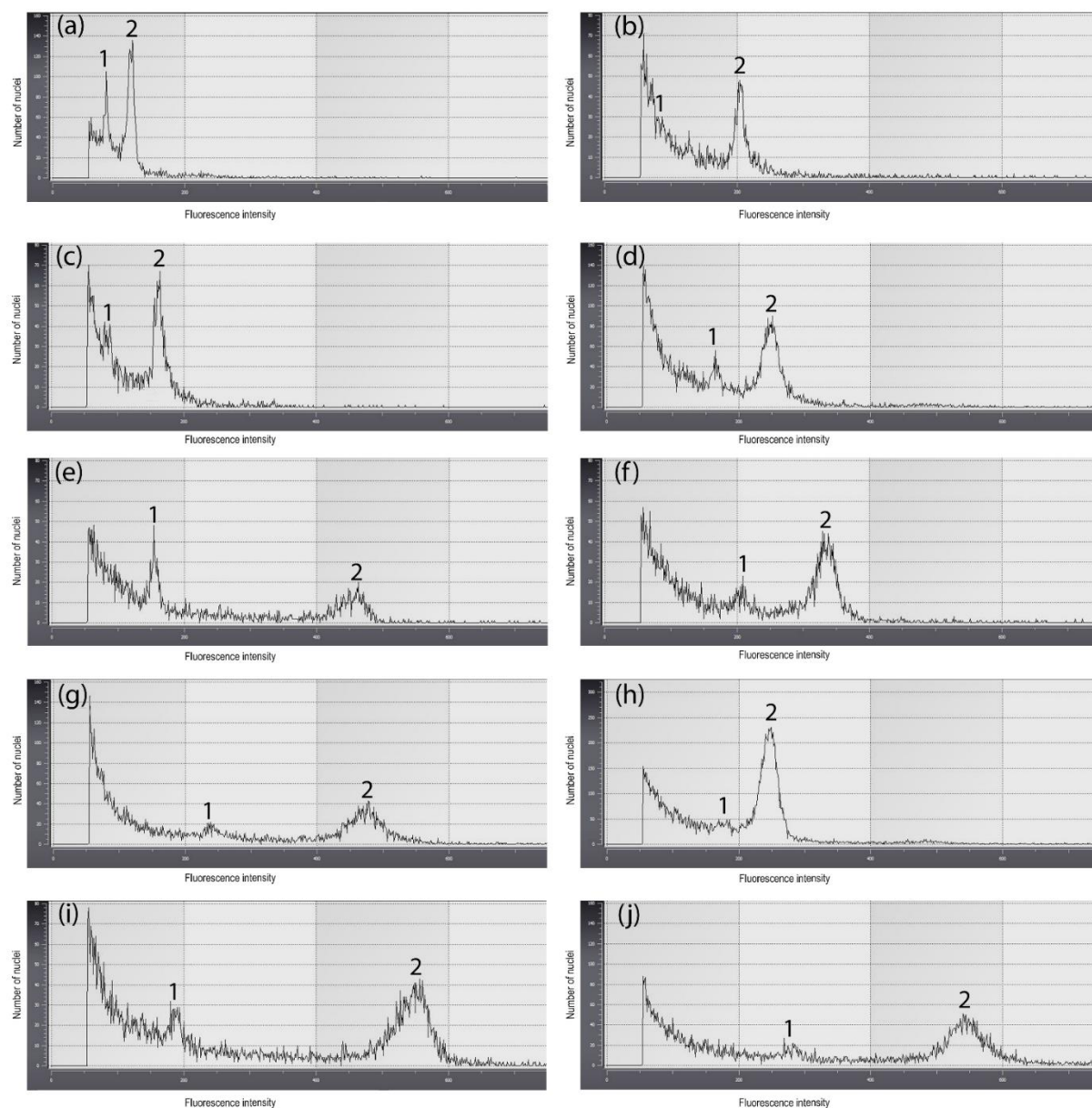




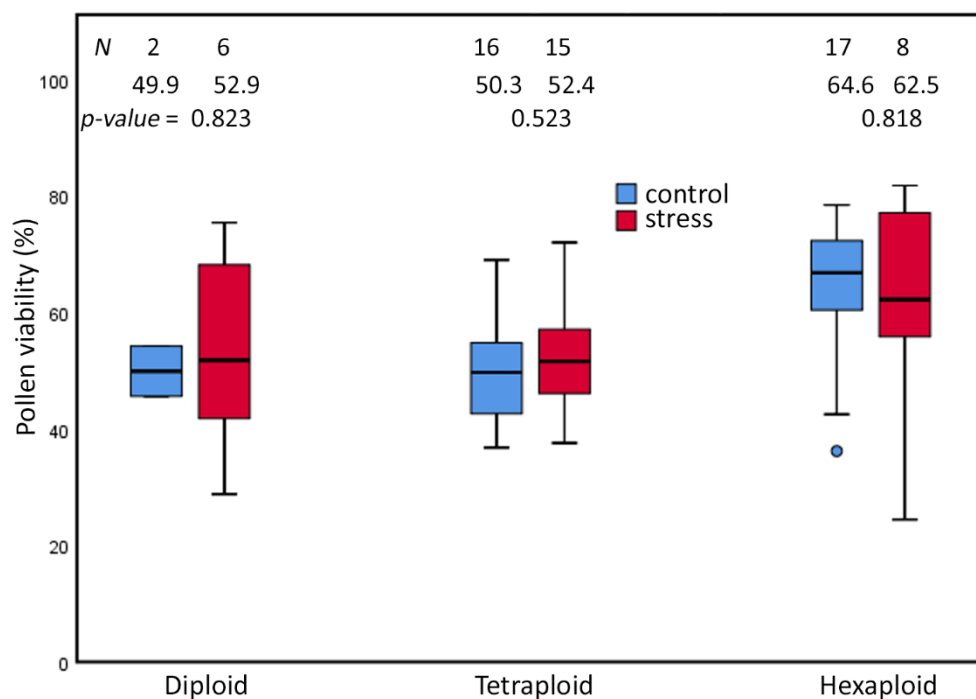
**Supplementary Figure 3.** Key reproductive stage of ovule development in facultative apomictic hexaploid *Ranunculus carpaticola x cassubicifolius*. **(a-b)** One asexual ovule in two different layers with megaspore tetrad cells in alignment (a) and an aposporous initial cell near chalazal pole (b); **(c)** Asexual ovule with functional megaspore and an AIC; **(d)** Ovule with young embryo sac after second nuclear division produced four nuclei; **(e-f)** One ovule in two different layers showing an embryo sac with an egg cell, polar nuclei, and Antipodal cells at chalazal pole; Plant individual: **(a-b)** 29/15-3V2/04; **(c)** 29/15-1L3/01; **(d)** 8492/6-2/04; **(e-f)** 29/15-3V2/27. AIC, Aposporous Initial Cell; AP, Antipodal Cells; DM, degenerating megaspores; EC, Egg Cell; ES, Embryo Sac; ii, inner integument; MT, Megaspore Tetrad; PN, Polar Nuclei, ●, chalazal pole; \*, micropylar pole. Scale bar: 50 µm.



**Supplementary Figure 4:** Mean proportions of sexual and asexual ovules from each developmental stage in three cytotypes of the *R. auricomus* complex (both treatments pooled). MMC, Megaspore Mother Cell; Dyad, first meiotic product; Tetrad, completed meiosis has produced four megaspores; FM, Functional Megaspore (only the chalazal megaspore developed while the other three cells aborted); ES, young embryo sac.



**Supplementary Figure 5.** Flow cytometry histograms of the *Ranunculus auricomus* complex. **(a)** diploid sexual seed; **(b)** diploid pseudogamous apomictic; **(c)** diploid autonomous apomictic; **(d)** tetraploid sexual; **(e)** tetraploid pseudogamous apomictic; **(f-g)** tetraploid BIII\_hybrid; **(h)** hexaploid sexual; **(i)** hexaploid pseudogamous apomictic; **(j)** hexaploid BIII\_hybrid. General peak labelling: 1 embryo peak, 2 endosperm peak. Plant individual: **(a)** J20xJ2/22; **(b)** F10xJ33/9; **(c)** F3xJ6/05; **(d)** LH1406030G1-16; **(e)** LH1406030B4-01; **(f)** LH1406030B2-07; **(g)** LH1406030B1-02; **(h-i)** 29/15-5K/31; **(j)** 29/15-6J/02.



**Supplementary Figure 6.** Proportions of viable pollen in the *R. auricomus* complex plants grown in climatic chamber under prolonged photoperiod (stress) and shortened photoperiod (control). Mean values and statistical significance are given in figure. N = number of individuals. For the test statistic, see Suppl. Table S2.





## Supplementary Tables

**Supplementary Table 1.** Plant material list of *Ranunculus auricomus* complex from three different cytotypes. \* indicated the plants used in different treatment in 2017 and 2018

Species	2017		2018	
	Control	Stress	Control	Stress
<i>R. carpaticola x notabilis</i> (2x)	F3XJ6/23	J10XJ2/22	F3xJ6/07	F3xJ6/04
		J24XJ22/10	F3xJ6/25	F3xJ6/05
		F3XJ6/10	J10xJ14/18	J10xJ30/12
		J10XJ30/12		J24xJ22/03
		J20XJ2/25		J24xJ22/23
		J24XJ22/18		F3xJ6/19
		J6XF3/23		F10xJ33/13
		F10XF7/01		F10xJ3/03
				J6xF3/06
				J24xJ22/09
<i>Ranunculus variabilis</i> (4x)	LH1406030B1-03*	LH1406030B1-01*	LH1406030B1-01*	LH1406030B1-03*
	LH1406030B5-18*	LH140603G1-07*	LH1406030B1-02*	LH1406030B1-04*
	LH1406030B2-02*	LH1406030B1-02*	LH1406030B2-03*	LH1406030B2-01
	LH1406030B4-06	LH1406030B1-05*	LH1406030B2-04	LH1406030B2-07
	LH1406030B4-10*	LH1406030B3-01*	LH1406030B3-01*	LH1406030B4-01
	LH1406030B4-11	LH1406030B2-03*	LH1406030B4-02	LH1406030B4-17
	LH1406030B4-14	LH1406030B4-7	LH1406030B4-08	LH1406030B4-20
	LH1406030B4-15	LH1406030B5-06	LH1406030B4-09	LH1406030B4-21
	LH1406030B4-19	LH1406030B5-07*	LH1406030B4-16	LH1406030B2-02*
	LH1406030B4-04	LH1406030B5-19*	LH1406030B4-18	LH1406030B5-08
	LH1406030B5-10*	LH1406030B4-07	LH1406030B5-07*	LH1406030B5-09
	LH1406030B4-10	LH1406030G1-07	LH1406030B5-12	LH1406030B5-10*
	LH1406030B5-04		LH1406030B5-16	LH1406030B5-13
			LH1406030B5-19*	LH1406030B5-18*
			LH140603G1-15	LH1406030B4-10*
			LH140603G1-07*	LH1406030G1-8
			LH4B005	LH1406030G1-16
			LH1406030G1-18	
<i>Ranunculus carpaticola x cassubicifolius</i> (6x)	29/15-6J/12	8492/27-1B/03	29/15-3N/02	29/15-3V2/03
	29/15-1L3/01	29/15-3V2/22	29/15-3V2/27	29/15-1L3/02
		35/28-1/14	29/15-5K/05	29/15-1L3/11
		29/15-3V2/03	29/15-5K/09	29/15-3V2/04
			35/28-4*/13	29/15-5K/29
			35/28-3/61	35/28-1/16
			35/28-4*/19	29/15-5K/07
			29/15-5K/31	29/15-3N/22
			29/15-6J/02	
			8492/6-2/04	
			29/15-6J/12	
			29/15-1L3/01	

**Supplementary Table 2.** Statistical characteristic of the effect of light extension on the reproductive mode among ploidies of *Ranunculus auricomus* complex plants. P-values in bold indicate significances between light treatment.

	<b>Diploid</b>		<b>Tetraploid</b>		<b>Hexaploid</b>	
	<b>Control</b>	<b>Stress</b>	<b>Control</b>	<b>Stress</b>	<b>Control</b>	<b>Stress</b>
<b>Proportion of sexual ovule</b>						
Median	80.37	99.26	57.90	80.29	52.61	70.36
Mean	80.37	100.00	58.97	84.34	56.94	80.00
SD	19.38	1.26	8.79	10.67	26.11	20.04
N	2	13	16	13	26	26
<i>p-value</i>	0.001		0.001		0.006	
<b>Seed-set</b>						
Median	35.09	50.00	29.02	29.14	43.40	43.59
Mean	39.84	50.22	31.09	28.97	42.17	43.04
SD	23.02	14.89	9.66	7.75	12.65	10.92
N	5	16	17	20	16	9
<i>p-value</i>	0.300		0.459		0.880	
<b>Reproduction mode</b>						
Median	100.00	100.00	2.50	0.00	10.00	3.60
Mean	100.00	98.74	6.59	3.88	9.66	5.08
SD	0.00	3.30	8.27	4.75	11.15	5.32
N	5	15	17	18	13	8
<i>p-value</i>	0.337		0.251		0.293	
<b>Pollen viability</b>						
Median	49.90	51.80	49.70	51.60	66.94	62.20
Mean	49.90	52.97	50.33	52.44	64.62	60.70
SD	6.08	17.38	9.22	9.51	11.73	19.95
N	2	6	16	15	17	11
<i>p-value</i>	0.777		0.536		0.605	

**Supplementary Table 3.** Pairwise comparison with Tukey HSD tests were conducted to determine the simple main effect of photoperiod on the proportion of sexual ovules among ploidies.

Treatment	Ploidy (I)	Ploidy (J)	Mean Difference (I-J)	Std. Error	p-value	95% Confidence Interval	
						Lower Bound	Upper Bound
Stress	Diploid	Tetraploid	0.554*	0.094	0.000*	0.366	0.743
	Diploid	Hexaploid	0.677*	0.081	0.000*	0.514	0.84
	Tetraploid	Hexaploid	0.123	0.081	0.137	-0.040	0.286
Control	Diploid	Tetraploid	0.356	0.198	0.08	-0.044	0.756
	Diploid	Hexaploid	0.396*	0.194	0.047*	0.005	0.788
	Tetraploid	Hexaploid	0.040	0.084	0.633	-0.129	0.21

Based on observed means.

\* The mean difference is significant at the 0.05 level.

**Supplementary Table 4.** Two-way ANOVAs were conducted to determine the interaction effect of photoperiod and ploidy level on the proportion of well-developed seeds.

Source	Type III Sum of Squares	df	Mean Square	F	p-value
Ploidy	0.445	2	0.222	11.167	0.000
Treatment	0.018	1	0.018	0.887	0.349
Ploidy x Treatment	0.050	2	0.025	1.246	0.293

a. R Squared = 0.307 (Adjusted R Squared = 0.262)

**Supplementary Table 5.** Multiple comparisons with Tukey HSD tests were conducted to determine the simple main effect of photoperiod on the proportion of well-developed seeds among ploidies

Ploidy (I)	Ploidy (J)	Mean Difference (I-J)	Std. Error	p-value	95% Confidence Interval	
					Lower Bound	Upper Bound
Diploid	Tetraploid	0.173*	0.043	0.000	0.088	0.259
Diploid	Hexaploid	0.036	0.047	0.445	-0.057	0.129
Tetraploid	Hexaploid	-0.138*	0.037	0.000	-0.212	-0.063

Based on observed means.

\* The mean difference is significant at the 0.05 level.

**Supplementary Table 6.** P-values for the Mann-Whitney U-test were conducted to determine the interaction effect of photoperiod and ploidy level on the proportion of sexual seeds.

	<b>Diploid</b>	<b>Tetraploid</b>	<b>Hexaploid</b>
Mann-Whitney U	30	118.5	47
Wilcoxon W	150	271.5	83
Z	-1.053	-0.678	-0.366
Asymp. Sig. (2-tailed)	0.292	0.497	0.714
Exact Sig. [2*(1-tailed Sig.)]	0.553c	0.533	0.750

**Supplementary Table 7.** Multiple comparisons with Tukey HSD tests were conducted to determine the simple main effect of photoperiod on the proportion of viable pollen among ploidies

Ploidy (I)	Ploidy (J)	Mean Difference (I-J)	Std. Error	p-value	95% Confidence Interval	
					Lower Bound	Upper Bound
Diploid	Tetraploid	0.015	0.063	0.968	-0.136	0.167
Diploid	Hexaploid	-0.015	0.063	0.968	-0.167	0.136
Tetraploid	Hexaploid	-0.152*	0.042	0.001	-0.253	-0.053

Based on observed means.

\* The mean difference is significant at the 0.05 level.

## **Chapter 3: Ploidy-dependent effects of prolonged photoperiod on photosynthesis performance of the *Ranunculus auricomus* complex (Ranunculaceae)**

Fuad Bahrul Ulum, Franz Hadacek and Elvira Hörandl

In prep to submit to Biology

### **3.1 Simple Summary**

Polyploidy enhances stress-tolerance compared to their diploid progenitors. Prolonged photoperiod in plants influences flowering, photosynthesis, growth, and metabolite profiles. A previous study suggested ploidy-dependent effects of photoperiod on mode of reproduction in three cytotypes of the *Ranunculus auricomus* complex. In this study we investigated the ploidy-dependent effect of photosynthesis performance under different photoperiods. Among cytotypes, diploids were more sensitive to the extended photoperiod compared to polyploids. In tetraploids, the fraction of excess light was quenched into photochemistry, but another fraction exceeded the capacity of photon trapping, hence dissipated as non-photochemical quenching. The hexaploids presented a high variation of photosynthesis performance among two clones which might relate to different ecotypes. Photosynthesis performance of *R. auricomus* relates to the mode of ovule formation, as diploids showed the highest sensitivity to prolonged photoperiod concomitant to the highest proportions of sexual ovules, followed by tetraploids. Hexaploids, however, exhibited a very large variance in the proportions of sexual ovules, which we also observed here in photosynthesis performance

### **3.2 Abstract**

Polyploidy (whole-genome duplication), enhances tolerance to drastic environmental stress compared to their diploid progenitor by diversifying genetic regulatory mechanisms. Prolongation of photoperiod influences flowering, photosynthesis, growth, and metabolite profiles of plants. Among plant organs, the reproductive part is most sensitive to stress. Light stress creates photodamage due to the inhibition of photosystem II (PSII) repair and alteration in the photosynthetic redox signaling pathways. Following a previous study on the ploidy-dependent effect of photoperiod on the female reproductive organs in three cytotypes of the *Ranunculus auricomus* complex, we investigated the possible role of polyploidy in photosynthesis performance by applying an extensive analysis of chlorophyll a fluorescence. We examined photosynthesis activity based on the parameters maximum efficiency of PSII ( $\phi$ PSII), maximum quantum yield (QY\_max), relative electron transport rate (rETR), non-photochemical quenching (NPQ), photochemical quenching (PQ), quenching coefficients, and fast fluorescence transient (OJIP) curves on the first basal leaves, which appear



synchronously with flower buds. We applied different photoperiods (12 hours and 16.5 hours) in two climate growth chambers and kept all other conditions equal (light intensity, temperature, and humidity). We hypothesized that prolonged photoperiod would affect photosynthetic efficiencies and hence redox homeostasis differentially in the three cytotypes. The results of *rETR*, PSII, and QY\_max indicated the light intensity of the climatic chamber was sufficient for photosynthesis. Among cytotypes, diploids were more sensitive to the extended photoperiod compared to polyploids as indicated by the alternation of non-photochemical quenching parameters ( $NPQ$ ,  $q_E$ ,  $NPQ_E$ , and  $q_M$ ), specific energy flux parameters ( $ABS/RC$ ,  $DI_o/RC$ , and  $TR_o/RC$ ), and performance index on absorption basis ( $PI_{Abs}$ ). In tetraploids, the fraction of light excess was quenched into photochemistry ( $qP$ ), but another fraction exceeded the capacity of photon trapping ( $TR_o/RC$ ), hence dissipated as non-photochemical quenching ( $qL$ ). The hexaploids presented a high variation of photosynthesis performance among two clones in all parameters, which might relate to their origins from different habitats. However, the photosynthesis performance of *R. auricomus* relates to the mode of ovule formation, as diploids showed the highest sensitivity to prolonged photoperiod concomitant to the highest proportions of sexual ovules, followed by tetraploids. Hexaploids, however, exhibited a very large variance in the proportions of sexual ovules, which we also observed here in photosynthesis performance. We detected here that this variation is mostly referable to two different ecotypes, supporting a hypothesis of a higher flexibility of high polyploids in their stress response.

**Keywords:** Cytotype, photoperiod, photochemistry, photosynthesis, polyploidy, quenching, *Ranunculus*

### 3.3 Introduction

Polyploidy, whole-genome duplication, is the presence of double or multiple chromosome sets by either genome doubling in a single species (autopolyploidy) or hybridization of two species with associated genome doubling (allopolyploidy) (Landis et al., 2018). Polyploidy enhances stress tolerance in response to drastic environmental change by enabling more extensive adaptations as consequences of gene and genome duplication (Van de Peer et al., 2020) and acts as drivers of evolution and speciation in plants (Alix et al., 2017). Compared to their diploid progenitor, polyploids exhibit a better stress resistance, e.g., an increase of the ABA signaling pathway under drought stress (Rao et al., 2020) or cold stress (Wu et al., 2004). Polyploid plants alter metabolite profiles and photosynthesis under cold stress (Lourkisti et al., 2020), increase xanthophyll pigment (Coate et al., 2013), and show a greater antioxidant activity under light stress (Oustric et al., 2018). Polyploid plants perform photosynthesis more efficiently (Warner and Edwards, 1993; Oustric et al., 2018) because they have larger

mesophyll cells containing more chloroplasts, higher chlorophyll content, and higher contents of the enzyme RuBisCo (Ribulose-1,5-bisphosphate-carboxylase/-oxygenase) than their diploid relatives (Coate et al., 2012; Münzbergová and Haisel, 2019). Moreover, the diversity of genomes, transcriptomes, and metabolomes of polyploids increases their resistance to environmental stress (Schoenfelder and Fox, 2015). Alternation of metabolite profiles in polyploids also has been reported (Iannicelli et al., 2020).

Photoperiod is the daily illumination received by an organism, naturally promoted by the tilt of the earth's axis (Jackson, 2009). In plants, photoperiod extension influences flowering (Jeong and Clark, 2005; Jackson, 2009), photosynthesis (Bauerle et al., 2012; Kinoshita et al., 2020), growth (Wu et al., 2004), metabolite profiles (Sulpice et al., 2014; de Castro et al., 2019), and production of reactive oxygen species (ROS) (Abuelsoud et al., 2020). Bauerle et al. (2012) reported that photosynthesis was more substantially associated with photoperiod than temperature regime in 23 tree species. Several studies addressed stress effects of photoperiod, e.g., modification of leaf structure and metabolism of *Ginkgo biloba* (Kinoshita et al., 2020) and destruction of flower meristem development (Jeong and Clark, 2005). In *Arabidopsis*, photoperiod altered trehalose 6-phosphate and amino acid biosynthesis intermediate shikimate as key coordinators for growth rate (Sulpice et al., 2014).

Light stress in plants occurs whenever absorption of environmental illumination in the leaves is higher than energy use and cannot be safely dissipated (Müller et al., 2001). Under natural conditions, plant exposure to the sunlight severed unfavorable risk to the photosynthetic component due to the formation of reactive oxygen species (ROS) as a by-product of light excess (Demmig-Adams and Adams III, 2006). This light stress creates photodamage due to the inhibition of photosystem II (PSII) repair and alternation in the photosynthetic redox signaling pathways (Gururani et al., 2015). When the photodamage rate exceeds the repair rate, PSII is downregulated, and this condition is called photoinhibition (Vass, 2012). Plants can escape this situation by applying regulation for the repartition of absorbed light between photochemistry and energy dissipating pathways as a photoprotective mechanism (Lavaud, 2007). The photoprotection accommodates light residue via leaf and chloroplast, modification of light-harvesting antenna, scavenging of ROS, and regulate thermal dissipation (Murchie and Niyogi, 2011). Among plant organs, the reproductive part is most sensitive to stress, e.g., reduction of seed set appeared under moderate temperature stress (Sato et al., 2006). Destructive effects on male and female development were reported by influenced of water, temperature, light, and oxidative stress review in Ma et al. (2020).

The expression of apomixis, i.e., the asexual reproduction via seeds (Asker and Jerling, 1992), is influenced by stress. Frequencies of asexual reproduction in facultative apomictic plants

were altered after stress, e.g., in *Boechera* (Mateo de Arias, 2015), *Ranunculus* (Klatt et al., 2016; Ulum et al., 2020), *Eragrostis* (Selva et al., 2020), and *Paspalum* (Karunaratne et al., 2020). Apomeiosis, the production of unreduced embryo sacs, is the key developmental step in gametophytic apomixis, the type that is relevant here (Asker and Jerling, 1992; Hodač et al., 2014). Apomeiotic versus meiotic development is influenced by ROS scavenging (Mateo de Arias et al., 2020). In *Arabidopsis*, photoperiod stress induces ROS scavenging system associated with catalase reduction and an increase of apoplastic peroxidase (Abuelsoud et al., 2020). The excess of ROS in reproductive tissue generates oxidative stress (Stangherlin and Reddy, 2013; Milev and Reddy, 2015). In the archespor, oxidative stress might lead to DNA double strand-breaks and induction of meiosis as a DNA repair mechanism (Hörandl and Hadacek, 2013). Stress-adapted plants are able to maintain the metabolic network in ROS scavenging including compatible solutes, antioxidants and stress-responsive proteins (Obata and Fernie, 2012). Increase of ROS scavenging secondary metabolites, e.g., of flavonoids, are linked to the increase of ROS in reproductive tissue e.g. (Paupière et al., 2017). In polyploid plants, the higher stress tolerance reduces oxidative stress (Wu et al., 2004; Coate et al., 2013; Oustric et al., 2018; Lourkisti et al., 2020; Rao et al., 2020). Hence, in facultative apomictic polyploids, lowered stress levels could result in a decrease of proportions of meiotic ovules and favor apomeiotic development (Hörandl and Hadacek, 2013). This effect was as observed after different photoperiod treatments in three cytotypes of the *Ranunculus auricomus* complex (Klatt et al., 2016; Ulum et al., 2020). A recent study on the *Ranunculus auricomus* complex over a large geographical area in Europe revealed that among many climatic parameters, light intensity was positively correlated to the distribution of sexual reproduction (Karbstein et al., 2021). Based on these results we focus here on light treatments as the most effective natural abiotic stress factor in this group. However, so far, no experimental study is available to test effects of different photoperiods on photosynthesis performance on different cytotypes. This information is crucial to establish the hypothetical causal link between light stress and mode of reproduction.

The *Ranunculus auricomus* complex comprises diploid to tetraploid sexual species and polyploid facultative apomictic, aposporous, and pseudogamous lineages (Nogler, 1984b; Hodač et al., 2014; Karbstein et al., 2021). Three cytotypes were studied previously for testing the reproduction mode and their stress sensitivity to extended light (Klatt et al., 2016; Ulum et al., 2020). These studies presented a stress buffer effect of polyploidy on the formation of meiotic ovules. Our study aim was to investigate the possible role of polyploidy in the photosynthesis performance of *R. auricomus* complex by extending the photoperiod. Three cytotypes of *R. auricomus* complex (diploids, tetraploids, and hexaploids (Ulum et al., 2020) were exposed to prolonged photoperiods as moderate stress and compared to controls with

short photoperiods. We examined the photosynthetic capacity under stress and control conditions by measuring chlorophyll fluorescence as an indicator of the photoprotective mechanism. The Chl a fluorescence is widely used for the analysis of photosynthesis performance in stressed plants (Maxwell and Johnson, 2000; Demmig-Adams and Adams III, 2006; Baker, 2008; Ptushenko et al., 2013). Measurement of Chl a fluorescence provided information on the efficiency of photochemical processes in photosystem II (“photochemical quenching”) and heat dissipation of excess light (“non-photochemical quenching”) (Maxwell and Johnson, 2000; Ptushenko et al., 2013; Lazár, 2015; Torres et al., 2021). In this study, we compare the parameters of PSII maximum efficiency ( $\phi_{PSII}$ ), maximum quantum efficiency of PSII photochemistry (QY\_max), relative electron transport rate (ETR), non-photochemical quenching (NPQ), photochemical quenching (PQ), quenching coefficients, and fast fluorescence transient curve (OJIP curve). We hypothesized that prolonged photoperiod would affect photosynthetic efficiencies and hence redox homeostasis differentially in the three cytotypes. A detailed study correlating photosynthesis data, metabolite profiles, and mode of the reproduction will be presented elsewhere.

### 3.4 Material and Methods

#### 3.4.1 Plant material and growth condition

*Ranunculus auricomus* plants comprise the same individuals as in a previously published study (Ulum et al., 2020). Diploids comprised synthetic F2 hybrids crosses of the sexual taxa *R. carpaticola* x *R. notabilis* (Barke et al., 2018; Barke et al., 2020), tetraploid plants were grown from seeds of plants that were originally collected near Schönau, Mühlkreis, Austria (48°22'46.00"N 14°44'46.00"E, wet meadow) by L. Hodač and K. Spitzer (LH002, GOET), and hexaploid plants were grown from seeds of natural hybrids of *R. carpaticola* x *R. cassubicifolius* (original clone 29 from a forest margin and clone 35 from a meadow (Hörandl et al., 2009; Klatt et al., 2016). Materials are documented in Table S1. All seedlings were grown under equal conditions in the Old Botanical Garden of the University of Göttingen. At all ploidy levels, plants represented closely related hybrid genotypes (Ulum et al., 2020). Hexaploids showed great variance in all photosynthetic parameters and hence were grouped into two separate clones (clone 6x\_29 and 6x\_35) due to their distinctive photosynthesis performance (Table S1). Growth conditions for control and stress treatments have been optimized in a previous study (Klatt et al., 2016). The climatic chambers were set at a temperature of 18°C, 60% humidity, and an average light intensity of about 250  $\mu\text{mol photons m}^{-2} \text{s}^{-1}$ . The photoperiod spanned 10 h for control and 16.5 h for light stress treatment (Klatt et al., 2016).

### 3.4.2 Photosynthesis

We analyzed the effect of extended photoperiod on photosynthesis efficiency as a proxy of stress conditions. All photosynthesis analyses were performed on 3 -11 plants per ploidy per treatment to a fully developed basal leaf (upper side) that supported the inflorescence. Measurement was started from the first weeks after sprouting of plants in March 2019 when plants produce flower buds. During this developmental step, the separation between meiotic versus apomeiotic development takes place in the ovules and hence is the stress-sensitive period (Hodač et al., 2014; Ulum et al., 2020). Flower buds are covered by green sepals as photosynthetic tissue, and hence we expect the same photosynthetic performance and stress effects as in the basal leaves.

The photosynthesis performances were observed by measurement of chlorophyll fluorescent intensity with a PAM fluorometer, PAR-FluorPen FP 110 (Photon Systems Instruments, Drásov, Czech Republic). Parameter formulae and explanations of photosynthesis efficiency were provided in Table S2. By using the preprogrammed device protocol, first, we measured the leaves without pre-dark adaptation to record the PSII maximum efficiency ( $\phi_{PSII} = F'_V/F'_M$ ). Then, plants were dark-adapted for at least 30 min for further parameter measurements, i.e., light curve to extract relative electron transport rate (rETR), fluorescence induction curve (IC) of non-photochemical quenching (NPQ), and fast fluorescence transient curve (OJIP curve). The maximum quantum efficiency of PSII photochemistry ( $QY_{max} = F_V/F_M$ ) was extracted from all dark-adapted measurements (LC, IC, and JIP-test).  $QY_{max}$  values quantify the maximum photochemical capacity of open PSII complexes (Roháček et al., 2008).

#### 3.4.2.1 Relative electron transport rate

rETR was assessed using light curve 1 (LC1). The measurement was started with an initial saturating super pulse in the dark, and subsequently, similar pulses were applied during an actinic light phase with increasing intensity, 10, 20, 50, 100, 300, and 500  $\mu\text{mol photons m}^{-2} \text{s}^{-1}$  (at photosynthesis photon flux density (PPFD)). Higher light intensities were not used due to the strong intensity decrease at 500  $\mu\text{mol photons m}^{-2} \text{s}^{-1}$  actinic light intensity. The measuring pulse was set to 0.09  $\mu\text{mol photons m}^{-2} \text{s}^{-1}$ , the saturating and super pulses to 2400  $\mu\text{mol photons m}^{-2} \text{s}^{-1}$ , and the actinic light to 300  $\mu\text{mol photons m}^{-2} \text{s}^{-1}$ .  $QY_{max}$  was extracted from the saturating pulse, and  $\phi_{PSII}$  values were extracted from the respective actinic light intensities. rETR was calculated with the equation  $\text{ETR} = \phi_{PSII} \times \text{PPFD} \times 0.5$  (Duarte et al., 2015).

### 3.4.2.2 Fluorescence quenching analysis of induction curve

IC was attained using NPQ1 program. The measuring pulse was the same as in the light curve (LC1) analysis. After the initial saturating super pulse, actinic light was switched on and lasted for 1 min. Within this time period, five additional super pulses were applied, the first one after 7 s and the following in a 12 s interval. The subsequent dark period lasted 88 s, during which three super pulses were applied, the first one after 11 s and the following in a 26 s interval. From IC of each light phase, we extracted quenching coefficients of baseline (minimum) and maximum fluorescence and fluorescence at a certain time, i.e., in the first dark-adapted state:  $F_0$  and  $F_M$ ; in the light-adapted state:  $F'_0$ ,  $F'_M$ , and  $F(t)$ ; and in darkness:  $F''_0$  and  $F''_M$  (Supplementary Figure 1). Following (Lazár, 2015), a number of IC parameters were extracted from the quenching coefficient, i.e., total non-photochemical quenching (NPQ) and photochemical quenching (PQ); quenching analysis to discriminate types of NPQ, i.e., energy dependent non-photochemical Chl fluorescence quenching ( $q_E$ ), photoinhibition non-photochemical Chl fluorescence quenching ( $q_I$ ), and NPQ parameter related to  $q_E$  and  $q_I$  ( $NPQ_E$  and  $NPQ_I$ ); and energy partitioning under consideration of active centers only, i.e., quenching coefficient of photochemical ( $q_P$ ), quenching coefficient of non-photochemical ( $q_N$ ), and quenching coefficient of non-photochemical that is formed only upon illumination to regulate the amount of absorbed light in avoiding damage effect ( $q_L$ ).

### 3.4.2.3 Fast fluorescence transient

OJIP curve followed the method of Strasser et al. (2000). The OJIP curve was induced by a pulse red light of 3000  $\mu\text{mol photons m}^{-2} \text{s}^{-1}$ . The relative fluorescence intensity of the OJIP curve at points O, J, I, P ( $F_0$ ,  $F_J$ ,  $F_I$ , and  $F_M$ , respectively) correspond to times of 0, 2, 30, and 1000 ms. Analysis of the change of relative variable fluorescence at point J, I, P was conducted with JIP-test parameters. Several OJIP measurements were taken from additional individuals due to the limited number of remaining basal leaves (Table S1).

### 3.4.3 Statistical analysis

All statistical analyses were conducted in R Studio (version 1.0.153), running R for windows (version 4.0.2, R Foundation for Statistical Computing). Data handling and visualization were performed using the *dplyr*, *tidyr*, *purrr*, and *ggplot2* package. Before all analyses, we checked the data's normality distribution by visual inspection of their frequency histograms and qq-plots using the *ggpubr* package. The photoperiods' effect on photosynthetic performance among different ploidy levels was tested using linear models (lm) when the normality distribution assumptions were met. When the assumptions were not met, generalized linear mixed models

with beta regression distribution were used or alternatively Kruskal-Wallis test for a lower sample number.

The  $\Phi$ PSII and QY\_max data (continuous variables with values ranging from 0 to 1) displayed left-skewed distributions and were calculated as a beta distribution. Therefore we run the analysis of  $\Phi$ PSII and QY\_max with a generalized mixed model framework that can handle beta distribution (Ferrari and Cribari-Neto, 2004). We employed generalized linear mixed models (GLMMs) using the *glmmTMB* package (Brooks et al., 2017) to explore the effect of extended photoperiod on the  $\Phi$ PSII and QY\_max among ploidy levels. GLMMs analyzed the relationship between  $\Phi$ PSII or QY\_max as a response variable, ploidy level, photoperiod, and their interactions as predictor variables, and logit link function and a beta distribution as well. Plant ID was treated as a random effect in  $\Phi$ PSII modeling, while the measurement origin (Data = NPQ, ETR, and JIP-test) was added as a random effect to account for the repeated measures in QY\_max modeling. Stepwise model simplification and selection were conducted based on *Akaike Information Criteria (AIC)* using *bbmle* package (Bolker and Bolker, 2020). Model fit was assessed by tests for overdispersion and residual fit tests using the *DHARMA* package (version 0.1.6) (Hartig and Hartig, 2017). Subsequently, the best model followed an analysis of variance (function *Anova.glmmTMB*) using the Wald  $\chi^2$  statistic (Type II) function for statistical value. The curve-fitting procedure for analysis of rETR curve, IC, and OJIP curve was performed using *ggplot2*.

## 3.5 Results

### 3.5.1 PSII maximum efficiency

Prolonged photoperiod did not enhance PSII maximum efficiency ( $\Phi$ PSII). Two-way ANOVAs revealed that  $\Phi$ PSII was not significantly different between treatments ( $\chi^2 = 0.54$ ,  $p = 0.464$ ), but significantly different between ploidy levels ( $\chi^2 = 80.08$ ,  $p < 0.000$ ) (Table 3.3.). The  $\Phi$ PSII values between treatments among three cytotypes of *R. auricomus* were presented in Figure 3.1. The highest mean value of  $\Phi$ PSII was observed in the diploid control, and in hexaploids clone 29 of both control and stress treatment ( $0.72$  (mean)  $\pm 0.03$  (SD)), and the lowest mean value was observed in hexaploid clone 35 of the control treatment ( $0.62 \pm 0.07$ ) (Table S3). We report the test statistic for  $\Phi$ PSII to factors ploidy levels, treatments, and their interaction in generalized linear mixed models Table S4. Pairwise comparisons among different ploidy levels and hexaploid clones exhibited that the  $\Phi$ PSII of hexaploid clone 35 was significantly lower compared to other groups except for tetraploid stress treatments (Table S5).

### 3.5.2 Maximum quantum efficiency of PSII photochemistry

The prolonged photoperiod did not enhance the maximum quantum efficiency of PSII photochemistry (QY\_max). Two-way ANOVAs revealed that QY\_max was not significantly different between treatments ( $\chi^2 = 2.39$ ,  $p = 0.121$ ), but significantly different between ploidy levels ( $\chi^2 = 180.19$ ,  $p < 0.001$ ) (Table 3.3.). The QY\_max values between treatments among three cytotypes of *R. auricomus* were presented in Figure 3.1b. The highest mean value of QY\_max was observed in tetraploids ( $0.83 \pm 0.02$ ) and hexaploid clone 29 ( $0.83 \pm 0.01$ ), both growing under control treatment. A slightly lower mean value of 0.81-0.82 was observed in diploids from both treatments and in tetraploids, and in hexaploid clone 29 growing under stress treatment. The hexaploid clone 35 had the lowest mean value of QY\_max, i.e.,  $0.71 \pm 0.08$  in the control treatment and  $0.66 \pm 0.09$  in stress treatment. The test statistics for the linear models of QY\_max to factors ploidy, treatments, and their interaction in generalized linear mixed models were displayed in Table S6. Pairwise comparisons among different ploidy levels and hexaploid clones exhibited that QY\_max of hexaploid clone 35 was significantly lower compared to other groups (Table S7).

### 3.5.3 Relative electron transport rate

The relative electron transport rate (rETR) curves linearly increased following the increase of light intensity, measured as photosynthesis photon flux density PPFD (Figure 3.2a). The mean values of rETR in each light intensity and their proportion alternation between the treatments is reported in Table 3.1, and boxplots are shown in Figure 3.3. Under extended photoperiod, rETR values were higher in diploids at 10 PPFD and in tetraploids at 10, 20, and 50 PPFD, but no significant alternation appeared in hexaploids. At higher light intensities, no differences appeared between treatments (Table 3.1). Kruskal-Wallis-Tests revealed that rETR from all light intensities (10-500 PPFD) were significantly different among diploids, tetraploid, and the two hexaploid clones in both treatments except in 10 PPFD of the control treatment (Table 3.2). Pairwise comparisons presented the significant values in each light intensity (Table S8). In the control treatment, the rETR of hexaploid clone 35 was significantly lower compared to tetraploids at lower light intensities (50 PPFD). But at higher light intensities (300 – 500 PPFD), tetraploids were significantly lower compared to hexaploid clone 29. In stress treatment, the ETR at a lower light intensity of hexaploid clone 35 was significantly lower compared to diploids (10-50 PPFD) and tetraploids (10 – 100 PPFD), but the ETR at higher light intensities (500 PPFD) of tetraploids was significantly lower compared to diploids.



Table 3.3. *P*-values of the two-way ANOVAs for determination of the effects of prolong photoperiod on PSII maximum efficiency ( $\Phi$ PSII) and maximum quantum efficiency of PSII photochemistry (QY\_max) between treatment and among different ploidy and hexaploid clones. Significant results are in bold. QY\_max: maximum photochemical efficiency of PSII photochemistry;  $\Phi$ PSII: actual quantum yield of PSII

	( $\Phi$ PSII)			(QY_max)		
	Chisq	Df	Pr(>Chisq)	Chisq	Df	Pr(>Chisq)
Treatment	0.536	1	0.46400	2.397	1	0.12160
Ploidy	80.082	3	<b>&lt;0.00000</b>	180.187	3	<b>&lt;0.000001</b>
Treatment:Ploidy	22.542	3	<b>0.00005</b>	1.474	3	0.68820

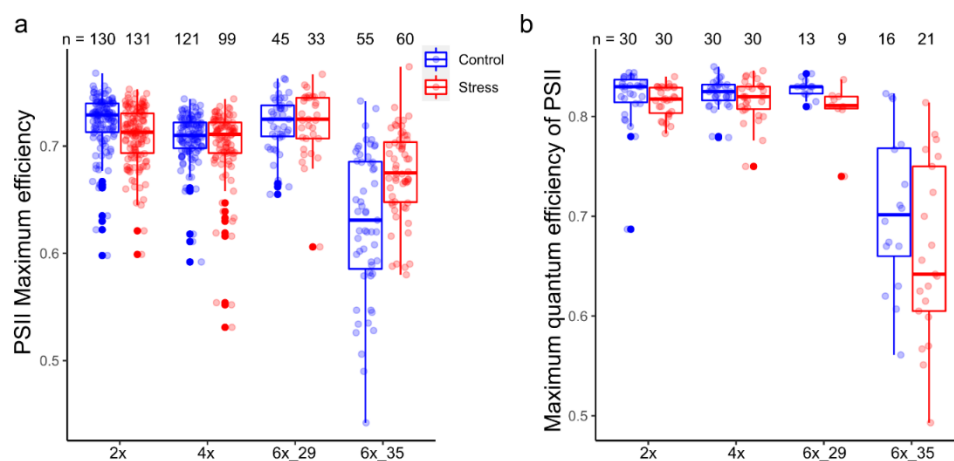


Figure 3.1 Photosynthesis performance of *Ranunculus auricomus* complex between treatment and among different ploidy and hexaploid clones. a. Boxplots of PSII maximum efficiency ( $\Phi$ PSII); b. Boxplots of maximum quantum efficiency of PSII photochemistry (QY\_max); Boxplots show the 25<sup>th</sup>, median, and 75<sup>th</sup> percentile range, and jitter plots represent the exact data distribution. n = number of measurements from 3-14 individuals per group.

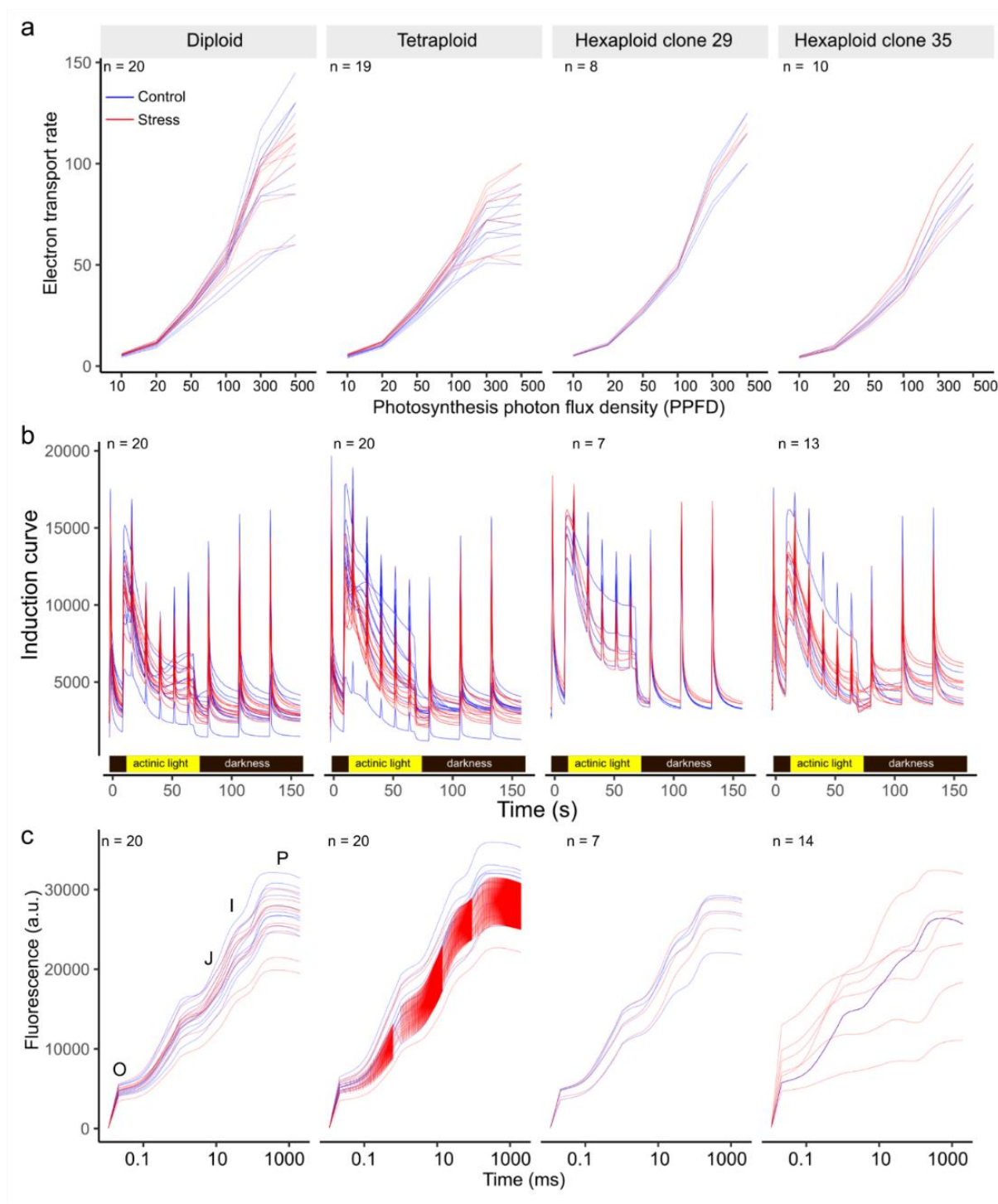


Figure 3.2 Effect photoperiod on the relative electron transport rate, induction curves, and fast fluorescence transient curves (OJIP) between treatment and among different ploidy levels and hexaploid clones. a. Relative electron transport rate (rETR) curve under different light intensities (10-500 PPFD). b. Induction and relaxation of non-photochemical quenching (NPQ) curves; c. OJIP curves. Each line in the curves is an individual value. n = number of measurements from 3-10 individuals per group.

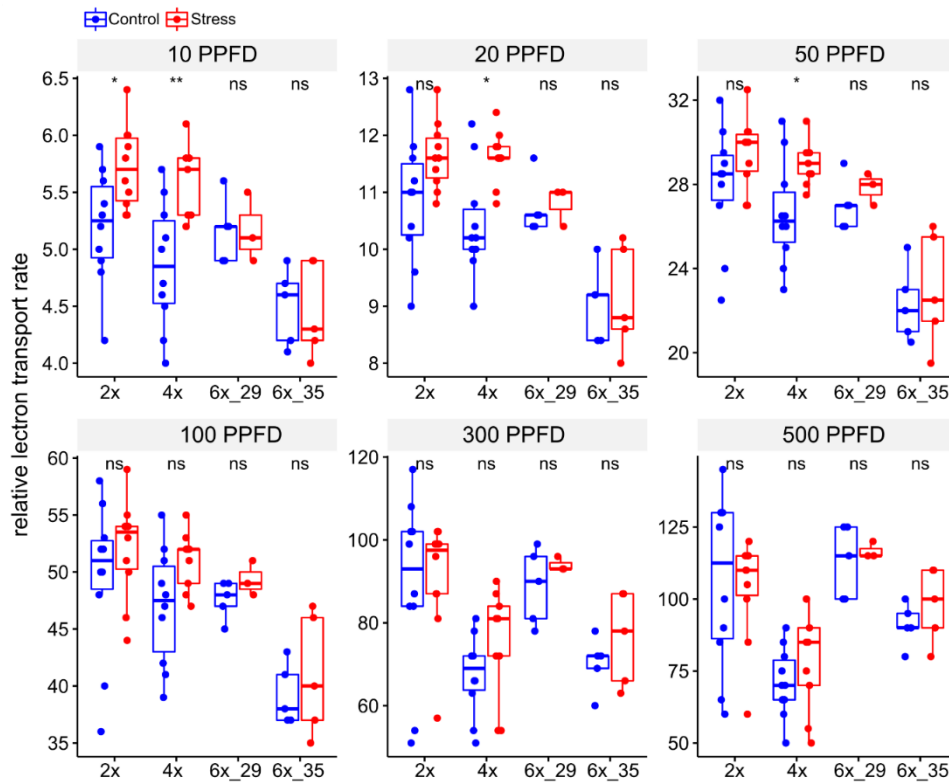


Figure 3.3 Photoperiod effect on relative electron transport rate between treatment and among different ploidies and hexaploid clones under different light intensities (10-500 PPFD). PPFD = photosynthesis photon flux density. Boxplots show the 25<sup>th</sup>, median, and 75<sup>th</sup> percentile range, and jitter plots represent the exact data distribution. n = 3-10 individuals per group, see details in Table 3.1.

### 3.5.4 Fluorescence quenching analysis of induction curve

The induction curves (IC) of all plants under actinic light and darkness were provided in Figure 3.2b. The IC was indicating a slightly higher fluorescence curve of plants under stress treatment even though a general overlapping pattern was observed. The quenching coefficients and other parameters extracted from the IC curve were provided in Table S9. The mean values of quenching parameters and their proportion alteration between the treatments were reported in Table 3.4 and visualized as boxplots in Figure 3.4. In diploids, extended light significantly increased four parameters, i.e., nonphotochemical quenching (NPQ) (S-C 20.44 %, p-value = 0.0185), energy-dependent nonphotochemical quenching coefficient ( $q_E$ ) (S-C 23.60 %, p-value = 0.0147), fraction of NPQ related to  $q_E$  (NPQ<sub>E</sub>) (S-C 24.15 %, p-value = 0.0232) and non-photochemical quenching coefficient ( $q_N$ ) (S-C 10.43 %, p-value = 0.0433). In tetraploids, extended light significantly increased parameters of coefficient of photochemical quenching ( $q_P$ ) (S-C 7.87 %, p-value = 0.0089) and non-photochemical that is formed only upon illumination ( $q_L$ ) (S-C 15.04 %, p-value = 0.0147). In the two hexaploid clones, no parameters were enhanced. Kruskal-Wallis tests of the IC parameters among different ploidies discriminated a total of eight parameters were altered only in control plants, i.e., NPQ,  $q_E$ ,  $q_L$ , NPQ<sub>E</sub>, NPQ<sub>I</sub>,  $q_P$ , and  $q_N$ , while in stress treatment a total of five parameters, i.e., PQ,  $q_L$ , NPQ<sub>I</sub>,

$qN$ , and  $qL$  was altered (Table 3.2). Pairwise comparison marked the significant values among cytotype and hexaploid clones (Table S9). In control treatment, diploids performed a significantly lower NPQ ( $p_{\text{adj}} = 0.023$ ),  $q_l$  ( $p_{\text{adj}} = 0.031$ ), and  $NPQ_l$  ( $p_{\text{adj}} = 0.031$ ) than tetraploids, but diploids performed a significantly higher PQ than hexaploid clone 29 ( $p_{\text{adj}} = 0.012$ ) and hexaploid clone 35 ( $p_{\text{adj}} = 0.048$ ). Diploids also performed a significantly higher  $qP$  than tetraploids ( $p_{\text{adj}} = 0.017$ ) and hexaploid clone 29 ( $p_{\text{adj}} = 0.012$ ). Tetraploid performed a significantly higher  $q_l$  ( $p_{\text{adj}} = 0.012$ ) and  $NPQ_l$  ( $p_{\text{adj}} = 0.012$ ) than hexaploid clone 29. On the other hand, in stress treatment, hexaploid clone 35 performed a significantly lower PQ than diploids ( $p_{\text{adj}} = 0.004$ ) and tetraploids ( $p_{\text{adj}} = 0.002$ ), but performed a significantly higher  $qN$  than diploids ( $p_{\text{adj}} = 0.025$ ). Hexaploid clone 29 performed a significantly lower  $q_l$  ( $p_{\text{adj}} = 0.042$ ) and  $NPQ_l$  ( $p_{\text{adj}} = 0.042$ ) than tetraploids.

Table 3.1 Summary statistics and P- values of Wilcoxon-Mann-Whitney-Test for determination effects of prolonged photoperiod on relative electron transport rate between treatments under different light intensities (PPFD 10-500). S-C: proportion of alternation of the mean value, calculated as (Stress - Control)/(Stress + Control)\*100. Significant results are **in bold**

Light intensity	Ploidy	Control treatment (C)			Stress treatment (S)			S - C (%)	p-value
		n	mean	sd	n	mean	sd		
10	2x	10	5.20	0.50	10	5.72	0.36	4.76	<b>0.02070</b>
	4x	10	4.86	0.56	9	5.58	0.33	6.88	<b>0.00601</b>
	6x_29	5	5.16	0.29	3	5.17	0.31	0.07	0.87800
	6x_35	5	4.50	0.34	5	4.46	0.42	-0.45	1.00000
20	2x	10	10.86	1.11	10	11.64	0.60	3.47	0.07450
	4x	10	10.44	0.95	9	11.62	0.48	5.36	<b>0.01230</b>
	6x_29	5	10.72	0.50	3	10.80	0.35	0.37	0.64300
	6x_35	5	9.04	0.67	5	9.12	0.94	0.44	0.83300
50	2x	10	27.95	2.85	10	29.50	1.68	2.70	0.18300
	4x	10	26.60	2.49	9	29.00	1.03	4.32	<b>0.02690</b>
	6x_29	5	27.00	1.23	3	27.83	0.76	1.52	0.28200
	6x_35	5	22.30	1.79	5	23.00	2.74	1.55	0.60200
100	2x	10	49.50	6.79	10	52.00	4.42	2.46	0.34300
	4x	10	47.00	5.12	9	51.00	2.55	4.08	0.05870
	6x_29	5	47.60	1.67	3	49.33	1.53	1.79	0.21900
	6x_35	5	39.20	2.68	5	41.00	5.34	2.24	0.75100
300	2x	10	88.80	21.87	10	90.90	13.93	1.17	0.90900
	4x	10	67.50	9.62	9	75.00	13.33	5.26	0.09810
	6x_29	5	88.80	9.15	3	94.00	1.73	2.85	0.54600
	6x_35	5	70.20	6.57	5	76.20	11.35	4.10	0.39900
500	2x	10	106.00	30.07	10	103.50	18.27	-1.19	0.56900
	4x	10	71.00	11.97	9	78.89	17.99	5.26	0.23400
	6x_29	5	113.00	12.55	3	116.67	2.89	1.60	0.87700
	6x_35	5	91.00	7.42	5	98.00	13.04	3.70	0.33700

Table 3.2 *P*-values of Kruskal-Wallis-Tests for determination of significant differences of relative electron transport rate, induction curve parameters, and specific energy fluxes parameters of JIP-test among different ploidy and hexaploid clones. Significant results are **in bold**

	Control treatment				Stress treatment			
	n	statistic	df	p-value	n	statistic	df	p-value
Electron transport rate at PPFD								
10	30	7.61	3	0.0547	27	14.97	3	<b>0.00184</b>
20	30	10.26	3	<b>0.0165</b>	27	15.06	3	<b>0.00177</b>
50	30	11.49	3	<b>0.00934</b>	27	14.42	3	<b>0.00239</b>
100	30	9.61	3	<b>0.0222</b>	27	11.53	3	<b>0.00919</b>
300	30	11.72	3	<b>0.00839</b>	27	11.06	3	<b>0.0114</b>
500	30	13.68	3	<b>0.00337</b>	27	13.32	3	<b>0.00399</b>
Inductive curve parameters								
NPQ	28	13.31	3	<b>0.00402</b>	32	6.88	3	0.07570
PQ	28	12.01	3	<b>0.00736</b>	32	17.14	3	<b>0.00066</b>
q <sub>E</sub>	28	12.22	3	<b>0.00668</b>	32	6.50	3	0.08980
q <sub>I</sub>	28	13.16	3	<b>0.00431</b>	32	10.66	3	<b>0.01370</b>
NPQ <sub>E</sub>	28	12.89	3	<b>0.00489</b>	32	7.65	3	0.05380
NPQ <sub>I</sub>	28	13.16	3	<b>0.00431</b>	32	10.66	3	<b>0.01370</b>
qP	28	12.08	3	<b>0.00713</b>	32	5.79	3	0.12200
qN	28	11.97	3	<b>0.00749</b>	32	12.05	3	<b>0.00723</b>
qL	28	7.26	3	0.06400	32	9.72	3	<b>0.02110</b>
Specific energy fluxes parameters of JIP-test								
PI_Abs	31	14.69	3	<b>0.0021</b>	31	14.36	3	<b>0.00246</b>
ABS/RC	31	9.29	3	<b>0.0256</b>	31	13.79	3	<b>0.00321</b>
TRo/RC	31	17.44	3	<b>0.000573</b>	31	16.80	3	<b>0.000775</b>
ETo/RC	31	1.76	3	0.624	31	16.36	3	<b>0.000957</b>
DIo/RC	31	12.62	3	<b>0.00553</b>	31	17.17	3	<b>0.000651</b>

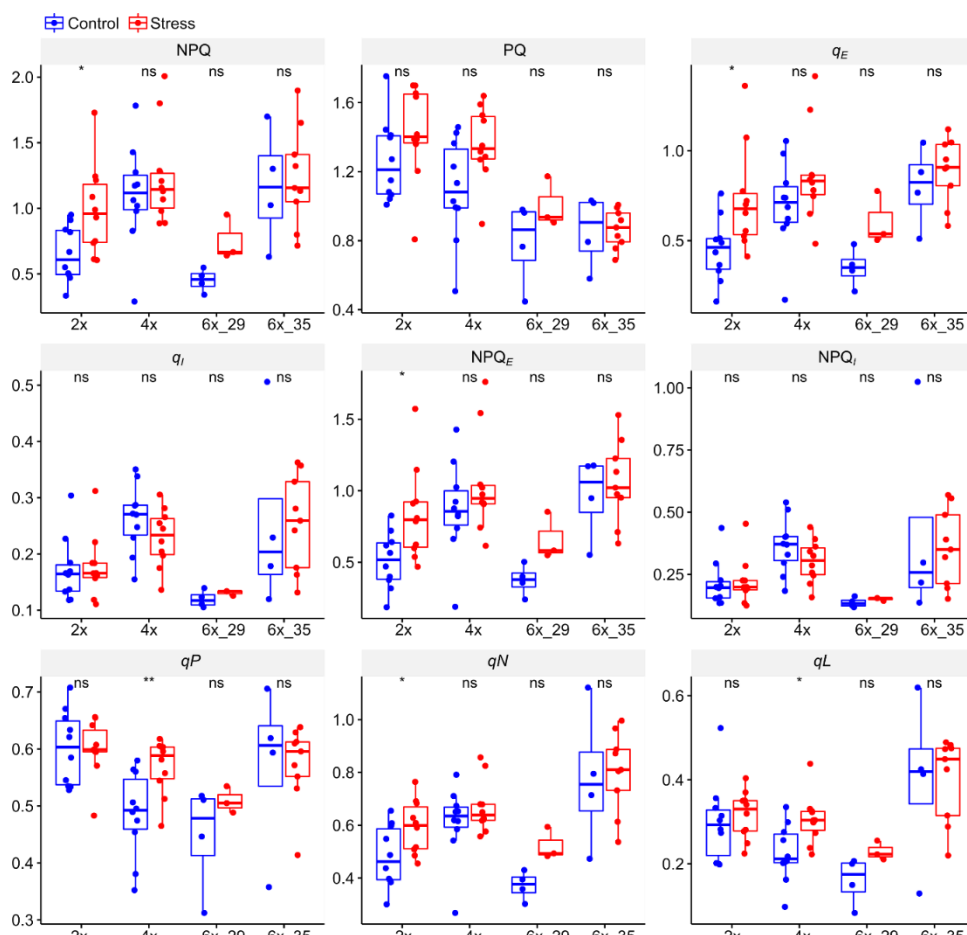


Figure 3.4 Photoperiod effect on induction curve parameters between treatment and among different ploidies and hexaploid clones and hexaploid clones. NPQ = Non-photochemical quenching,  $NPQ_E$  = energy dependent non-photochemical Chl fluorescence quenching,  $NPQ_i$  = photoinhibitory non-photochemical Chl fluorescence quenching, PQ = photochemical quenching,  $q_E$  = energy dependent non-photochemical Chl fluorescence quenching coefficient,  $q_i$  = photoinhibitory non-photochemical Chl fluorescence quenching coefficient,  $q_P$  = quenching coefficient of photochemical,  $q_N$  = quenching coefficient of non-photochemical,  $q_L$  = quenching coefficient of non-photochemical that is formed only upon illumination to regulate the amount of absorbed light in avoiding damage effect. Boxplots show the 25<sup>th</sup>, median, and 75<sup>th</sup> percentile range, and jitter plots represent the exact data distribution. n = 3-10 individuals per group, see detail in Table 3.3.

Table 3.3 Summary statistic and *P*- values of Wilcoxon-Mann-Whitney-Test for determination of effects of prolonged photoperiod on induction curves parameters between treatments . **S-C**: proportion of alternation of the mean value, calculated as (Stress - Control)/(Stress + Control)\*100. Significant results are in **bold**.

Parameter	Ploidy	Control treatment (C)			Stress treatment (S)			S - C (%)	p-value
		n	mean	sd	n	mean	sd		
NPQ	2x	10	0.654	0.213	10	0.99	0.347	20.44	<b>0.0185</b>
	4x	10	1.102	0.39	10	1.241	0.376	5.93	0.631
	6x_29	4	0.451	0.088	3	0.753	0.173	25.08	0.0571
	6x_35	4	1.164	0.451	9	1.237	0.381	3.04	0.71
PQ	2x	10	1.263	0.238	10	1.425	0.276	6.03	0.218
	4x	10	1.093	0.296	10	1.358	0.218	10.81	0.0524
	6x_29	4	0.789	0.248	3	1.004	0.147	11.99	0.629
	6x_35	4	0.856	0.214	9	0.869	0.111	0.75	0.71
$q_E$	2x	10	0.45	0.178	10	0.728	0.289	23.60	<b>0.0147</b>
	4x	10	0.698	0.244	10	0.869	0.269	10.91	0.123
	6x_29	4	0.35	0.108	3	0.605	0.149	26.70	0.0571
	6x_35	4	0.801	0.225	9	0.889	0.18	5.21	0.414
$q_I$	2x	10	0.172	0.057	10	0.178	0.057	1.71	0.912
	4x	10	0.263	0.06	10	0.229	0.052	-6.91	0.19
	6x_29	4	0.12	0.015	3	0.131	0.005	4.38	0.4
	6x_35	4	0.258	0.171	9	0.256	0.085	-0.39	0.71
NPQ <sub>E</sub>	2x	10	0.512	0.198	10	0.838	0.33	24.15	<b>0.0232</b>
	4x	10	0.871	0.33	10	1.044	0.349	9.03	0.315
	6x_29	4	0.375	0.109	3	0.662	0.167	27.68	0.0571
	6x_35	4	0.962	0.294	9	1.06	0.289	4.85	0.604
NPQ <sub>I</sub>	2x	10	0.213	0.092	10	0.222	0.093	2.07	0.912
	4x	10	0.365	0.11	10	0.302	0.086	-9.45	0.19
	6x_29	4	0.136	0.02	3	0.151	0.006	5.23	0.4
	6x_35	4	0.419	0.409	9	0.359	0.156	-7.71	0.71
$q_P$	2x	10	0.601	0.065	10	0.6	0.05	-0.08	0.912
	4x	10	0.486	0.075	10	0.569	0.049	7.87	<b>0.00893</b>
	6x_29	4	0.447	0.095	3	0.509	0.023	6.49	0.629
	6x_35	4	0.569	0.149	9	0.573	0.069	0.35	0.825
$q_N$	2x	10	0.481	0.117	10	0.593	0.101	10.43	<b>0.0433</b>
	4x	10	0.611	0.139	10	0.669	0.099	4.53	0.529
	6x_29	4	0.371	0.055	3	0.524	0.061	17.09	0.0571
	6x_35	4	0.776	0.268	9	0.802	0.153	1.65	0.604
$q_L$	2x	10	0.299	0.097	10	0.317	0.057	2.92	0.353
	4x	10	0.226	0.069	10	0.306	0.059	15.04	<b>0.0147</b>
	6x_29	4	0.16	0.057	3	0.23	0.023	17.95	0.0571
	6x_35	4	0.397	0.202	9	0.402	0.101	0.63	0.71

### 3.5.5 Fast fluorescence transient curve

All fast fluorescence transient curve (OJIP) transients among ploidies from both light treatments showed a typical polyphasic rise of the OJIP curve with a slight decrease in stressed diploids at the I-P phase, tetraploids at the J-I and I-P phase, and a higher alternation of all phase in hexaploid clone 35. The hexaploid clone 29 did not show a clear shift of the OJIP phase between treatments (Figure 3.2c). The JIP-test parameters were provided in Table S10. The mean values of the JIP-test and their proportion alternation between the treatments were reported in Table 3.4 and visualized as boxplots in Figure 3.5. The JIP-test revealed that extended light significantly altered a total of fourteen parameters in diploids and a total of two parameters in tetraploids and hexaploid clone 35, but none of the parameters were altered in hexaploid clone 29. Stress in diploids altered the proportion of alternation of the mean S-C value by decreasing  $F_M/F_0$  (-4.40 %),  $F_V/F_0$  (-5.38 %),  $F_V/F_M$  or  $\Phi_{P_0}$  (-0.98 %),  $\Phi_{E_0}$  (-3.25%),  $S_S$  (-3.96 %), and  $PI_{Abs}$  (-15.66 %), by increasing:  $M_0$  (7.25%),  $V_i$  (3.31 %),  $\Phi_{Pav}$  (0.51 %),  $\Phi_{D_0}$  (4.35 %),  $ABS/RC$  (4.71%),  $TR_0/RC$  (3.75%), and  $DI_0/RC$  (9.07 %). Stress in tetraploids decreased the S-C parameter for  $Fix.Area$  (-14.12 %) and  $ET_0/RC$  (-5.09 %). Stress in the hexaploid clone 35 increased the S-C parameter for  $TR_0/RC$  (8.95 %) and  $ET_0/RC$  (13.72 %) (see p-values in Table S10). Selected parameters, namely the specific energy fluxes and  $PI_{Abs}$ , were presented in Table 3.4 and visualized as boxplots in Figure 3.5. Kruskal-Wallis tests of the specific energy fluxes and  $PI_{Abs}$  parameters among different ploidy indicated that all parameters were significantly different in both treatments except  $ET_0/RC$  in the control treatment (Table 3.2). Pairwise comparison marked the significant values between cytotypes (Table S12). In both treatments, hexaploid clone 35 had a lower mean value of  $PI_{Abs}$  compared to diploids and tetraploids, but had a higher mean value of  $ABS/RC$  and  $DI_0/RC$  compared to diploids and tetraploid, and a higher mean value of  $TR_0/RC$  than diploids, tetraploids, and hexaploid clone 29 (only control treatment). In the stress treatment, tetraploids had a lower mean value of  $ET_0/RC$  than diploids and hexaploid clone 35.

### 3.6 Discussion

Plant growth and development are sensitive to the photoperiod, which affects the metabolite profile (de Castro et al., 2019), photosynthesis (Bauerle et al., 2012; Sulpice et al., 2014; Kinoshita et al., 2020), growth (Wu et al., 2004; Fortini et al., 2020), and flower initiation (Jeong and Clark, 2005). Extended photoperiod altered the mode of reproduction in hexaploid plants of the *Ranunculus auricomus* complex by increasing proportions of sexual ovules (Klatt et al., 2016) and showed a more substantial effect in lower ploidy levels (Ulum et al., 2020). The present study analyzed the photosynthesis efficiency of three cytotypes of *Ranunculus*



*auricomus* under control and stress conditions with extended photoperiod. Combining the current result with our previous study on the same plant material (Ulum et al., 2020), we tested the hypothesis that extended photoperiod alters the photosynthetic performance, with the expectation of a buffering effect by polyploidy.

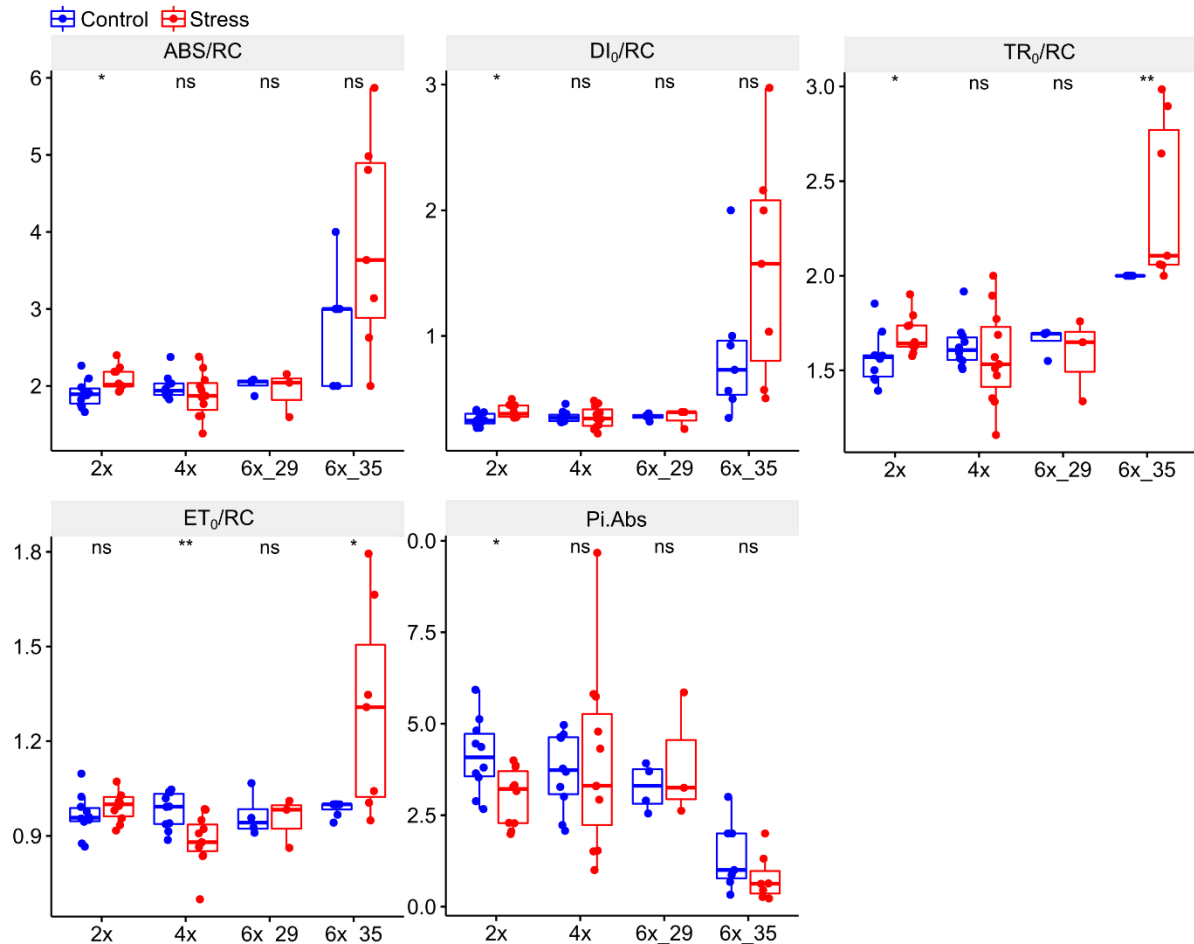


Figure 3.5 Photoperiod effect on specific energy fluxes parameters of JIP-test between treatment and among different ploidy and hexaploid clones. ABS/RC = absorption flux per reaction center (RC) (apparent antenna size of an active PSII), DI<sub>0</sub>/RC = dissipated energy flux per reaction center (RC), ET<sub>0</sub>/RC = electron transport flux per reaction center (RC), Pi\_Abs = performance index on absorption basis related to the overall photosynthetic activity of PSII, TR<sub>0</sub>/RC = trapped energy flux per RC. Boxplots show the 25<sup>th</sup>, median, and 75<sup>th</sup> percentile range, and jitter plots represent the exact data distribution. n = 3-11 individuals per group, see detail in Table 3.4

### 3.6.1 Ploidy dependent effects of photoperiod on photosynthetic capacity

Photoperiod alternation modulating plant photosynthesis was reported in several studies (e.g., (Fr chet te et al., 2016; de Castro et al., 2019; Elkins and van Iersel, 2020). Here we examined the prolonged photoperiod effects on photosynthesis performance of *R. auricomus* cytotypes marked by  $\Phi$ PSII, rETR, and QY<sub>max</sub>. The three cytotypes of *R. auricomus* complex exhibited in either short (10 h) or long (16.5 h) photoperiod a similar capacity to capture the climatic chamber's light for the PSII (photosystem II) photochemistry under different photoperiod

treatments, as observed in our  $\Phi$ PSII data. The  $\Phi$ PSII photosynthesis parameter estimates the theoretical proportion of absorbed light used by Chlorophyll associated with PSII and hence measures the efficiency of photosystem II (Ghashghaie et al., 1992; Baker, 2008). However, there was a significant difference between ploidy levels (Table 3.3.), caused mainly by lower  $\Phi$ PSII values of the hexaploid clone 35.

The light intensity of our climatic chamber ( $250 \text{ m}^{-2} \text{ s}^{-1}$ ) provided sufficient energy for the reaction center in PSII and kept the PSII reaction center at the open stage as indicated by relative electron transport (rETR) values at 100 and 300 PPFD (Figure 3.3). rETR curve illustrates the physiological flexibility of plant photosynthetic capacity to rapid irradiation changes (Schreiber and Berry, 1977; Ralph and Gademann, 2005). In our study, rETR confirmed that in lower light intensities (10–50 PPFD), diploids and tetraploids had a higher photosynthetic capacity after longer photoperiods treatment, but no differences appeared at higher light intensities (100–500 PPFD) in both treatments. The increase of rETR in diploids and tetraploids might be related to the convexity response of  $\Phi$ PSII to Photosynthetic photon flux density (PPFD) as the same pattern was reported in *Lactuca sativa* (Weaver and van Iersel, 2020). Our rETR curves also suggested different photosynthesis performances between ploidy and hexaploid clones (Table S8). Diploids and hexaploid clone 29 were more adaptive to a wider range of light intensity, but tetraploids and hexaploid clone 35 were more sensitive to the change of light intensity. Tetraploids performed a better rETR in lower light intensity (<300 PPFD), but hexaploid clone 35 improved the rETR within the increase of light intensity (>300 PPFD). The rETR values, however, must be interpreted with caution as they are calculated on assumptions of constant values for a fraction of absorbed PPFD that is received by PSII (0.5), and these assumptions are often not met (Baker, 2008).

Plants under excess light exposure might damage photosystem II or activate photoinhibition in the photosynthetic reaction center (RC) of PSII (Takahashi and Murata, 2008).  $C_3$  plants have relatively constant  $F_v/F_m$  ratios, with mean values of  $QY_{\text{max}}$  of  $\sim 0.83$  under unstressed conditions, whereas deviating values indicate the presence of photoinhibition (Björkman and Demmig, 1987). The photoperiod treatments did not activate photoinhibition in *R. auricomus* as indicated by the maximum quantum efficiency of PSII photochemistry ( $QY_{\text{max}}$ ) in almost all plants around 0.83, except for the hexaploid clone 35. In this clone, the low  $QY_{\text{max}}$  value might be related to photoinhibition, as indicated by  $\Phi$ PSII and rETR. However, this clone also exhibited a slower development of leaves during the measurement period, which also may explain deviating results. The  $QY_{\text{max}}$  value of 0.81 from the congeneric species *Ranunculus asiaticus* L. was reported to be close to the optimal value (Carillo et al., 2019). The result of our study with a range of mean values of  $QY_{\text{max}}$  between 0.81 - 0.83 in almost all of the

plants was close to the optimal value, suggesting that in the presence of light excess *R. auricomus* is prone to perform heat dissipation as the main photoprotective mechanism. Another study in *Lippia alba* also confirmed the same pattern that photoperiod extension affected the NPQ and ETR, but neither affected the QY\_max (de Castro et al., 2019).

Table 3.4 Summary statistics and *P*- values of Wilcoxon-Mann-Whitney-Test for determination of effects of prolonged photoperiod on specific energy fluxes parameters of JIP-test between treatments . **S-C**: proportion of alternation of the mean value, calculated as (Stress - Control)/(Stress + Control)\*100. Significant results are in **bold**

Parameter	Ploidy	Control treatment (C)			Stress treatment (S)			S - C (%)	p-value
		n	mean	sd	n	mean	sd		
ABS/RC	2x	10	1.902	0.181	10	2.09	0.154	4.709	0.01400
	4x	10	1.987	0.162	11	1.885	0.29	-2.634	0.38700
	6x_29	4	2.017	0.099	3	1.931	0.295	-2.178	0.85700
	6x_35	7	2.714	0.756	7	3.866	1.399	17.508	0.10500
DI <sub>0</sub> /RC	2x	10	0.336	0.052	10	0.403	0.054	9.066	0.01150
	4x	10	0.356	0.045	11	0.354	0.087	-0.282	0.86300
	6x_29	4	0.357	0.028	3	0.35	0.078	-0.990	0.62900
	6x_35	7	0.867	0.551	7	1.545	0.905	28.109	0.12800
TR <sub>0</sub> /RC	2x	10	1.566	0.134	10	1.688	0.102	3.749	0.01470
	4x	10	1.631	0.12	11	1.572	0.251	-1.842	0.42600
	6x_29	4	1.659	0.073	3	1.582	0.219	-2.376	0.85700
	6x_35	7	2	0	7	2.393	0.434	8.946	0.00372
ET <sub>0</sub> /RC	2x	10	0.964	0.067	10	0.992	0.047	1.431	0.21200
	4x	10	0.981	0.057	11	0.886	0.081	-5.088	0.00365
	6x_29	4	0.965	0.071	3	0.952	0.079	-0.678	1.00000
	6x_35	7	0.987	0.023	7	1.301	0.331	13.724	0.01870
Pi_Abs	2x	10	4.121	1.014	10	3.005	0.786	-15.661	0.02880
	4x	10	3.696	1.044	11	3.99	2.502	3.825	1.00000
	6x_29	4	3.267	0.65	3	3.909	1.715	8.946	0.85700
	6x_35	7	1.41	0.949	7	0.787	0.645	-28.357	0.12400

### 3.6.2 Ploidy dependent effects of photoperiod on quenching processes

The photosynthesis pigments in plants absorb the energy from the photon, which is mostly used in photosynthetic electron transport (photochemical quenching), but the excess light energy is dissipated as heat (non-photochemical quenching) and/or re-emitted as fluorescence (Walker, 1987). These three fates occur in competition, as they rely on the same energy source, and the increase of one factor decreases the others (Kautsky and Hirsch, 1931; Maxwell and Johnson, 2000). Heat dissipation was observed to some extent in both photoperiods in this study. An enhancement of the non-photochemical quenching after extended photoperiod was observed only in diploids but absent in tetraploids and hexaploids, indicating the stress buffer in polyploid plants. NPQ corresponds to the excess light dissipation

to heat (Brestic and Zivcak, 2013). A better capacity of polyploids for regulating non-photochemical quenching was also observed in tetraploid *Glycine max* (Coate et al., 2012). A higher photosynthesis rate and better quenching of destructive light in polyploids compared to their diploid progenitor were suggested as the advantages of the higher DNA content per cell (Warner and Edwards, 1993) and more photosynthetic pigments as reported in polyploids of *Vicia cracca* (Münzbergová and Haisel, 2019).

The component of NPQ is discriminated into  $q_E$  quenching and  $q_I$  quenching based on relaxation analysis in high illumination (D'Ambrosio et al., 2008; Lazár, 2015). In diploids, prolonged photoperiod activated mechanism of thermal dissipation as indicated by NPQ<sub>E</sub> and  $q_E$ , instead of photoinhibition of photosynthesis (NPQ<sub>I</sub> and  $q_I$ ). Under consideration of the active center, the  $q_N$  was the only quenching coefficient altered by extended photoperiod in diploids.  $q_N$  reflecting the fraction of variable Chl fluorescence is quenched by non-photochemical process (Lazár, 2015) rather than being used for photosynthetic electron transport (Genty et al., 1989). Our result of  $\phi$ PSII and QY<sub>max</sub> on diploids was concomitant with this quenching data. In tetraploids, an enhanced quenching coefficient  $q_P$  and  $q_L$  suggested that the light excess from 16.5 h photoperiod was quenched into photochemistry, but a certain fraction absorbed light was dissipated into heat. The  $q_P$  (coefficient of photochemical quenching) indicated that excess light is quenched by photochemistry (Lazár, 2015) and reflected the degree of open reaction centers in which primary quinone acceptor Q<sub>A</sub> PSII is capable of photoreduction (Krause and Weis, 1991). The  $q_L$  estimates non-photochemical is formed only upon illumination to regulate the amount of absorbed light in avoiding damage effect (Kramer et al., 2004).

The pairwise comparison among ploidy levels in control treatments confirmed that hexaploid clone 29 and clone 35 performed a lower PQ than diploids. PQ of hexaploid clone 35 was also lower in stress treatment compared to diploids and tetraploids, which was probably due to the less optimal light intensity of the growth condition as suggested by  $\phi$ PSII and QY<sub>max</sub>. The PQ parameter indicated the de-excitation pathway of absorbed light energy (Porcar-Castell et al., 2014). Hexaploid clone 29 also performed a lower  $q_I$  than tetraploids in both treatments. Hence, we cannot make a general conclusion on hexaploids, but we rather detected a great variation in response to prolonged photoperiods, probably depending on the original habitat of the source population. The hexaploid clones/populations of this hybrid lineage are genetically all very similar, but nevertheless occupy a broad range of habitats from forest understory to forest margins and open meadows (Paun et al., 2006; Hörandl et al., 2009).

### 3.6.3 Fast fluorescence transient curve

The OJIP curve illustrates the reduction of the acceptor side of PSII (represented as O-J phase), partial reduction of the PQ pool (represented as J-I phase), and the reduction of the acceptor side of PSI (represented as I-P phase) (Yusuf et al., 2010; Ripoll et al., 2016). Our OJIP curves indicated that prolonged photoperiod altered the I-P phase in diploids, the J-I and I-P phase in tetraploids, all phases in hexaploid clone 35. Since the JIP-test parameters provide a more detailed characterization of fluorescence transient for screening the environmental effect on photosynthesis behavioral in plants e.g., Strasser et al. (2000), we extended the observation of the stress effect between diploids and tetraploids with JIP-tests.

The JIP-test between the treatments presented a stronger effect in diploids marked by a reduction of the value of  $Pi\_Abs$  (performance index on absorption basis).  $Pi\_Abs$  quantifies the overall performance of PSII electron flow (Stirbet et al., 2018). Prolonged photoperiod in diploids altered parameters of specific energy flux per reaction center (RC), affecting the antenna molecules in the photosynthetic membrane, then resulted in higher closure of reaction center ( $ABS/RC$ ), reduced the capacity of photon trapping ( $TR_0/RC$ ); hence, photons dissipated to a higher extent ( $DI_0/RC$ ). Single turn-over ( $S_s$ ) represents the total amount of primary PSII acceptor ( $Q_A$ ) (Strasser et al., 2004) and corresponds to the O-J phase (Bordenave et al., 2019) as presented by a slightly higher O-J phase. The study of Rusaczek et al. (2015) on *Arabidopsis thaliana* proposed that the inhibition of photosynthetic electron transport after UV stress might have originated from an increase in UV sensitivity of the light-dependent reactions ( $\Phi_{D_0}$ ). In our study, the diploids in prolonged photoperiods might have an increased sensitivity of the light-dependent reactions. The specific energy fluxes of diploids were reduced, e.g., absorption flux per reaction center (RCs) (apparent antenna size of an active PSII) ( $ABS/RC$ ), dissipated energy flux per RCs ( $DI_0/RC$ ), and trapped energy flux per RCs ( $TR_0/RC$ ).  $ABS/RC$  estimates the ratio of the total number of photons absorbed by Chlorophyll of all reaction centers (RCs) in PSII to the number of active RCs. In *A. thaliana*, the increase of  $ABS/RC$  was an indication of inactivation of PSII center after UV-C stress, a higher  $TR_0/RC$  was an indication of reduction of plastoquinone  $Q_A$  pool, and increasing of  $DI_0/RC$  was an indication of PSII RCs damage and reduction of the efficiency in trapping photons (Rusaczek et al., 2015). The stressed diploid *Ranunculus auricomus* plants presented a higher dissipated energy flux per reaction center ( $DI_0/RC$ ), which correlates with the result of higher dissipated heat (NPQ in this study) and fluorescence ( $\Phi_{P_0}$ ). A similar pattern was also reported in Çiçek et al. (2020) after UV-B stress in Scots pine, and the absorbed energy could not be directed to PSII for photochemistry but was dissipated as heat and fluorescence.

In tetraploids, only a slight effect of prolonged photoperiod was observed by the reduction of  $ET_0/RC$  and  $Fix.Area$  (area below the fluorescence curve between  $F_{20\mu s}$  and  $F_{1s}$ ). Under stress treatment, the mean value of  $ET_0/RC$  of tetraploid was lower than in the other cytotypes.  $ET_0/RC$  was the later stage of electron transport per reaction center. The reduction of  $ET_0/RC$  might indicate the blockage of PSII electron transport beyond  $Q_A^-$  (Stirbet et al., 2018). Following Rusaczonk et al. (2015) that reduction of  $ET_0/RC$  is related to an increase of inactive reaction centers of PSII, and hence in tetraploids, extended photoperiod might not affect the antenna molecules in the photosynthetic membrane as indicated by quenching coefficient  $qP$ , but exceeding the capacity of photon trapping ( $TR_0/RC$ ); hence the excess light dissipated as non-photochemical quenching as indicated by quenching coefficient  $qL$ .

In hexaploids, again, the differentiation of the two clones was apparent. The hexaploid clone 35 performed a better photon trapping capacity ( $TR_0/RC$ ) and electron transport flux per RCs ( $ET_0/RC$ ) in the longer photoperiod. Specific energy fluxes parameter confirmed a higher photosynthesis performance of this clone and the  $PI_{Abs}$  indicating the requirement of higher light intensity for optimal photosynthesis. In clone 29, no differences appeared between treatments in any of the OJIP parameters. The variation of photosynthesis performance of hexaploids among two clones might relate to different habitats.

### **3.7 Conclusion on ploidy-dependent light stress effects and on mode of reproduction**

Our study revealed differential responses of cytotypes in photosynthesis parameters to prolonged photoperiods. However, the response of photosynthesis performance is complex and differs in various parameters and does not follow a linear pattern of better stress tolerance with higher ploidy levels. Although we raised the plants under equal garden conditions, we suppose that different pre-adaptations from original habitats of the provenances may still influence the photosynthesis performance. Diploids originated from crosses of forest plants and hence might be preadapted to low light conditions (Hörandl et al., 2009). They respond to prolonged photoperiod in most photosynthesis parameters and tend to reduce excess energy via non-photochemical quenching. Tetraploids were raised from light-adapted meadow plants, and also the hexaploid clone 35 was a typical sun-adapted plant that originated from a meadow population with more sunlight exposure (Paun et al., 2006; Hörandl et al., 2009), clone 35 = VRU2), whereas hexaploid clone 29 (= TRE) originated from a half-shaded habitat at forest margins). Tetraploids showed altogether not much sensitivity to the change of photoperiod and appeared to be adapted to high light conditions. Hexaploids, however strongly differentiated according to their provenances. We suppose an influence of habitat as other factors are unlikely. All cytotypes originate from sites in Central Europe (at 47- 48° latitude and from the same altitudinal zone), and hence we can rather rule out that differential

light intensities due to strong latitude (or altitude) gradients, as observed in Karbstein et al. (2021) over whole Europe, would influence the pattern. The variability of polyploid ecotypes may rely on a greater variance of gene expression patterns as they have highly heterozygous genomes (Karbstein et al., 2021). In tetraploid *Glycine max*, overexpression of oxidative stress-regulating genes compared to the diploid progenitors correlated to differential photosynthetic performance and adaptation to higher light intensities (Coate et al., 2012). Also, epigenetic control mechanisms may play a role. A study on cytosin-methylation of diploid and tetraploid *R. kuepferi* revealed not only different profiles between cytotypes but also indicated two different epigenetic groups within tetraploids, correlating to different temperature conditions (Schinkel et al., 2020).

The photosynthesis performance of *R. auricomus* cytotypes, however, does relate to mode of ovule formation, as diploids showed the highest sensitivity to prolonged photoperiod concomitant to the highest proportions of sexual ovules, followed by tetraploids (Ulum et al., 2020). Hexaploids, however, exhibited a very large variance in the proportions of sexual ovules, which we also observed here in photosynthesis performance. We detected here that this variation is mostly referable to two different ecotypes. We suppose that differential levels of oxidative stress influence the mode of reproduction, as in *Boechera* (Mateo de Arias et al., 2020). Different levels of oxidative stress in the reproductive tissues, however, need further investigation of metabolite profiles as important factors for the maintenance of redox homeodynamics.

**Patents:** Not applicable.

**Author Contributions:** EH and FH conceived and designed the study; FU performed the photo-synthesis analysis. Data were analyzed by FU and FH, and FU, EH, and FH wrote and consented to the manuscript.

**Funding:** This project was founded by The German Research Fund DFG (DFG Hörandl Ho 4395 4-1) to EH and by the Indonesia endowment fund for education, grant no. PRJ-2369/LPDP.3/2016 to FBU.

**Data Availability Statement:** The raw data are deposited at GöttingenResearchOnline (<https://data.goettingen-research-online.de/dataset.xhtml?persistentId=doi:10.25625/S7RGG7>).

**Acknowledgments:** Silvia Friedrichs for nursing the plants; referees for valuable comments on the manuscript.

**Conflicts of Interest:** The authors declare no conflict of interest

Supplementary Materials:

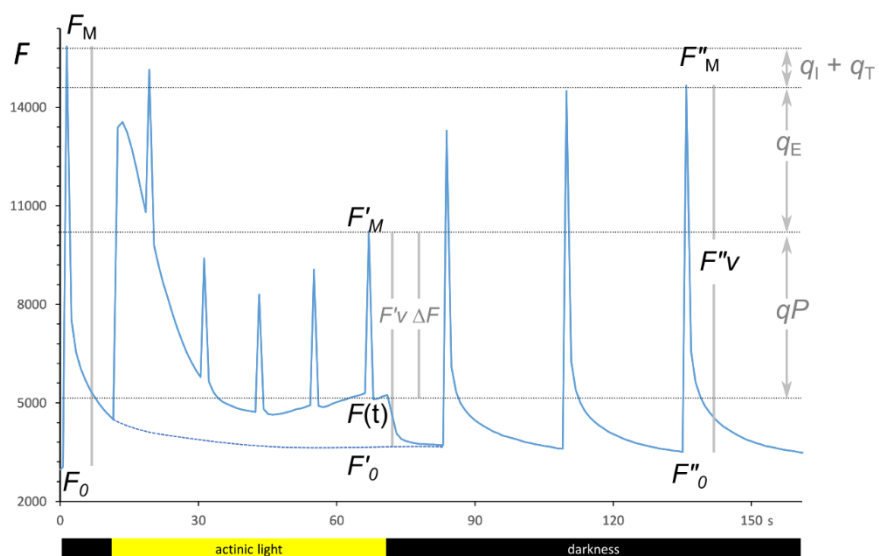


Figure S1: Induction curve and annotation of coefficients.



**Table S1.** Plant material used in the treatments and for measurements of photosynthesis parameters.

Ploidy	Treatment	Sample code	Plant code	Photosynthesis				
				PSII	ETR	IC	OJIP	
2x	Control	C2-12	J10xJ30/03	x				
		C2-13	J10xJ30/11	x	x	x	x	
		C2-15	J20xJ2/16	x	x	x	x	
		C2-19	J24xJ22/12	x	x	x	x	
		C2-21	F3xJ6/25	x	x	x	x	
		C2-24	J10xJ14/18	x		x	x	
		C2-25	J6xF3/19		x	x	x	
		C2-26	J10xJ30/05	x	x			
		C2-27	J6xF3/14		x	x	x	
		C2-4	F3xJ6/28	x				
		C2-7	J6xF3/14	x	x	x	x	
		C2-8	J6xF7/12	x	x	x	x	
		C2-9	J6xF7/14	x	x	x	x	
		Stress	S2-1	F3xJ6/01	x	x	x	x
			S2-18	J24xJ22/03	x	x	x	x
	S2-2		F3xJ6/04	x	x	x	x	
	S2-21		F3xJ6/1	x	x	x	x	
	S2-23		F10xJ3/03	x	x	x	x	
	S2-24		J6xF3/06	x	x	x	x	
	S2-25		J10xJ14/09	x				
	S2-27		J24xJ22/09	x				
	S2-3		F3xJ6/05	x	x	x	x	
	S2-6		J6xF3/02	x	x	x	x	
	S2-7		J6xF3/05	x	x	x	x	
	S2-9	J6xF7/08	x	x	x	x		
	4x	Control	C4-11	LH1406030B4-08	x	x	x	x
C4-13			LH1406030B4-16	x	x	x	x	
C4-15			LH1406030B4-18	x	x	x	x	
C4-19			LH1406030B5-07	x	x	x	x	
C4-21			LH1406030B5-16	x	x	x	x	
C4-22			LH1406030B5-17	x	x	x	x	
C4-23			LH1406030B5-19	x	x	x	x	
C4-26			LH4B005	x				
C4-5			LH1406030B2-04	x	x	x	x	
C4-8			LH1406030B4-02	x	x	x	x	
C4-9			LH1406030B4-05	x	x	x	x	

Ploidy	Treatment	Sample code	Plant code	Photosynthesis			
				PSII	ETR	IC	OJIP
	Stress	S4-11	LH1406030B4-19	x	x	x	x
		S4-14	LH1406030B2-02	x	x	x	
		S4-14	LH1406030B2-02	x			x
		S4-16	LH1406030B5-05	x			x
		S4-2	LH1406030B1-04	x		x	
		S4-20	LH1406030B5-13	x			x
		S4-21	LH1406030B5-18	x	x	x	
		S4-22	LH1406030B5-20	x			
		S4-23	LH1406030B4-10	x	x	x	x
		S4-24	LH1406030G1-8	x			x
		S4-25	LH1406030G1-16		x	x	x
		S4-26	LH1406030G1-18		x	x	
		S4-27	LH1406030B5-04	x			
		S4-4	LH1406030B2-01	x			x
		S4-5	LH1406030B2-07	x	x	x	
		S4-6	LH1406030B4-01		x	x	x
		S4-8	LH1406030B4-11	x	x	x	
6x clone 29	Control	C6-1	29/15-3N/02	x	x		
		C6-12	29/15-5K/21	x	x	x	x
		C6-5	29/15-5K/02	x	x	x	x
		C6-6	29/15-5K/05	x	x	x	x
		C6-7	29/15-5K/09	x	x	x	x
	Stress	S6-39	29/15-5K/20	x	x	x	x
		S6-9	29/15-5K/06	x	x	x	x
S6-1		29/15-5K/03	x	x	x	x	
6x clone 35	Control	C6-15	35/28-4*/26	x			x
		C6-16	35/28-4*/28	x	x	x	x
		C6-22	35/28-4a/16	x			x
		C6-23	35/28-4*/27		x	x	x
		C6-25	35/28-4a/22	x	x	x	x
		C6-33	35/28-4Q/82	x	x		x
		C6-15	35/28-4*/26	x	x	x	
	Stress	S6-17	35/28-4*/03	x	x	x	x
		S6-19	35/28-4*/18	x	x	x	x
		S6-21	35/28-4*/24		x	x	x
		S6-22	35/28-4*/22			x	
		S6-24	35/28-4*/26		x	x	x
		S6-25	35/28-4*/40		x	x	x
		S6-29	35/28-4Q/27	x		x	
		S6-33	35/28-4Q/28	x		x	
S6-37	35/28-4a/40			x	x		

**Table S2.** Formulae and definitions of terms used in photosynthesis parameters (Strasser and Govindjee, 1992; Strasser et al., 2004; Baker, 2008; Tsimilli-Michael and Strasser, 2013; Lazár, 2015; Rusaczoněk et al., 2015)

Parameter formula	Explanation
$\phi_{PSII} = F^V/F^M$	PSII maximum efficiency
$QY_{max} = F_v/F_M$	maximum quantum efficiency of PSII photochemistry
$ETR = \phi_{PSII} \times PPFD \times 0.5$	Electron transport rate; PPFD: Photosynthetic photon flux density
Fluorescence quenching analysis of induction curve	
$PQ = (F_M/F(t)) - (F_M/F^M)$	Photochemical quenching (PQ)
$NPQ = (F_M/F^M)/F^M$	Non-photochemical quenching (NPQ)
$qE = (F^M - F^V)/F^M$	Energy-dependent non-photochemical quenching coefficient
$qI = 1 - (F^V/F_V)$	Photoinhibitory non-photochemical quenching coefficient
$NPQE = (F_M/F^M) - (F_M/F^M)$	Energy-dependent non-photochemical quenching coefficient
$NPQI = (F_V/F^V) - 1$	Photoinhibitory non-photochemical quenching coefficient
$qP = \Delta F / (F^M - F^0)$	coefficient of photochemical quenching
$qN = (F^M - F^0)/F_v$	Non-photochemical quenching coefficient
$qL = ((F^M - F(t))/(F^M - F^0)) \times (F^0/F(t))$	Estimates the fraction of "open" PSII centers (lake model)
JIP-test parameter	
$F_0 = F_{50\mu s}$	Fluorescence intensity at 50 $\mu s$
$F_j$	Fluorescence intensity at J-step (at 2ms)
$F_i$	Fluorescence intensity at I-step (at 30 ms)
$F_M$	Maximum fluorescence intensity
$F_v = F_M - F_0$	Maximal variable fluorescence
$F_M/F_0$	Ratio of fluorescence
$F_V/F_0$	Efficiency of the oxygen-evolving complex
Area	Area between fluorescence curve and $F_M$ (background subtracted)
Fix.Area	Area below the fluorescence curve between $F_{20\mu s}$ and $F_1s$ (background subtracted)
$M_0 = TR_0/RC - ET_0/RC = 4 (F_{300} - F_0) / (F_M - F_0)$	Approximated initial slope (in $ms^{-1}$ ) of the fluorescence transient normalized on the maximal variable fluorescence $F_V$
$SM = Area / (F_M - F_0)$	The normalized area above the OJIP curve
$S_s$	The smallest SM turn-over (single turn-over)
$N = SM \times M_0 \times (1/V_j)$	Turn-over number QA
$\Phi_{iP_0} = 1 - (F_0/F_M)$ (or $F_V/F_M$ )	Maximum quantum yield of primary photochemistry
$V_i = (F_i - F_0)/(F_M - F_0)$	Relative variable fluorescence at the I-step
$V_j = (F_j - F_0)/(F_M - F_0)$	Relative variable fluorescence at the J-step
$\Phi_{iD_0} = 1 - \Phi_{iP_0} - (F_0 - F_M)$	Quantum yield of energy dissipation
$\Phi_{iE_0} = (1 - (F_0/F_M)) \times \Psi_{i_0}$	Quantum yield of electron transport at time zero
$\Phi_{iP_0} = 1 - (F_0/F_M)$ (or $F_V/F_M$ )	Maximum quantum yield of primary photochemistry

Parameter formula	Explanation
$\Psi_0 = 1 - V_j$	Probability that a trapped exciton moves an electron into the electron transport chain beyond QA-
$\Phi_{Pav} = \Phi_{P0} (SM/tFM)$ tFM = time to reach Fm (in ms)	Time to reach maximum chlorophyll fluorescence level (in ms)
Specific energy fluxes (per active PSII):	
$ABS/RC = (M0/V_j)/\Phi_{P0}$	Absorption flux per reaction center (RC) (apparent antenna size of an active PSII)
$TR0/RC = M0/V_j$	Trapped energy flux per RC
$ET0/RC = (M0/V_j) \times \Psi_0$	Electron transport flux per reaction center (RC)
$DI0/RC = ABS/RC - TR0/RC$	Dissipated energy flux per reaction center (RC)
$PI_{Abs} = (RC/ABS) \times \Phi_{P0}/(1 - \Phi_{P0}) \times \Psi_0/(1 - \Psi_0)$	Performance index on absorption basis related to the overall photosynthetic activity of PSII

## References:

- Baker, N.R. (2008). Chlorophyll fluorescence: a probe of photosynthesis in vivo. *Annu. Rev. Plant Biol.* 59, 89-113.
- Lazár, D. (2015). Parameters of photosynthetic energy partitioning. *Journal of Plant Physiology* 175, 131-147.
- Rusaczonok, A., Czarnocka, W., Kacprzak, S., Witoń, D., Ślesak, I., Szechyńska-Hebda, M., et al. (2015). Role of phytochromes A and B in the regulation of cell death and acclimatory responses to UV stress in *Arabidopsis thaliana*. *Journal of experimental botany* 66(21), 6679-6695.
- Strasser, R.J., and Govindjee (1992). "The Fo and the O-J-I-P Fluorescence Rise in Higher Plants and Algae," in *Regulation of Chloroplast Biogenesis*, ed. J.H. Argyroudi-Akoyunoglou. (Boston, MA: Springer US), 423-426.
- Strasser, R.J., Tsimilli-Michael, M., and Srivastava, A. (2004). "Analysis of the chlorophyll a fluorescence transient," in *Chlorophyll a fluorescence*. Springer), 321-362.
- Tsimilli-Michael, M., and Strasser, R.J. (2013). The energy flux theory 35 years later: formulations and applications. *Photosynthesis research* 117(1), 289-320.

**Table S3.** Summary statistics of PSII maximum efficiency ( $\Phi$ PSII) and maximum quantum efficiency of PSII photochemistry (QY\_max) between treatment and among different ploidies and hexaploid clones. n = number of measurements from 9 -14 individual per group.

Ploidy	Treatment	$\Phi$ PSII				QY_max			
		n	mean	sd	median	n	mean	sd	median
2x	Control	130	0.721	0.028	0.729	30	0.819	0.03	0.83
	Stress	131	0.710	0.027	0.713	30	0.816	0.015	0.817
4x	Control	121	0.707	0.024	0.710	30	0.823	0.016	0.825
	Stress	99	0.700	0.037	0.711	30	0.817	0.021	0.82
6x_29	Control	45	0.720	0.026	0.725	13	0.828	0.009	0.83
	Stress	33	0.722	0.031	0.725	9	0.808	0.027	0.811
6x_35	Control	55	0.628	0.068	0.631	16	0.705	0.08	0.702
	Stress	60	0.675	0.041	0.675	21	0.664	0.088	0.642

**Table S4.** Summary of generalized linear mixed models analysis for change in PSII maximum efficiency ( $\Phi$ PSII) to factors treatment and ploidy level (hexaploid separated in to two clones).

	<b>Estimate</b>	<b>Std. Error</b>	<b>z value</b>	<b>Pr(&gt; z )</b>	
Intercept	0.94215	0.03053	30.859	<0.000001	***
Stress treatment	-0.04569	0.04318	-1.058	0.29	
4x	-0.06073	0.04337	-1.400	0.161	
6x_29	0.00058	0.05910	0.010	0.992	
6x_35	-0.46562	0.05185	-8.980	<0.0000001	***
Stress:4x	-0.00401	0.06045	-0.066	0.947	
Stress:6x_29	0.05802	0.08860	0.655	0.513	
Stress:6x_35	0.30527	0.07169	4.258	0.00002	***

**Table S5.** Pairwise comparison of PSII maximum efficiency ( $\Phi$ PSII) among different ploidies and hexaploid clones of each treatment. Significant results are in bold.

Contrast		Control				Stress			
		estimate	SE	t.ratio	p.value	estimate	SE	t.ratio	p.value
2x	4x	0.06	0.04	1.40	0.85050	0.06	0.04	1.54	0.77740
2x	6x_29	0.00	0.06	-0.01	1.00000	-0.06	0.07	-0.89	0.98630
2x	6x_35	0.47	0.05	8.98	<.0001	0.16	0.05	3.24	0.02570
4x	6x_29	-0.06	0.06	-1.04	0.96710	-0.12	0.07	-1.89	0.54690
4x	6x_35	0.40	0.05	7.78	<.0001	0.10	0.05	1.97	0.49150
6x_29	6x_35	0.47	0.07	7.10	<.0001	0.22	0.07	3.11	0.03810

**Table S6.** Summary of generalized linear mixed model analysis for change in maximum quantum efficiency of PSII photochemistry (QY\_max) to factors treatment and ploidy level (hexaploid separated in to two clones).

	<b>Estimate</b>	<b>Std. Error</b>	<b>z value</b>	<b>Pr(&gt; z )</b>	
Intercept	1.52182	0.05718	26.61300	<0.000001	***
Stress treatment	-0.03586	0.08185	-0.43800	0.66100	
4x	0.01244	0.08201	0.15200	0.87900	
6x_29	0.03794	0.10358	0.36600	0.71400	
6x_35	-0.64995	0.09362	-6.94200	0.00000	***
Stress:4x	0.00751	0.11378	0.06600	0.94700	
Stress:6x_29	-0.08429	0.15974	-0.52800	0.59800	
Stress:6x_35	-0.12520	0.12657	-0.98900	0.32300	



**Table S7.** Pairwise comparisons of QY\_max among different ploidy levels and hexaploid clones of each treatment. Significant results are in bold.

Contrast		Control					Stress				
		estimate	SE	df	t.ratio	p.value	estimate	SE	df	t.ratio	p.value
2x	4x	-0.01	0.08	169	-0.15	1.000	-0.02	0.08	169	-0.25	1.000
2x	6x_29	-0.04	0.10	169	-0.37	1.000	0.05	0.12	169	0.38	1.000
2x	6x_35	0.65	0.09	169	6.94	<.0001	0.78	0.09	169	9.10	<.0001
4x	6x_29	-0.03	0.10	169	-0.24	1.000	0.07	0.12	169	0.56	0.999
4x	6x_35	0.40	0.05	664	7.78	<.0001	0.80	0.08	169	9.78	<.0001
6x_29	6x_35	0.66	0.09	169	7.00	<.0001	0.73	0.12	169	5.92	<.0001

**Table S8.** Pairwise comparison of relative electron transport rate among different ploidy and hexaploid clones of each treatment under different light intensities (10-500). Significant results (p adj. signif.) are in bold.

PPFD	Ploidy		Control			Stress		
			statistic	p	p.adj.signif	statistic	p	p.adj.signif
10	2x	4x	68.000	0.185	1.0000	57.500	0.322	1.0000
	2x	6x_29	28.500	0.711	1.0000	26.500	0.062	0.3710
	2x	6x_35	45.000	0.017	0.1000	50.000	0.003	<b>0.0160</b>
	4x	6x_29	17.000	0.357	1.0000	23.000	0.093	0.5560
	4x	6x_35	34.500	0.269	1.0000	45.000	0.003	<b>0.0190</b>
	6x_29	6x_35	24.000	0.020	0.1180	14.000	0.067	0.4010
20	2x	4x	63.500	0.324	1.0000	43.500	0.934	1.0000
	2x	6x_29	27.500	0.805	1.0000	27.000	0.050	0.3020
	2x	6x_35	46.000	0.012	0.0710	50.000	0.003	<b>0.0160</b>
	4x	6x_29	15.000	0.242	1.0000	24.000	0.060	0.3620
	4x	6x_35	45.000	0.016	0.0970	45.000	0.003	<b>0.0190</b>
	6x_29	6x_35	25.000	0.011	0.0670	15.000	0.036	0.2150
50	2x	4x	67.000	0.211	1.0000	56.500	0.366	1.0000
	2x	6x_29	34.500	0.267	1.0000	24.500	0.123	0.7380
	2x	6x_35	47.000	0.008	0.0500	50.000	0.003	<b>0.0150</b>
	4x	6x_29	20.000	0.577	1.0000	22.500	0.110	0.6600
	4x	6x_35	47.000	0.008	<b>0.0490</b>	45.000	0.003	<b>0.0190</b>
	6x_29	6x_35	25.000	0.012	0.0700	15.000	0.036	0.2140
100	2x	4x	66.500	0.225	1.0000	55.500	0.412	1.0000
	2x	6x_29	37.500	0.140	0.8400	22.500	0.233	1.0000
	2x	6x_35	43.000	0.032	0.1900	46.500	0.010	0.0590
	4x	6x_29	24.000	0.951	1.0000	19.500	0.303	1.0000
	4x	6x_35	45.500	0.014	0.0850	44.500	0.004	<b>0.0240</b>
	6x_29	6x_35	25.000	0.012	0.0700	15.000	0.036	0.2140
300	2x	4x	82.000	0.017	0.1010	76.000	0.012	0.0730
	2x	6x_29	30.500	0.539	1.0000	17.500	0.732	1.0000
	2x	6x_35	40.000	0.075	0.4500	41.000	0.054	0.3260
	4x	6x_29	2.000	0.006	<b>0.0330</b>	0.000	0.016	0.0930
	4x	6x_35	21.500	0.708	1.0000	22.000	1.000	1.0000
	6x_29	6x_35	24.500	0.016	0.0940	15.000	0.035	0.2080
500	2x	4x	82.500	0.015	0.0910	78.000	0.008	<b>0.0460</b>
	2x	6x_29	25.000	1.000	1.0000	5.500	0.117	0.7020
	2x	6x_35	32.500	0.387	1.0000	34.500	0.264	1.0000
	4x	6x_29	0.000	0.003	<b>0.0160</b>	0.000	0.016	0.0940
	4x	6x_35	3.500	0.010	0.0580	8.500	0.070	0.4180
	6x_29	6x_35	24.000	0.019	0.1150	15.000	0.035	0.2080

**Table S9.** Summary statistics and *P*- values of Wilcoxon-Mann-Whitney-Test for determination of effects of prolonged photoperiod on induction curves parameters between treatments. **S-C**: proportion of alternation of the mean value, calculated as  $(\text{Stress} - \text{Control})/(\text{Stress} + \text{Control}) \times 100$ . Significant results are in **bold**

Parameter	Ploidy	Control treatment (C)			Stress treatment (C)			S-C	p
		n	mean	sd	n	mean	sd		
Fv	2x	10	11770	2725.722	10	12189.4	1169.17	1.75	0.912
	4x	10	12835.5	2900.151	10	11953.8	1696.967	-3.56	0.165
	6x_29	4	14050.25	1202.819	3	14311.67	779.973	0.92	1
	6x_35	4	9874	3098.879	9	9624.778	2099.756	-1.28	0.94
Fv'	2x	10	6605.592	2261.851	10	5403.539	1376.386	-10.01	0.165
	4x	10	5423.215	2000.658	10	4496.728	1119.035	-9.34	0.218
	6x_29	4	9071.828	1417.599	3	7190.53	506.356	-11.57	0.229
	6x_35	4	3878.085	2756.17	9	3279.352	1252.866	-8.37	0.94
Fv''	2x	10	9854.2	2627.07	10	10056	1379.529	1.01	0.623
	4x	10	9522.3	2394.021	10	9224.7	1420.841	-1.59	0.436
	6x_29	4	12358	921.55	3	12436	673.143	0.31	1
	6x_35	4	7547	3681.889	9	7168.222	1717.041	-2.57	0.825
F(t)	2x	10	5085.4	1422.407	10	4500.6	954.277	-6.10	0.247
	4x	10	5098.8	1740.582	10	4129.4	752.516	-10.50	0.0892
	6x_29	4	7709.25	1707.153	3	6413.333	476.708	-9.18	0.229
	6x_35	4	4896.75	2058.913	9	4542	741.238	-3.76	0.71
F0	2x	10	2698.9	655.178	10	2718	231.407	0.35	0.705
	4x	10	2622.1	582.257	10	2693.3	467.979	1.34	1
	6x_29	4	2801.75	118.829	3	3278.667	44.106	7.84	0.0571
	6x_35	4	4114.75	1468.216	9	4352	987.434	2.80	0.71
F0'	2x	10	2389.208	522.211	10	2310.361	256.488	-1.68	0.481
	4x	10	2206.885	479.607	10	2180.172	331.323	-0.61	0.579
	6x_29	4	2605.422	132.82	3	2877.47	66.768	4.96	0.0571
	6x_35	4	2920.165	486.316	9	3112.537	556.611	3.19	0.71
F0''	2x	10	2959.2	776.997	10	2965.1	324.253	0.10	0.912
	4x	10	3137.7	718.385	10	3030.5	521.163	-1.74	0.307
	6x_29	4	3280	29.439	3	3675.333	54.501	5.68	0.0571
	6x_35	4	4325	804.503	9	4726.222	935.938	4.43	0.604
FM	2x	10	14468.9	3023.335	10	14907.4	1255.799	1.49	1
	4x	10	15457.6	3457.08	10	14647.1	1985.781	-2.69	0.241
	6x_29	4	16852	1295.326	3	17590.33	808.047	2.14	0.629
	6x_35	4	13988.75	2801.748	9	13976.78	1935.453	-0.04	0.817
FM'	2x	10	8994.8	2502.283	10	7713.9	1574.58	-7.67	0.143
	4x	10	7630.1	2339.183	10	6676.9	1275.26	-6.66	0.247
	6x_29	4	11677.25	1523.304	3	10068	570.071	-7.40	0.229
	6x_35	4	6798.25	2672.861	9	6391.889	1322.82	-3.08	0.825

Parameter	Ploidy	Control treatment (C)			Stress treatment (C)			S-C	p
		n	mean	sd	n	mean	sd		
FM''	2x	10	12813.4	3032.888	10	13021.1	1587.794	0.80	0.796
	4x	10	12660	3036.018	10	12255.2	1678.656	-1.62	0.315
	6x_29	4	15638	920.906	3	16111.33	681.414	1.49	0.629
	6x_35	4	11872	3116.23	9	11894.44	1568.051	0.09	0.643
$\Delta F$	2x	10	3909.4	1204.87	10	3213.3	740.585	-9.77	0.112
	4x	10	2531.3	713.406	10	2547.5	643.174	0.32	1
	6x_29	4	3968	568.674	3	3654.667	99.485	-4.11	0.857
	6x_35	4	1901.5	678.819	9	1849.889	655.695	-1.38	1
NPQ	2x	10	0.654	0.213	10	0.99	0.347	20.44	0.0185
	4x	10	1.102	0.39	10	1.241	0.376	5.93	0.631
	6x_29	4	0.451	0.088	3	0.753	0.173	25.08	0.0571
	6x_35	4	1.164	0.451	9	1.237	0.381	3.04	0.71
PQ	2x	10	1.263	0.238	10	1.425	0.276	6.03	0.218
	4x	10	1.093	0.296	10	1.358	0.218	10.81	0.0524
	6x_29	4	0.789	0.248	3	1.004	0.147	11.99	0.629
	6x_35	4	0.856	0.214	9	0.869	0.111	0.75	0.71
$q_E$	2x	10	0.45	0.178	10	0.728	0.289	23.60	0.0147
	4x	10	0.698	0.244	10	0.869	0.269	10.91	0.123
	6x_29	4	0.35	0.108	3	0.605	0.149	26.70	0.0571
	6x_35	4	0.801	0.225	9	0.889	0.18	5.21	0.414
$q_I$	2x	10	0.172	0.057	10	0.178	0.057	1.71	0.912
	4x	10	0.263	0.06	10	0.229	0.052	-6.91	0.19
	6x_29	4	0.12	0.015	3	0.131	0.005	4.38	0.4
	6x_35	4	0.258	0.171	9	0.256	0.085	-0.39	0.71
NPQ <sub>E</sub>	2x	10	0.512	0.198	10	0.838	0.33	24.15	0.0232
	4x	10	0.871	0.33	10	1.044	0.349	9.03	0.315
	6x_29	4	0.375	0.109	3	0.662	0.167	27.68	0.0571
	6x_35	4	0.962	0.294	9	1.06	0.289	4.85	0.604
NPQ <sub>I</sub>	2x	10	0.213	0.092	10	0.222	0.093	2.07	0.912
	4x	10	0.365	0.11	10	0.302	0.086	-9.45	0.19
	6x_29	4	0.136	0.02	3	0.151	0.006	5.23	0.4
	6x_35	4	0.419	0.409	9	0.359	0.156	-7.71	0.71
$q_P$	2x	10	0.601	0.065	10	0.6	0.05	-0.08	0.0433
	4x	10	0.486	0.075	10	0.569	0.049	7.87	0.529
	6x_29	4	0.447	0.095	3	0.509	0.023	6.49	0.912
	6x_35	4	0.569	0.149	9	0.573	0.069	0.35	0.00893
$q_N$	2x	10	0.481	0.117	10	0.593	0.101	10.43	0.629
	4x	10	0.611	0.139	10	0.669	0.099	4.53	0.825
	6x_29	4	0.371	0.055	3	0.524	0.061	17.09	0.0571
	6x_35	4	0.776	0.268	9	0.802	0.153	1.65	0.604

Parameter	Ploidy	Control treatment (C)			Stress treatment (C)			S-C	p
		n	mean	sd	n	mean	sd		
<i>qL</i>	2x	10	0.299	0.097	10	0.317	0.057	2.92	0.353
	4x	10	0.226	0.069	10	0.306	0.059	15.04	0.0147
	6x_29	4	0.16	0.057	3	0.23	0.023	17.95	0.0571
	6x_35	4	0.397	0.202	9	0.402	0.101	0.63	0.71

**Table S10.** Pairwise comparison of inductive curve parameters in different treatments. Significant results are in bold.

Parameter	group1	group2	Control			Stress		
			statistic	p	p.adj	statistic	p	p.adj
NPQ	2x	4x	13	0.00400	<b>0.02300</b>	31	0.16500	0.99000
	2x	6x_29	32	0.10600	0.63600	21	0.37100	1.00000
	2x	6x_35	5	0.03600	0.21600	27	0.15600	0.93600
	4x	6x_29	36	0.02400	0.14400	28	0.02800	0.16800
	4x	6x_35	18	0.83900	1.00000	44	0.96800	1.00000
	6x_29	6x_35	0	0.02900	0.17200	2	0.03600	0.21800
PQ	2x	4x	67	0.21800	1.00000	64	0.31500	1.00000
	2x	6x_29	40	0.00200	<b>0.01200</b>	27	0.04900	0.29400
	2x	6x_35	38	0.00800	<b>0.04800</b>	84	0.00065	<b>0.00400</b>
	4x	6x_29	35	0.03600	0.21600	27	0.04900	0.29400
	4x	6x_35	29	0.24000	1.00000	86	0.00026	<b>0.00200</b>
	6x_29	6x_35	5	0.48600	1.00000	20	0.28200	1.00000
$q_E$	2x	4x	18	0.01500	0.08800	29	0.12300	0.73800
	2x	6x_29	27	0.37400	1.00000	17	0.81100	1.00000
	2x	6x_35	3	0.01400	0.08400	25	0.11300	0.67800
	4x	6x_29	36	0.02400	0.14400	25	0.11200	0.67200
	4x	6x_35	15	0.53900	1.00000	35	0.44700	1.00000
	6x_29	6x_35	0	0.02900	0.17200	2	0.03600	0.21800
$q_I$	2x	4x	14	0.00500	<b>0.03100</b>	22	0.03500	0.21300
	2x	6x_29	34	0.05400	0.32300	24	0.16100	0.96600
	2x	6x_35	12	0.30400	1.00000	21	0.05400	0.32100
	4x	6x_29	40	0.00200	<b>0.01200</b>	30	0.00700	<b>0.04200</b>
	4x	6x_35	26	0.45400	1.00000	37	0.54900	1.00000
	6x_29	6x_35	2	0.11400	0.68400	2	0.03600	0.21800
NPQ <sub>E</sub>	2x	4x	13	0.00400	<b>0.02300</b>	30	0.14300	0.85800
	2x	6x_29	28	0.30400	1.00000	20	0.46900	1.00000
	2x	6x_35	5	0.03600	0.21600	23	0.07900	0.47300
	4x	6x_29	36	0.02400	0.14400	28	0.02800	0.16800
	4x	6x_35	16	0.63500	1.00000	39	0.66100	1.00000
	6x_29	6x_35	0	0.02900	0.17200	2	0.03600	0.21800
NPQ <sub>I</sub>	2x	4x	14	0.00500	<b>0.03100</b>	22	0.03500	0.21300
	2x	6x_29	34	0.05400	0.32300	24	0.16100	0.96600
	2x	6x_35	12	0.30400	1.00000	21	0.05400	0.32100
	4x	6x_29	40	0.00200	<b>0.01200</b>	30	0.00700	<b>0.04200</b>
	4x	6x_35	26	0.45400	1.00000	37	0.54900	1.00000
	6x_29	6x_35	2	0.11400	0.68400	2	0.03600	0.21800
$q_P$	2x	4x	88	0.00300	<b>0.01700</b>	66	0.24700	1.00000
	2x	6x_29	40	0.00200	<b>0.01200</b>	27	0.04900	0.29400
	2x	6x_35	21	0.94500	1.00000	54	0.49700	1.00000
	4x	6x_29	24	0.63500	1.00000	26	0.07700	0.46100
	4x	6x_35	9	0.14200	0.85200	38	0.60400	1.00000

Parameter	group1	group2	Control			Stress		
			statistic	p	p.adj	statistic	p	p.adj
<i>qN</i>	2x	4x	21	0.02900	0.17300	33	0.21800	1.00000
	2x	6x_29	31	0.14200	0.85200	22	0.28700	1.00000
	2x	6x_35	5	0.03600	0.21600	11	0.00400	<b>0.02500</b>
	4x	6x_29	36	0.02400	0.14400	28	0.02800	0.16800
	4x	6x_35	10	0.18800	1.00000	24	0.09500	0.56800
	6x_29	6x_35	0	0.02900	0.17200	1	0.01800	0.10900
<i>qL</i>	2x	4x	68	0.19000	1.00000	60	0.48100	1.00000
	2x	6x_29	35	0.03600	0.21600	28	0.02800	0.16800
	2x	6x_35	12	0.30400	1.00000	22	0.06500	0.39200
	4x	6x_29	32	0.10600	0.63600	27	0.04900	0.29400
	4x	6x_35	9	0.14200	0.85200	22	0.06500	0.39200
	6x_29	6x_35	3	0.20000	1.00000	2	0.03600	0.21800

**Table S11.** Summary statistics and *P*- values of Wilcoxon-Mann-Whitney-Test for determination of effects of prolonged photoperiod on JIP-test parameters between treatments. Summary statistic of treatment. **S-C**: proportion of alternation of the mean value, calculated as  $(\text{Stress} - \text{Control})/(\text{Stress} + \text{Control}) * 100$ . Significant results are in bold.

Parameter	Group	Control treatment			Stress treatment			S-C	p
		n	mean	sd	n	mean	sd		
V <sub>i</sub>	2x	10	0.715	0.031	10	0.764	0.021	3.313	0.00105
	4x	10	0.792	0.025	11	0.792	0.045	0.000	0.80500
	6x_29	4	0.748	0.018	3	0.759	0.041	0.730	1.00000
	6x_35	7	0.741	0.077	7	0.687	0.11	-3.782	0.31800
V <sub>j</sub>	2x	10	0.382	0.033	10	0.41	0.036	3.535	0.12300
	4x	10	0.396	0.051	11	0.412	0.085	1.980	0.83300
	6x_29	4	0.418	0.036	3	0.394	0.043	-2.956	0.62900
	6x_35	7	0.462	0.053	7	0.447	0.057	-1.650	0.62000
F <sub>M</sub> /F <sub>0</sub>	2x	10	5.71	0.425	10	5.228	0.326	-4.407	0.00893
	4x	10	5.602	0.295	11	5.448	0.587	-1.394	0.65400
	6x_29	4	5.656	0.188	3	5.597	0.497	-0.524	0.85700
	6x_35	7	3.848	1.03	7	2.991	1.051	-12.531	0.12800
F <sub>v</sub> /F <sub>0</sub>	2x	10	4.71	0.425	10	4.228	0.326	-5.393	0.00893
	4x	10	4.602	0.295	11	4.448	0.587	-1.702	0.65400
	6x_29	4	4.656	0.188	3	4.597	0.497	-0.638	0.85700
	6x_35	7	2.848	1.03	7	1.991	1.051	-17.710	0.12800
F <sub>v</sub> /F <sub>M</sub>	2x	10	0.824	0.013	10	0.808	0.012	-0.980	0.01260
	4x	10	0.821	0.009	11	0.815	0.021	-0.367	0.67200
	6x_29	4	0.823	0.006	3	0.82	0.015	-0.183	0.85700
	6x_35	7	0.724	0.072	7	0.633	0.111	-6.706	0.11000
M <sub>0</sub>	2x	10	0.601	0.092	10	0.695	0.095	7.253	0.03550
	4x	10	0.65	0.125	11	0.643	0.205	-0.541	0.86000
	6x_29	4	0.694	0.072	3	0.63	0.151	-4.834	0.85700
	6x_35	7	0.935	0.225	7	1.043	0.229	5.460	0.45600
Area	2x	10	11413795	1795993	10	10500268	1472647	-4.169	0.39300
	4x	10	9861305	1895808	11	7946877	3442061	-10.750	0.38700
	6x_29	4	10785254	2097474	3	11355959	590010.4	2.578	0.40000
	6x_35	7	15959414	8015471	7	24223637	14561164	20.566	0.80500
Fix.Area	2x	10	27204510	2434725	10	25168040	3171928	-3.888	0.28000
	4x	10	30394650	2801993	11	22873332	9660293	-14.120	0.00479
	6x_29	4	26113779	3276642	3	26233125	1841156	0.228	0.62900
	6x_35	7	30091663	3752652	7	22856067	7499010	-13.666	0.05300
Sm	2x	10	499.066	100.227	10	504.429	50.166	0.534	0.57900
	4x	10	391.935	96.541	11	385.584	109.357	-0.817	0.65400
	6x_29	4	488.675	65.249	3	515.18	12.911	2.640	0.40000
	6x_35	7	753.133	511.619	7	2034.586	1436.457	45.968	0.25900
Ss	2x	10	0.643	0.052	10	0.594	0.035	-3.961	0.01720
	4x	10	0.616	0.042	11	0.665	0.093	3.825	0.17300
	6x_29	4	0.604	0.028	3	0.641	0.094	2.972	0.85700
	6x_35	7	0.508	0.079	7	0.444	0.096	-6.723	0.25900



Parameter	Group	Control treatment			Stress treatment			S-C	p
		n	mean	sd	n	mean	sd		
N	2x	10	777.587	151.779	10	850.901	98.376	4.502	0.07530
	4x	10	634.705	138.84	11	593.303	170.98	-3.371	0.91800
	6x_29	4	810.54	112.543	3	813.34	99.779	0.172	1.00000
	6x_35	7	1585.056	1294.919	7	5217.227	4045.185	53.396	0.31800
Phi_Po	2x	10	0.824	0.013	10	0.808	0.012	-0.980	0.01260
	4x	10	0.821	0.009	11	0.815	0.021	-0.367	0.67200
	6x_29	4	0.823	0.006	3	0.82	0.015	-0.183	0.85700
	6x_35	7	0.724	0.072	7	0.633	0.111	-6.706	0.11000
Psi_0	2x	10	0.617	0.033	10	0.59	0.036	-2.237	0.12300
	4x	10	0.604	0.051	11	0.588	0.085	-1.342	0.83300
	6x_29	4	0.582	0.036	3	0.606	0.043	2.020	0.62900
	6x_35	7	0.538	0.053	7	0.553	0.057	1.375	0.62000
Phi_E0	2x	10	0.509	0.029	10	0.477	0.034	-3.245	0.02560
	4x	10	0.496	0.044	11	0.48	0.08	-1.639	0.69800
	6x_29	4	0.479	0.032	3	0.497	0.042	1.844	0.62900
	6x_35	7	0.392	0.068	7	0.348	0.056	-5.946	0.25000
Phi_Pav	2x	10	930.326	9.949	10	939.887	4.589	0.511	0.01850
	4x	10	937.974	8.581	11	928.619	32.596	-0.501	0.91800
	6x_29	4	936.878	9.82	3	943.21	6.593	0.337	0.40000
	6x_35	7	940	8.907	7	948.514	12.36	0.451	0.20900
Phi_D0	2x	10	0.176	0.013	10	0.192	0.012	4.348	0.01260
	4x	10	0.179	0.009	11	0.185	0.021	1.648	0.67200
	6x_29	4	0.177	0.006	3	0.18	0.015	0.840	0.85700
	6x_35	7	0.276	0.072	7	0.367	0.111	14.152	0.11000
ABS/RC	2x	10	1.902	0.181	10	2.09	0.154	4.709	0.01400
	4x	10	1.987	0.162	11	1.885	0.29	-2.634	0.38700
	6x_29	4	2.017	0.099	3	1.931	0.295	-2.178	0.85700
	6x_35	7	2.714	0.756	7	3.866	1.399	17.508	0.10500
DI0/RC	2x	10	0.336	0.052	10	0.403	0.054	9.066	0.01150
	4x	10	0.356	0.045	11	0.354	0.087	-0.282	0.86300
	6x_29	4	0.357	0.028	3	0.35	0.078	-0.990	0.62900
	6x_35	7	0.867	0.551	7	1.545	0.905	28.109	0.12800
TR0/RC	2x	10	1.566	0.134	10	1.688	0.102	3.749	0.01470
	4x	10	1.631	0.12	11	1.572	0.251	-1.842	0.42600
	6x_29	4	1.659	0.073	3	1.582	0.219	-2.376	0.85700
	6x_35	7	2	0	7	2.393	0.434	8.946	0.00372
ET0/RC	2x	10	0.964	0.067	10	0.992	0.047	1.431	0.21200
	4x	10	0.981	0.057	11	0.886	0.081	-5.088	0.00365
	6x_29	4	0.965	0.071	3	0.952	0.079	-0.678	1.00000
	6x_35	7	0.987	0.023	7	1.301	0.331	13.724	0.01870
Pi_Abs	2x	10	4.121	1.014	10	3.005	0.786	-15.661	0.02880
	4x	10	3.696	1.044	11	3.99	2.502	3.825	1.00000
	6x_29	4	3.267	0.65	3	3.909	1.715	8.946	0.85700
	6x_35	7	1.41	0.949	7	0.787	0.645	-28.357	0.12400

**Table S12.** Pairwise comparison of JIP-test parameters in different treatments. Significant results are in bold.

Parameter	group1	group2	Control			Stress		
			statistic	p	p.adj	statistic	p	p.adj
ABS/RC	2x	4x	36	0.31500	1.00000	81	0.07200	0.26700
	2x	6x_29	12	0.30400	1.00000	18	0.67200	1.00000
	2x	6x_35	6	0.00500	<b>0.03100</b>	6	0.00500	<b>0.02700</b>
	4x	6x_29	14	0.45400	1.00000	15	0.88500	1.00000
	4x	6x_35	12	0.02700	0.13600	3.5	0.00200	<b>0.01100</b>
	6x_29	6x_35	9	0.38600	1.00000	2	0.06700	0.26700
DI <sub>0</sub> /RC	2x	4x	39.5	0.45000	1.00000	76	0.15200	0.45600
	2x	6x_29	15	0.53900	1.00000	20	0.46900	0.93800
	2x	6x_35	3	0.00072	<b>0.00400</b>	0	0.00010	<b>0.00052</b>
	4x	6x_29	16	0.63500	1.00000	15	0.88500	0.93800
	4x	6x_35	5	0.00200	<b>0.01000</b>	0	0.00006	<b>0.00038</b>
	6x_29	6x_35	3	0.04200	0.17000	0	0.01700	0.06700
TR <sub>0</sub> /RC	2x	4x	33	0.21800	0.65400	77	0.13200	0.39600
	2x	6x_29	12	0.30400	0.65400	17	0.81100	1.00000
	2x	6x_35	0	0.00049	<b>0.00300</b>	0	0.00010	<b>0.00062</b>
	4x	6x_29	14	0.45400	0.65400	16	1.00000	1.00000
	4x	6x_35	0	0.00049	<b>0.00300</b>	0.5	0.00068	<b>0.00300</b>
	6x_29	6x_35	0	0.00300	<b>0.01300</b>	0	0.01700	0.06700
ET <sub>0</sub> /RC	2x	4x	41.5	0.54500	1.00000	99	0.00200	<b>0.01100</b>
	2x	6x_29	22	0.83900	1.00000	19	0.55400	0.62200
	2x	6x_35	22	0.21700	1.00000	13.5	0.04000	0.16100
	4x	6x_29	23	0.73300	1.00000	9.5	0.31100	0.62200
	4x	6x_35	32	0.80500	1.00000	3	0.00044	<b>0.00300</b>
	6x_29	6x_35	8	0.27600	1.00000	3	0.11700	0.35100
Pi_Abs	2x	4x	59	0.52900	1.00000	44	0.46800	1.00000
	2x	6x_29	29	0.24000	0.72000	11	0.57300	1.00000
	2x	6x_35	68	0.00200	<b>0.00900</b>	69	0.00021	<b>0.00100</b>
	4x	6x_29	25	0.53900	1.00000	16	1.00000	1.00000
	4x	6x_35	68	0.00200	<b>0.00900</b>	73	0.00075	<b>0.00400</b>
	6x_29	6x_35	26	0.02900	0.11800	21	0.01700	0.06700

## Chapter 4: Discussion

In this thesis, I had obtained better insights into the role of polyploidy in the complex environmental stress of the photoperiod alternation that contributed to the physiological process of photosynthesis, hence concomitant to reproductive mode. Even though the present study is not complete in any way to deal with the various issues of plant evolution related to polyploidy, the model plants of facultative apomictic *R. auricomus* complex with three cytotype levels (diploid, tetraploid, and hexaploid) presented the role of polyploidy in buffering light stress. Results indicated a higher stress sensitivity of diploids as observed in ovule development and photosynthetic organ but a lesser stress effect in tetraploid and a stronger stress-tolerance in hexaploids. The establishment of apomixis seed development is complex. It involves three components: apomeiosis (formation of unreduced embryo sac), parthenogenesis (embryo development without fertilization of egg cell), and functional endosperm development (Nogler, 1984a; Kaushal et al., 2018). The photoperiod stress only affected the apomeiosis but not the later stages.

### 4.1 Mode of ovule formation

The comprehensive investigation of ovule development with cytological analysis of a total of 6505 ovules from the three cytotypes *R. auricomus* complex has shown the typical Polygonum type embryo sac and at a similar timing. In the sexual ovule, during megasporogenesis, the meiotic division of a megaspore mother cell produced four cells (megaspore tetrad), in which only one remains to develop into a functional megaspore, while the other three aborted. At megagametogenesis, the functional megaspore enlarged with the presence of vacuoles and continued with three times of nuclear division, producing a total of eight nuclei of embryo sac structure. On the other hand, in the asexual ovule, at megasporogenesis, one or more aposporous initial cell/s developed from an enlarged somatic cell near to functional megaspore. The aposporous cell grows faster than the megaspore and takes over the embryo sac development (Hojsgaard et al., 2014a). Under microscopic analysis, the hexaploids ovule presented a bigger cell size compared to tetraploids, while diploids presented the smaller size of the structure. Having a bigger cell size confers at least three consequences, i.e., first, increasing volume decreases surface area, which could impact cell signaling on limiting oxidative damage; second, impact on mechanical properties; and third, pertaining to the size of intracellular structure, e.g., spindle which contributes to cell division (Schoenfelder and Fox, 2015). The alternation of spindle structure in polyploid yeast leads to the increase of errors of chromosome segregation during the cell division process (Storchová et al., 2006). In reproductive tissues, polyploids release apomeiosis as a strategy to circumvent the unbalanced chromosomal segregation (Hojsgaard, 2018). Another study on disoriented

chromosomes during microsporogenesis in diploid and allopolyploid *R. auricomus* among cytotype is presented in (Barke et al., 2020). Further study on megasporogenesis will provide a clearer understanding of factors triggering apomixis.

The cytological analysis also discriminated the alternation of the proportions of sexual and asexual ovule between the treatments and showed the sign of buffering stress in the establishment of apomixis in polyploids. The prolonged photoperiod might cause the accumulation of reactive oxygen species (ROS) in the flower buds, which trigger oxidative stress (Klatt et al., 2016; Abuelsoud et al., 2020) e.g., as indicated by the accumulation of lipid peroxidation (Nitschke et al., 2016). In facultative apomixis, apomeiosis and meiotic cell division are regulated by metabolites that are related to ROS scavenging (Mateo de Arias et al., 2020). In diploids of *R. auricomus*, the 16.5 h photoperiod was categorized as a mild abiotic stressor that mobilized the meiotic DNA repair system in the megaspore mother cell and triggered meiosis and megasporogenesis (Hörandl and Hadacek, 2013). The proportion of sexual ovules was 80.4 % or c.a. 19.6 % apospory were observed in diploids synthetic hybrid, and this related to the low frequency of natural diploid apomixis. A recent flow cytometric seed screening study reported the frequency of 1% of diploid apomictic seed in *R. auricomus* from temperate Europe (Karbstein et al., 2021).

On the other hand, in tetraploids and hexaploids, probably due to the better ROS scavenging (Deng et al., 2012; Wei et al., 2019), the oxidative stress from the same photoperiod treatment might be less strong to induce the DNA double strand breaks (Hörandl and Hadacek, 2013), and consequently meiosis and megasporogenesis might be disturbed and released apomeiosis that occupies embryo sac development. An example study on allopolyploids of *Glycine dolichocarpa* addressed the better light stress-tolerance compared to the diploid relatives indicated by the alternation of non-photochemical quenching followed by ROS scavenging (Coate et al., 2013). This result is correlated to our finding that polyploids regulated a stress buffer on NPQ parameters (Chapter 2). Nevertheless, metabolites analysis addressing the ROS scavenging among cytotypes will be immensely supporting our assumption.

The advantages of gene redundancy (more DNA repair templates) of polyploids protect the DNA from stress (Schoenfelder and Fox, 2015); hence a higher dosage of stress would be required to break the DNA as a consequence of buffering stress in polyploids (Hörandl and Hadacek, 2013). Polyploidy, on the other hand, challenges proper gene regulation by epigenetic disability due to the interaction between parental genomes (Comai, 2005). The high variation of the proportions of sexual ovules among individual of polyploids compared to diploids follow the assumption of the epigenetic mechanism as the background of phenotypic

expression (Grimanelli, 2012; Schmidt et al., 2014). A similar pattern was reported from the same genus in *Ranunculus kuepferi* (Schinkel et al., 2020). Overall, the result of cytological analysis of ovule development supports the hypothesis of ploidy dependent-effects on the phenotypic feature of apomixis in angiosperms (Delgado et al., 2016; Kaushal et al., 2018) and under epigenetic regulation (Rodrigo et al., 2017).

## 4.2 Mode of seed formation

Mode of seed formation was analyzed with flow cytometry seed screening (FCSS) to a total of 14068 viable seeds from 83 individuals among three cytotypes growing in control and stress photoperiod. Hexaploids developed a bigger seed size, but diploids produced a higher quantity of seed set compared to polyploids. Nevertheless, high abortion rate of seeds compared to the rate of ovule formation was observed in all cytotypes and was still within the range (30 – 60 %) of similar studies in *R. auricomus* (Izmailow, 1996; Hörandl, 2008; Hörandl and Temsch, 2009; Klatt et al., 2016; Barke et al., 2018). The seed quantity is also related to the pollen quality. In Apomictic seed, the embryo development was independent of the male genome (parthenogenesis). But for endosperm development, the contribution of male gamete is essential (Pseudogamy) (Nogler, 1984a). The better quality of pollen of diploids and hexaploids was followed by a higher seed set, while in tetraploids, the lower pollen quality was also followed by a lower seed set. However, a high variation of pollen quality was reported in apomictic plants (Asker and Jerling, 1992). Our result revealed a neutral effect of photoperiod on the pollen quality and concomitant with the seed quality.

The formation of the viable seeds of *R. auricomus* requires the contribution of male gamete to fertilize the central nuclei for the development of endosperm. The FCSS results revealed that a low number of autonomous (poolen-independent) seeds (less than 10 seed per cytotype) were formed in all cytotypes, and that means almost all *R. auricomus*'s seeds developed pseudogamously. The lower number of apomictic seeds in diploids was related to their sensitivity to the genomic imprinting; a constant ratio 2:1 for maternal (m) and paternal (p) genome contributed to the endosperm (Spielman et al., 2003; Vinkenoog et al., 2003). This imprinting factor contributed to the reduction of the number of putative apomictic seeds in diploids growing under control treatment. In contrast, polyploids presented a lower number of sexual seeds but a higher number of apomictic pseudogamous seeds, and a conspicuous number of B<sub>III</sub> hybrids in tetraploids. The formation of pseudogamous endosperm is predominant in apomictic plants (Mogie, 1992). The relaxation of genomic imprinting in polyploids was suggested due to the epigenetic mutation during endosperm development (Kaushal et al., 2018) and addressing the better seed set of hexaploids compared to tetraploid as observed in this study and another study of *Potentilla puberula* (Dobeš et al., 2018). The

presence of  $B_{III}$  hybrids was suggested either by the longer receptivity of egg cell in tetraploids as reported in the synthetic hybrid of *R. auricomus* (Barke et al., 2018) or by the hybridity contribution on the establishment of apomixis (Schinkel, 2019).

The peak index (PI) of FCSS indicated the DNA content in embryo and endosperm and represented the mode of seed development (Klatt et al., 2016; Schinkel et al., 2016; Barke et al., 2018). In the sexual seed of diploids, the reduced egg cell (1m) is fertilized by a reduced sperm (1p) producing embryo with a set of the chromosome [1(m)+1(p)], whereas in endosperm, the two reduced polar nuclei (1m+1m) are fertilized by a reduced sperm cell (1p) producing endosperm [1(m)+1(m)+1(p)]. Within these set chromosomes in a seed, the PI value 1.5 indicated that the seed developed sexually. While in apomictic seed, PI value is 2.0, 2.5, 3.0 depending on the contribution of pollen nuclei to endosperm. The FCSS revealed that photoperiod treatments did not alter the development of the seeds of *R. auricomus*. The seeds of diploid plants generally developed sexually with a lower amount of apomictic seeds (3 seeds in total). In contrast, polyploids developed their seeds asexually (> 90% seeds). The lower sexual seed formation in polyploids indicated a higher aborting rate of meiotic megaspores and replacement by apomeiosis that completed the megagametogenesis. The development of sexual ovules was less competitive compared to the development of aposporous embryo sac (AES) during seed development (Hojsgaard et al., 2013; Klatt et al., 2016; Hodač et al., 2019). In aposporous embryo sac, the unreduced egg cell develops parthenogenetically (without fertilization with sperm nucleus) into an embryo, while the unreduced polar nuclei develop pseudogamously (fertilized by a sperm cell/s) into endosperm. The dominance of apomictic seed formation in polyploids in this study is in line with the general observation that apomixis mostly occurs in polyploid plants with the presence of a lower number in diploids, supporting the hypothesis that polyploidy facilitates the establishment of apomixis (Hojsgaard and Hörandl, 2019).

### 4.3 Photoprotective mechanisms

Alternation on the mode of ovule formation was influenced by mid stress effect from prolonged photoperiod. The presence of light stress effects in *R. auricomus* was observed by measurement of photosynthesis performance with Chlorophyll a fluorescent as a proxy of photoprotection mechanisms. Measurements were conducted in the first basal leaf that appeared with flower buds. The plant generates mechanism to avoid damage from light stress via movement of chloroplasts, change in leaf area and leaf angle, adjustment of antenna size, regulation of thermal dissipation, and scavenging reactive oxygen species to prevent oxidative stress (Takahashi and Murata, 2008; Murchie and Niyogi, 2011). The thermal dissipation can be measured as quenching of chlorophyll fluorescence with the common term of non-

photochemical quenching (NPQ) (Baker, 2008). From NPQ measurements, several parameters can be extracted to get the insight of energy dependence quenching ( $q_E$ ), photoinhibition of photosynthesis ( $q_I$ ), quenching coefficient by non-photochemical process ( $q_N$ ), photochemical coefficient quenching ( $q_P$ ), and quenching of NPQ during illumination ( $q_L$ ) (Lazár, 2015).

Prolonged photoperiod (16.5 h) led to light excess and influenced the photosynthesis performance of diploids and tetraploids. Diploids were more sensitive to stress compared to polyploids, as indicated by the alternation of non-photochemical quenching parameters ( $q_I$  and  $q_N$ ). Tetraploids experienced a lesser stress effect as indicated by an alternation of  $q_P$  and  $q_L$  parameters which means the light excess is quenched by photochemistry, and the fraction of light is dissipated into heat (Lazár, 2015).

The photosynthesis performance also observed by fast chlorophyll a fluorescence transient which provides that the fluorescence rise is related to the closure of some PSII reaction centers (Kalaji et al., 2016); the parameters of performance index on absorption basis (PI\_Abs) represent the sum of structural and functional criteria of absorption flux per reaction center (ABS/RC), trapped energy flux per RC (TR<sub>0</sub>/RC), electron transport flux per reaction center (ET<sub>0</sub>/RC), and Dissipated energy flux per reaction center (DI<sub>0</sub>/RC) (Brestic and Zivcak, 2013; Stirbet et al., 2018). The stress altered the performance index on an absorption basis in diploids. In diploids, the light stress influenced the antenna membrane resulted in a massive closure of the PSII reaction centers (ABS/RC), reduced the capacity of photon trapping (ET<sub>0</sub>/RC), and increased the photon dissipation (DI<sub>0</sub>/RC). In tetraploids, the lesser stress level might not have affected the antenna molecule in the photosynthetic membrane, but the fraction of light exceeding the capacity of photon trapping (ET<sub>0</sub>/RC), hence dissipated into non-photochemical quenching ( $q_L$ ).

The three cytotypes of *R. auricomus* had been raised from seedling in garden conditions and kept in cultivated for several years (Horandl et al., 1997; Paun et al., 2006; Hodač et al., 2014; Hojsgaard et al., 2014a; Barke et al., 2018), but their photosynthesis activity still followed the pre-adaptation to habitats of their mother plants from natural sites as observed in relative electron transport rate curves and photosynthesis efficiency parameters. The light intensity of our climatic chamber, i.e., c.a. 250  $\mu\text{mol photons m}^{-2} \text{s}^{-1}$  provided optimal condition to the plants as indicated by the absence of photoinhibition in all three cytotypes, except for hexaploid clone 35 as indicated by parameter PSII maximum efficiency ( $\phi_{\text{PSII}}$ ) and maximum quantum efficiency of PSII photochemistry (QY<sub>max</sub>). Measurement of relative electron curves revealed that diploids and hexaploid clone 29 were more adaptive to a wide range of light intensity. On the other hand, tetraploids performed better photosynthesis under lower

light intensity (below 300  $\mu\text{mol photons m}^{-2} \text{ s}^{-1}$  at PPF), whereas hexaploid clone 35 performed better photosynthesis under higher light intensity (more than 300  $\mu\text{mol photons m}^{-2} \text{ s}^{-1}$  at PPF). The contrasts of photosynthesis capacity of hexaploid clones might be related to the high level of heterozygosity in polyploidy, as reported recently (Karbstein et al., 2021). The advantage of heterozygosity is the potential for diversifying the gene function by altering redundant copies of important or essential genes (Comai, 2005). An example was presented in tetraploid *Glycine max* with overexpression of oxidative stress-regulating genes compared to the diploid progenitors, which correlated to differential photosynthetic performance and adaptation to higher light intensities (Coate et al., 2012). Epigenetic studies on polyploids of *R. auricomus* will be beneficial to combine the current result with the phenotypic variation among hexaploid clones and among cytotypes. In diploid and tetraploid *R. kuepferi* a study on cytosin-methylation indicated different epigenetic profiles within cytotype and between habitats (Schinkel et al., 2020).



## References

- Abuelsoud, W., Cortleven, A., and Schumling, T. (2020). Photoperiod stress alters the cellular redox status and is associated with an increased peroxidase and decreased catalase activity. *bioRxiv*. doi: 10.1101/2020.03.05.978270.
- Acuña-Rodríguez, I.S., Newsham, K.K., Gundel, P.E., Torres-Díaz, C., and Molina-Montenegro, M.A. (2020). Functional roles of microbial symbionts in plant cold tolerance. *Ecology Letters* 23(6), 1034-1048. doi: <https://doi.org/10.1111/ele.13502>.
- Alix, K., Gérard, P.R., Schwarzacher, T., and Heslop-Harrison, J.S. (2017). Polyploidy and interspecific hybridization: partners for adaptation, speciation and evolution in plants. *Annals of Botany* 120(2), 183-194. doi: 10.1093/aob/mcx079.
- Aliyu, O.M., Schranz, M.E., and Sharbel, T.F. (2010). Quantitative variation for apomictic reproduction in the genus *Boechera* (Brassicaceae). *American Journal of Botany* 97(10), 1719-1731.
- Anneberg, T.J., and Segraves, K.A. (2019). Intraspecific polyploidy correlates with colonization by arbuscular mycorrhizal fungi in *Heuchera cylindrica*. *American Journal of Botany* 106(6), 894-900. doi: <https://doi.org/10.1002/ajb2.1294>.
- Asker, S.E., and Jerling, L. (1992). *Apomixis in plants*. CRC Press.
- Baker, N.R. (2008). Chlorophyll fluorescence: a probe of photosynthesis in vivo. *Annu. Rev. Plant Biol.* 59, 89-113. doi: 10.1146/annurev.arplant.59.032607.092759.
- Baniaga, A.E., Marx, H.E., Arrigo, N., and Barker, M.S. (2020). Polyploid plants have faster rates of multivariate niche differentiation than their diploid relatives. *Ecology Letters* 23(1), 68-78. doi: <https://doi.org/10.1111/ele.13402>.
- Barke, B.H., Daubert, M., and Hörandl, E. (2018). Establishment of Apomixis in Diploid F2 Hybrids and Inheritance of Apospory From F1 to F2 Hybrids of the *Ranunculus auricomus* Complex. *Frontiers in Plant Science* 9(1111). doi: 10.3389/fpls.2018.01111.
- Barke, B.H., Karbstein, K., Daubert, M., and Hörandl, E. (2020). The relation of meiotic behaviour to hybridity, polyploidy and apomixis in the *Ranunculus auricomus* complex (Ranunculaceae). *BMC Plant Biology* 20(1), 523. doi: 10.1186/s12870-020-02654-3.
- Bauerle, W.L., Oren, R., Way, D.A., Qian, S.S., Stoy, P.C., Thornton, P.E., et al. (2012). Photoperiodic regulation of the seasonal pattern of photosynthetic capacity and the implications for carbon cycling. *Proceedings of the National Academy of Sciences* 109(22), 8612-8617. doi: 10.1073/pnas.1119131109.
- Bicknell, R.A., and Koltunow, A.M. (2004). Understanding apomixis: recent advances and remaining conundrums. *The Plant Cell* 16(suppl 1), S228-S245. doi: 10.1105/tpc.017921.
- Bicknell, R.A., Lambie, S.C., and Butler, R.C. (2003). Quantification of progeny classes in two facultatively apomictic accessions of *Hieracium*. *Hereditas* 138(1), 11-20. doi: 10.1034/j.1601-5223.2003.01624.x.
- Björkman, O., and Demmig, B. (1987). Photon yield of O<sub>2</sub> evolution and chlorophyll fluorescence characteristics at 77 K among vascular plants of diverse origins. *Planta* 170(4), 489-504. doi: 10.1007/BF00402983.
- Bolker, B., and Bolker, M.B. (2020). " Package 'bbmle'. Tools for General Maximum Likelihood Estimation, 641
- Bordenave, C.D., Rocco, R., Maiale, S.J., Campestre, M.P., Ruiz, O.A., Rodríguez, A.A., et al. (2019). Chlorophyll a fluorescence analysis reveals divergent photosystem II responses to saline, alkaline and saline-alkaline stresses in the two *Lotus japonicus*

- model ecotypes MG20 and Gifu-129. *Acta Physiologiae Plantarum* 41(9), 1-13. doi: 10.1007/s11738-019-2956-0.
- Brestic, M., and Zivcak, M. (2013). PSII fluorescence techniques for measurement of drought and high temperature stress signal in crop plants: protocols and applications. *Molecular stress physiology of plants*, 87-131. doi: 10.1007/978-81-322-0807-5.
- Brochmann, C., Brysting, A.K., Alsos, I.G., Borgen, L., Grundt, H.H., Scheen, A.-C., et al. (2004). Polyploidy in arctic plants. *Biological Journal of the Linnean Society* 82(4), 521-536. doi: 10.1111/j.1095-8312.2004.00337.x.
- Brooks, M.E., Kristensen, K., van Benthem, K.J., Magnusson, A., Berg, C.W., Nielsen, A., et al. (2017). glmmTMB balances speed and flexibility among packages for zero-inflated generalized linear mixed modeling. *The R journal* 9(2), 378-400. doi: 10.32614/RJ-2017-066.
- Carillo, P., Arena, C., Modarelli, G.C., De Pascale, S., and Paradiso, R. (2019). Photosynthesis in *Ranunculus asiaticus* L.: the influence of the hybrid and the preparation procedure of tuberous roots. *Frontiers in plant science* 10, 241. doi: 10.3389/fpls.2019.00241.
- Carman, J.G. (1997). Asynchronous expression of duplicate genes in angiosperms may cause apomixis, bispory, tetraspory, and polyembryony. *Biological Journal of the Linnean Society* 61(1), 51-94.
- Carman, J.G., Mateo de Arias, M., Gao, L., Zhao, X., Kowallis, B.M., Sherwood, D.A., et al. (2019). Apospory and Diplospory in Diploid *Boechea* (Brassicaceae) May Facilitate Speciation by Recombination-Driven Apomixis-to-Sex Reversals. *Frontiers in Plant Science* 10(724). doi: 10.3389/fpls.2019.00724.
- Chao, D.-Y., Dilkes, B., Luo, H., Douglas, A., Yakubova, E., Lahner, B., et al. (2013). Polyploids exhibit higher potassium uptake and salinity tolerance in Arabidopsis. *Science* 341(6146), 658-659.
- Çiçek, N., Kalaji, H.M., and Ekmekçi, Y. (2020). Special issue in honour of Prof. Reto J. Strasser—Probing the photosynthetic efficiency of some European and Anatolian Scots pine populations under UV-B radiation using polyphasic chlorophyll a fluorescence transient. *Photosynthetica* 58(SPECIAL ISSUE), 468-478. doi: 10.32615/ps.2019.151.
- Coate, J.E., Luciano, A.K., Seralathan, V., Minchew, K.J., Owens, T.G., and Doyle, J.J. (2012). Anatomical, biochemical, and photosynthetic responses to recent allopolyploidy in *Glycine dolichocarpa* (Fabaceae). *American Journal of Botany* 99(1), 55-67. doi: doi.org/10.3732/ajb.1100465.
- Coate, J.E., Powell, A.F., Owens, T.G., and Doyle, J.J. (2013). Transgressive physiological and transcriptomic responses to light stress in allopolyploid *Glycine dolichocarpa* (Leguminosae). *Heredity* 110(2), 160-170. doi: 10.1038/hdy.2012.77.
- Comai, L. (2005). The advantages and disadvantages of being polyploid. *Nature reviews genetics* 6(11), 836.
- Cosendai, A.-C., and Hörandl, E. (2010). Cytotype stability, facultative apomixis and geographical parthenogenesis in *Ranunculus kuepferi* (Ranunculaceae). *Annals of Botany* 105(3), 457-470.
- D'Ambrosio, N., Guadagno, C., and De Santo, A.V. (2008). Is qE always the major component of non-photochemical quenching? *Photosynthesis. Energy from the sun*, 1001-1004. doi: 10.1007/978-1-4020-6709-9\_218.
- de Castro, K.M., Batista, D.S., Fortini, E.A., Silva, T.D., Felipe, S.H.S., Fernandes, A.M., et al. (2019). Photoperiod modulates growth, morphoanatomy, and linalool content in *Lippia*

- alba* L.(Verbenaceae) cultured in vitro. *Plant Cell, Tissue and Organ Culture (PCTOC)* 139(1), 139-153. doi: 10.1007/s11240-019-01672-w.
- De Storme, N., and Geelen, D. (2014). The impact of environmental stress on male reproductive development in plants: biological processes and molecular mechanisms. *Plant, Cell & Environment* 37(1), 1-18. doi: <https://doi.org/10.1111/pce.12142>.
- del Pozo, J.C., and Ramirez-Parra, E. (2014). Deciphering the molecular bases for drought tolerance in *Arabidopsis* autotetraploids. *Plant, Cell & Environment* 37(12), 2722-2737.
- Delgado, L., Sartor, M.E., Espinoza, F., Soliman, M., Galdeano, F., and Ortiz, J.P.A. (2016). Hybridity and autopolyploidy increase the expressivity of apospory in diploid *Paspalum rufum*. *Plant Systematics and Evolution* 302(10), 1471-1481. doi: 10.1007/s00606-016-1345-z.
- Demmig-Adams, B., and Adams III, W.W. (2006). Photoprotection in an ecological context: the remarkable complexity of thermal energy dissipation. *New Phytologist* 172(1), 11-21. doi: 10.1111/j.1469-8137.2006.01835.x.
- Deng, B., Du, W., Liu, C., Sun, W., Tian, S., and Dong, H. (2012). Antioxidant response to drought, cold and nutrient stress in two ploidy levels of tobacco plants: low resource requirement confers polytolerance in polyploids? *Plant Growth Regulation* 66(1), 37-47. doi: 10.1007/s10725-011-9626-6.
- Dobeš, C., Scheffknecht, S., Fenko, Y., Prohaska, D., Sykora, C., and Hülber, K. (2018). Asymmetric reproductive interference: The consequences of cross-pollination on reproductive success in sexual–apomictic populations of *Potentilla puberula* (Rosaceae). *Ecology and evolution* 8(1), 365-381.
- Doyle, J.J., and Coate, J.E. (2019). Polyploidy, the Nucleotype, and Novelty: The Impact of Genome Doubling on the Biology of the Cell. *International Journal of Plant Sciences* 180(1), 1-52. doi: 10.1086/700636.
- Duarte, B., Gössling, J.W., Marques, J., and Caçador, I. (2015). Ecophysiological constraints of *Aster tripolium* under extreme thermal events impacts: merging biophysical, biochemical and genetic insights. *Plant Physiology and Biochemistry* 97, 217-228. doi: 10.1016/j.plaphy.2015.10.015.
- Elkins, C., and van Iersel, M.W. (2020). Longer photoperiods with the same daily light integral improve growth of *Rudbeckia* seedlings in a greenhouse. *HortScience* 1(aop), 1-7. doi: 10.21273/HORTSCI15200-20.
- Evans, L., and Knox, R. (1969). Environmental control of reproduction in *Themeda australis*. *Australian Journal of Botany* 17(3), 375-389.
- Ferrari, S., and Cribari-Neto, F. (2004). Beta regression for modelling rates and proportions. *Journal of applied statistics* 31(7), 799-815. doi: 10.1080/0266476042000214501.
- Fortini, E.A., Batista, D.S., de Castro, K.M., Silva, T.D., Felipe, S.H.S., Correia, L.N.F., et al. (2020). Photoperiod modulates growth and pigments and 20-hydroxyecdysone accumulation in Brazilian ginseng *Pfaffia glomerata* (Spreng.) Pedersen] grown in vitro. *Plant Cell, Tissue and Organ Culture (PCTOC)* 142(3), 595-611. doi: 10.1007/s11240-020-01886-3.
- Foyer, C.H., and Noctor, G. (2009). Redox regulation in photosynthetic organisms: signaling, acclimation, and practical implications. *Antioxidants & redox signaling* 11(4), 861-905.
- Fréchette, E., Chang, C.Y.-Y., and Ensminger, I. (2016). Photoperiod and temperature constraints on the relationship between the photochemical reflectance index and the light use efficiency of photosynthesis in *Pinus strobus*. *Tree physiology* 36(3), 311-324. doi: 10.1093/treephys/tpv143.

- Gao, L. (2018). *Pharmacologically Induced Meiosis Apomeiosis Interconversions in Boechea, Arabidopsis and Vigna*. Doctor of Philosophy (PhD) Dissertation, Utah State University.
- Genty, B., Briantais, J.-M., and Baker, N.R. (1989). The relationship between the quantum yield of photosynthetic electron transport and quenching of chlorophyll fluorescence. *Biochimica et Biophysica Acta (BBA)-General Subjects* 990(1), 87-92. doi: 10.1016/S0304-4165(89)80016-9.
- Ghashghaie, G.C.J., Genty, B., and Briantais, J. (1992). Leaf photosynthesis is resistant to a mild drought stress. *Photosynthetica* 27(3), 295-309. doi: 10.1007/0-306-48135-9\_14.
- Godfree, R.C., Marshall, D.J., Young, A.G., Miller, C.H., and Mathews, S. (2017). Empirical evidence of fixed and homeostatic patterns of polyploid advantage in a keystone grass exposed to drought and heat stress. *Royal Society open science* 4(11), 170934.
- Gounaris, E., Sherwood, R., Gounaris, I., Hamilton, R., and Gustine, D. (1991). Inorganic salts modify embryo sac development in sexual and aposporous *Cenchrus ciliaris*. *Sexual Plant Reproduction* 4(3), 188-192.
- Grant, V. (1981). "Plant speciation". Columbia University Press).
- Grimanelli, D. (2012). Epigenetic regulation of reproductive development and the emergence of apomixis in angiosperms. *Current Opinion in Plant Biology* 15(1), 57-62. doi: <https://doi.org/10.1016/j.pbi.2011.10.002>.
- Grimanelli, D., Hernández, M., Perotti, E., and Savidan, Y. (1997). Dosage effects in the endosperm of diplosporous apomictic *Tripsacum* (Poaceae). *Sexual Plant Reproduction* 10(5), 279-282.
- Gururani, M.A., Venkatesh, J., and Tran, L.S.P. (2015). Regulation of photosynthesis during abiotic stress-induced photoinhibition. *Molecular plant* 8(9), 1304-1320. doi: 10.1016/j.molp.2015.05.005.
- Halliwell, B. (2006). Reactive species and antioxidants. Redox biology is a fundamental theme of aerobic life. *Plant physiology* 141(2), 312-322.
- Hand, M.L., and Koltunow, A.M. (2014). The genetic control of apomixis: asexual seed formation. *Genetics* 197(2), 441-450.
- Hannweg, K., Steyn, W., and Bertling, I. (2016). In vitro-induced tetraploids of *Plectranthus esculentus* are nematode-tolerant and have enhanced nutritional value. *Euphytica* 207(2), 343-351. doi: 10.1007/s10681-015-1547-4.
- Harms, N., Shearer, J., Cronin, J.T., and Gaskin, J.F. (2020). Geographic and genetic variation in susceptibility of *Butomus umbellatus* to foliar fungal pathogens. *Biological Invasions* 22(2), 535-548. doi: 10.1007/s10530-019-02109-3.
- Hartig, F., and Hartig, M.F. (2017). "Package 'DHARMA'". 0.4.1. <https://cran.r-project.org/web/packages/DHARMA/vignettes/DHARMA.html>
- Hias, N., Leus, L., Davey, M.W., Vanderzande, S., Van Huylenbroeck, J., and Keulemans, J. (2017). Effect of polyploidization on morphology in two apple (*Malus domestica*) genotypes. *Horticultural Science* 44(2), 55-63.
- Hodač, L., Klatt, S., Hojsgaard, D., Sharbel, T.F., and Hörandl, E. (2019). A little bit of sex prevents mutation accumulation even in apomictic polyploid plants. *BMC evolutionary biology* 19(1), 1-11.
- Hodač, L., Scheben, A.P., Hojsgaard, D., Paun, O., and Hörandl, E. (2014). ITS Polymorphisms Shed Light on Hybrid Evolution in Apomictic Plants: A Case Study on the *Ranunculus auricomus* Complex. *PLOS ONE* 9(7), e103003. doi: 10.1371/journal.pone.0103003.

- Hojsgaard, D. (2018). Transient Activation of Apomixis in Sexual Neotriploids May Retain Genomically Altered States and Enhance Polyploid Establishment. *Frontiers in Plant Science* 9(230). doi: 10.3389/fpls.2018.00230.
- Hojsgaard, D., Greilhuber, J., Pellino, M., Paun, O., Sharbel, T.F., and Hörandl, E. (2014a). Emergence of apospory and bypass of meiosis via apomixis after sexual hybridisation and polyploidisation. *New Phytologist* 204(4), 1000-1012. doi: 10.1111/nph.12954.
- Hojsgaard, D., and Hörandl, E. (2019). The Rise of Apomixis in Natural Plant Populations. *Frontiers in plant science* 10, 358-358. doi: 10.3389/fpls.2019.00358.
- Hojsgaard, D., Klatt, S., Baier, R., Carman, J.G., and Hörandl, E. (2014b). Taxonomy and biogeography of apomixis in angiosperms and associated biodiversity characteristics. *Critical Reviews in Plant Sciences* 33(5), 414-427.
- Hojsgaard, D.H., Martínez, E.J., and Quarin, C.L. (2013). Competition between meiotic and apomictic pathways during ovule and seed development results in clonality. *New Phytologist* 197(1), 336-347.
- Hörandl, E. (1998). Species concepts in agamic complexes: Applications in the *Ranunculus auricomus* complex and general perspectives. *Folia Geobotanica* 33(3), 335-348. doi: 10.1007/BF03216210.
- Hörandl, E. (2008). Evolutionary implications of self-compatibility and reproductive fitness in the apomictic *Ranunculus auricomus* polyploid complex (ranunculaceae). *International journal of plant sciences* 169(9), 1219-1228. doi: 10.1086/591980.
- Hörandl, E., Dobes, C., and Lambrou, M. (1997). Chromosome and pollen studies on Austrian species of the apomictic *Ranunculus auricomus* complex. *Botanica Helvetica* 107(2), 195-209.
- Hörandl, E., Greilhuber, J., Klímová, K., Paun, O., Temsch, E., Emadzade, K., et al. (2009). Reticulate evolution and taxonomic concepts in the *Ranunculus auricomus* complex (Ranunculaceae): insights from analysis of morphological, karyological and molecular data. *Taxon* 58(4), 1194-1216. doi: 10.1002/tax.584012.
- Hörandl, E., and Hadacek, F. (2013). The oxidative damage initiation hypothesis for meiosis. *Plant reproduction* 26(4), 351-367.
- Hörandl, E., and Temsch, E.M. (2009). Introgression of apomixis into sexual species is inhibited by mentor effects and ploidy barriers in the *Ranunculus auricomus* complex. *Annals of Botany* 104(1), 81-89.
- Huang, H., Ullah, F., Zhou, D.-X., Yi, M., and Zhao, Y. (2019). Mechanisms of ROS regulation of plant development and stress responses. *Frontiers in Plant Science* 10.
- Iannicelli, J., Guariniello, J., Tossi, V.E., Regalado, J.J., Di Ciaccio, L., Van Baren, C.M., et al. (2020). The "polyploid effect" in the breeding of aromatic and medicinal species. *Scientia Horticulturae* 260, 108854. doi: 10.1016/j.scienta.2019.108854.
- Izmailow, R. (1996). Reproductive strategy in the *Ranunculus auricomus* complex (Ranunculaceae). *Acta Societatis Botanicorum Poloniae* 65(1-2), 167-170.
- Jackson, S.D. (2009). Plant responses to photoperiod. *New Phytologist* 181(3), 517-531. doi: 10.1111/j.1469-8137.2008.02681.x.
- Jeong, S., and Clark, S.E. (2005). Photoperiod regulates flower meristem development in *Arabidopsis thaliana*. *Genetics* 169(2), 907-915. doi: 10.1534/genetics.104.033357.
- Jiang, J., Yuan, Y., Zhu, S., Fang, T., Ran, L., Wu, J., et al. (2019). Comparison of physiological and methylational changes in resynthesized *Brassica napus* and diploid progenitors under drought stress. *Acta Physiologiae Plantarum* 41(4), 45.

- Juranić, M., Tucker, M.R., Schultz, C.J., Shirley, N.J., Taylor, J.M., Spriggs, A., et al. (2018). Asexual female gametogenesis involves contact with a sexually-fated megaspore in apomictic *Hieracium*. *Plant physiology* 177(3), 1027-1049. doi: 10.1104/pp.18.00342.
- Kalaji, H.M., Jajoo, A., Oukarroum, A., Brestic, M., Zivcak, M., Samborska, I.A., et al. (2016). Chlorophyll a fluorescence as a tool to monitor physiological status of plants under abiotic stress conditions. *Acta Physiologiae Plantarum* 38(4), 102. doi: 10.1007/s11738-016-2113-y.
- Karbstein, K., Tomasello, S., Hodač, L., Lorberg, E., Daubert, M., and Hörandl, E. (2021). Moving beyond assumptions: polyploidy and environmental effects explain a geographical parthenogenesis scenario in European plants. *Molecular Ecology*. doi: 10.1111/mec.15919.
- Karunarathne, P., Reutemann, A.V., Schedler, M., Glücksberg, A., Martínez, E.J., Honfi, A.I., et al. (2020). Sexual modulation in a polyploid grass: a reproductive contest between environmentally inducible sexual and genetically dominant apomictic pathways. *Scientific reports* 10(1), 1-14. doi: 10.1038/s41598-020-64982-6.
- Kaushal, P., Dwivedi, K.K., Radhakrishna, A., Saxena, S., Paul, S., Srivastava, M.K., et al. (2018). Ploidy dependent expression of apomixis and its components in guinea grass (*Panicum maximum* Jacq.). *Euphytica* 214(9), 152. doi: 10.1007/s10681-018-2232-1.
- Kautsky, H., and Hirsch, A. (1931). Neue Versuche zur Kohlensäureassimilation. *Naturwissenschaften* 19(48), 964-964. doi: 10.1007/BF01516164.
- Keane, O.M., Toft, C., Carretero-Paulet, L., Jones, G.W., and Fares, M.A. (2014). Preservation of genetic and regulatory robustness in ancient gene duplicates of *Saccharomyces cerevisiae*. *Genome Research* 24(11), 1830-1841.
- Keeney, S., Lange, J., and Mohibullah, N. (2014). Self-organization of meiotic recombination initiation: general principles and molecular pathways. *Annual review of genetics* 48, 187-214.
- Kinoshita, T., Kume, A., and Hanba, Y.T. (2020). Seasonal variations in photosynthetic functions of the urban landscape tree species *Ginkgo biloba*: photoperiod is a key trait. *Trees*, 1-13. doi: 10.1007/s00468-020-02033-3.
- Klatt, S., Hadacek, F., Hodač, L., Brinkmann, G., Eilerts, M., Hojsgaard, D., et al. (2016). Photoperiod extension enhances sexual megaspore formation and triggers metabolic reprogramming in facultative apomictic *Ranunculus auricomus*. *Frontiers in plant science* 7, 278.
- Klatt, S., Schinkel, C.C., Kirchheimer, B., Dullinger, S., and Hörandl, E. (2018). Effects of cold treatments on fitness and mode of reproduction in the diploid and polyploid alpine plant *Ranunculus kuepferi* (Ranunculaceae). *Annals of botany* 121(7), 1287-1298.
- Knox, R. (1967). Apomixis: seasonal and population differences in a grass. *Science* 157(3786), 325-326.
- Koltunow, A.M. (1993). Apomixis: embryo sacs and embryos formed without meiosis or fertilization in ovules. *The plant cell* 5(10), 1425. doi: 10.1105/tpc.5.10.1425.
- Koltunow, A.M., and Grossniklaus, U. (2003). Apomixis: a developmental perspective. *Annual review of plant biology* 54(1), 547-574.
- Kramer, D.M., Johnson, G., Kiirats, O., and Edwards, G.E. (2004). New fluorescence parameters for the determination of  $Q_A$  redox state and excitation energy fluxes. *Photosynthesis research* 79(2), 209-218. doi: 10.1023/B:PRES.0000015391.99477.0d.

- Krause, G., and Weis, E. (1991). Chlorophyll fluorescence and photosynthesis: the basics. *Annual review of plant biology* 42(1), 313-349. doi: 10.1146/annurev.pp.42.060191.001525.
- Landis, J.B., Soltis, D.E., Li, Z., Marx, H.E., Barker, M.S., Tank, D.C., et al. (2018). Impact of whole-genome duplication events on diversification rates in angiosperms. *American journal of botany* 105(3), 348-363. doi: 10.1002/ajb2.1060.
- Lavaud, J. (2007). Fast regulation of photosynthesis in diatoms: mechanisms, evolution and ecophysiology. *Functional Plant Science and Biotechnology*, 2 1, 267-287.
- Lazár, D. (2015). Parameters of photosynthetic energy partitioning. *Journal of Plant Physiology* 175, 131-147. doi: 10.1016/j.jplph.2014.10.021.
- Liu, B., and Sun, G. (2019). Transcriptome and miRNAs analyses enhance our understanding of the evolutionary advantages of polyploidy. *Critical reviews in biotechnology* 39(2), 173-180.
- Lourkisti, R., Froelicher, Y., Herbette, S., Morillon, R., Tomi, F., Gibernau, M., et al. (2020). Triploid citrus genotypes have a better tolerance to natural chilling conditions of photosynthetic capacities and specific leaf volatile organic compounds. *Frontiers in plant science* 11, 330. doi: 10.3389/fpls.2020.00330.
- Ma, X., Su, Z., and Ma, H. (2020). Molecular genetic analyses of abiotic stress responses during plant reproductive development. *Journal of Experimental Botany* 71(10), 2870-2885. doi: 10.1093/jxb/eraa089.
- Martínez, L.M., Fernández-Ocaña, A., Rey, P.J., Salido, T., Amil-Ruiz, F., and Manzaneda, A.J. (2018). Variation in functional responses to water stress and differentiation between natural allopolyploid populations in the *Brachypodium distachyon* species complex. *Annals of Botany* 121(7), 1369-1382. doi: 10.1093/aob/mcy037.
- Masterson, J. (1994). Stomatal Size in Fossil Plants: Evidence for Polyploidy in Majority of Angiosperms. *Science* 264(5157), 421-424. doi: 10.1126/science.264.5157.421.
- Mateo de Arias, M. (2015). *Effects of plant stress on facultative apomixis in Boechera (Brassicaceae)*. Doctor of Philosophy (PhD) Dissertation, Utah State University.
- Mateo de Arias, M., Gao, L., Sherwood, D.A., Dwivedi, K.K., Price, B.J., Jamison, M., et al. (2020). Whether gametophytes are reduced or unreduced in angiosperms might be determined metabolically. *Genes* 11(12), 1449. doi: doi.org/10.3390/genes11121449.
- Maxwell, K., and Johnson, G.N. (2000). Chlorophyll fluorescence—a practical guide. *Journal of experimental botany* 51(345), 659-668. doi: 10.1093/jexbot/51.345.659.
- Milev, N.B., and Reddy, A.B. (2015). Circadian redox oscillations and metabolism. *Trends in Endocrinology & Metabolism* 26(8), 430-437. doi: 10.1016/j.tem.2015.05.012.
- Mogie, M. (1992). *The evolution of asexual reproduction in plants*. London: Chapman and Hall.
- Mráz, P., Chrtek, J., and Šingliarová, B. (2009). Geographical parthenogenesis, genome size variation and pollen production in the arctic-alpine species *Hieracium alpinum*. *Botanica Helvetica* 119(1), 41-51.
- Müller, P., Li, X.-P., and Niyogi, K.K. (2001). Non-photochemical quenching. A response to excess light energy. *Plant physiology* 125(4), 1558-1566. doi: 10.1104/pp.125.4.1558.
- Mungoma, C. (1988). *Photoperiod sensitivity in tropical maize accessions, early inbreds, and their crosses*. Iowa State University.
- Münzbergová, Z., and Haisel, D. (2019). Effects of polyploidization on the contents of photosynthetic pigments are largely population-specific. *Photosynthesis research* 140(3), 289-299. doi: 10.1007/s11120-018-0604-y.

- Murchie, E.H., and Lawson, T. (2013). Chlorophyll fluorescence analysis: a guide to good practice and understanding some new applications. *Journal of experimental botany* 64(13), 3983-3998. doi: 10.1093/jxb/ert208.
- Murchie, E.H., and Niyogi, K.K. (2011). Manipulation of photoprotection to improve plant photosynthesis. *Plant physiology* 155(1), 86-92. doi: 10.1104/pp.110.168831.
- Nitschke, S., Cortleven, A., Iven, T., Feussner, I., Havaux, M., Riefler, M., et al. (2016). Circadian Stress Regimes Affect the Circadian Clock and Cause Jasmonic Acid-Dependent Cell Death in Cytokinin-Deficient *Arabidopsis* Plants. *The Plant Cell* 28(7), 1616-1639. doi: 10.1105/tpc.16.00016.
- Nogler, G. (1984a). "Gametophytic apomixis," in *Embryology of angiosperms*. Springer, 475-518.
- Nogler, G. (1984b). Genetics of apospory in *Ranunculus auricomus* V, Conclusions. *Bot. Helv.* 94, 411-422.
- Obata, T., and Fernie, A.R. (2012). The use of metabolomics to dissect plant responses to abiotic stresses. *Cellular and Molecular Life Sciences* 69(19), 3225-3243. doi: 10.1007/s00018-012-1091-5.
- Orians, C.M. (2000). The effects of hybridization in plants on secondary chemistry: implications for the ecology and evolution of plant–herbivore interactions. *American Journal of Botany* 87(12), 1749-1756. doi: 10.2307/2656824.
- Otto, F. (1990). "Chapter 11 DAPI Staining of Fixed Cells for High-Resolution Flow Cytometry of Nuclear DNA," in *Methods in Cell Biology*, eds. Z. Darzynkiewicz & H.A. Crissman. Academic Press), 105-110.
- Otto, S.P. (2007). The Evolutionary Consequences of Polyploidy. *Cell* 131(3), 452-462. doi: <https://doi.org/10.1016/j.cell.2007.10.022>.
- Oustric, J., Morillon, R., Ollitrault, P., Herbette, S., Luro, F., Froelicher, Y., et al. (2018). Somatic hybridization between diploid *Poncirus* and *Citrus* improves natural chilling and light stress tolerances compared with equivalent doubled-diploid genotypes. *Trees* 32(3), 883-895. doi: 10.1007/s00468-018-1682-3.
- Ozias-Akins, P., and van Dijk, P.J. (2007). Mendelian genetics of apomixis in plants. *Annu. Rev. Genet.* 41, 509-537.
- Paun, O., Greilhuber, J., Temsch, E., and Hörandl, E. (2006). Patterns, sources and ecological implications of clonal diversity in apomictic *Ranunculus carpaticola* (*Ranunculus auricomus* complex, Ranunculaceae). *Molecular ecology* 15(4), 897-910. doi: 10.1111/j.1365-294X.2006.02800.x.
- Paupière, M.J., Müller, F., Li, H., Rieu, I., Tikunov, Y.M., Visser, R.G., et al. (2017). Untargeted metabolomic analysis of tomato pollen development and heat stress response. *Plant reproduction* 30(2), 81-94. doi: 10.1007/s00497-017-0301-6.
- Porcar-Castell, A., Tyystjärvi, E., Atherton, J., Van der Tol, C., Flexas, J., Pfündel, E.E., et al. (2014). Linking chlorophyll a fluorescence to photosynthesis for remote sensing applications: mechanisms and challenges. *Journal of experimental botany* 65(15), 4065-4095. doi: 10.1093/jxb/eru191.
- Ptushenko, V.V., Ptushenko, E.A., Samoilova, O.P., and Tikhonov, A.N. (2013). Chlorophyll fluorescence in the leaves of *Tradescantia* species of different ecological groups: induction events at different intensities of actinic light. *Biosystems* 114(2), 85-97. doi: 10.1016/j.biosystems.2013.08.001.
- Quarin, C.L. (1986). Seasonal changes in the incidence of apomixis of diploid, triploid, and tetraploid plants of *Paspalum cromyorrhizon*. *Euphytica* 35(2), 515-522. doi: 10.1007/bf00021860.



- Quarin, C.L. (1999). Effect of pollen source and pollen ploidy on endosperm formation and seed set in pseudogamous apomictic *Paspalum notatum*. *Sexual Plant Reproduction* 11(6), 331-335.
- Ralph, P.J., and Gademann, R. (2005). Rapid light curves: a powerful tool to assess photosynthetic activity. *Aquatic botany* 82(3), 222-237. doi: 10.1016/j.aquabot.2005.02.006.
- Ram, Y., and Hadany, L. (2016). Condition-dependent sex: who does it, when and why? *Philosophical Transactions of the Royal Society B: Biological Sciences* 371(1706), 20150539.
- Rambaut, A. (2007). "FigTree". v1.3.1. Available: <http://tree.bio.ed.ac.uk/software/figtree/> [Accessed 2017]
- Ramsey, J., and Schemske, D.W. (1998). Pathways, mechanisms, and rates of polyploid formation in flowering plants. *Annual Review of Ecology and Systematics* 29(1), 467-501. doi: 10.1146/annurev.ecolsys.29.1.467.
- Rao, S., Tian, Y., Xia, X., Li, Y., and Chen, J. (2020). Chromosome doubling mediates superior drought tolerance in *Lycium ruthenicum* via abscisic acid signaling. *Horticulture research* 7(1), 1-18. doi: 10.1038/s41438-020-0260-1.
- Rice, A., Šmarda, P., Novosolov, M., Drori, M., Glick, L., Sabath, N., et al. (2019). The global biogeography of polyploid plants. *Nature Ecology & Evolution* 3(2), 265-273. doi: 10.1038/s41559-018-0787-9.
- Ripoll, J., Bertin, N., Bidet, L.P., and Urban, L. (2016). A user's view of the parameters derived from the induction curves of maximal chlorophyll a fluorescence: perspectives for analyzing stress. *Frontiers in plant science* 7, 1679. doi: 10.3389/fpls.2016.01679.
- Rodrigo, J.M., Zappacosta, D.C., Selva, J.P., Garbus, I., Albertini, E., and Echenique, V. (2017). Apomixis frequency under stress conditions in weeping lovegrass (*Eragrostis curvula*). *PLOS ONE* 12(4), e0175852. doi: 10.1371/journal.pone.0175852.
- Roeber, V.M., Bajaj, I., Rohde, M., Schmülling, T., and Cortleven, A. (2021). Light acts as a stressor and influences abiotic and biotic stress responses in plants. *Plant, Cell & Environment* 44(3), 645-664. doi: <https://doi.org/10.1111/pce.13948>.
- Roháček, K., Soukupová, J., and Barták, M. (2008). Chlorophyll fluorescence: a wonderful tool to study plant physiology and plant stress. *Plant Cell Compartments-Selected Topics. Research Signpost, Kerala, India*, 41-104. doi: 10.1007/s13580-014-0006-9.
- Rusaczonok, A., Czarnocka, W., Kacprzak, S., Witoń, D., Ślesak, I., Szechyńska-Hebda, M., et al. (2015). Role of phytochromes A and B in the regulation of cell death and acclimatory responses to UV stress in *Arabidopsis thaliana*. *Journal of experimental botany* 66(21), 6679-6695. doi: 10.1093/jxb/erv375
- Saran, S., and de Wet, J. (1976). Environmental-control of reproduction in *Dichanthium-intermedium*. *Journal of Cytology and Genetics* 11, 22-28.
- Šarhanová, P., Vašut, R.J., Dančák, M., Bureš, P., and Trávníček, B. (2012). New insights into the variability of reproduction modes in European populations of *Rubus* subgen. *Rubus*: how sexual are polyploid brambles? *Sexual Plant Reproduction* 25(4), 319-335. doi: 10.1007/s00497-012-0200-9.
- Sato, S., Kamiyama, M., Iwata, T., Makita, N., Furukawa, H., and Ikeda, H. (2006). Moderate increase of mean daily temperature adversely affects fruit set of *Lycopersicon esculentum* by disrupting specific physiological processes in male reproductive development. *Annals of Botany* 97(5), 731-738. doi: 10.1093/aob/mcl037

- Schinkel, C.C.-F. (2019). *Reproductive strategies of alpine apomictic plants under different ecological conditions*. (Doctoral dissertation, Niedersächsische Staats- und Universitätsbibliothek Göttingen)
- Schinkel, C.C., Syngelaki, E., Kirchheimer, B., Dullinger, S., Klatt, S., and Hörandl, E. (2020). Epigenetic patterns and geographical parthenogenesis in the alpine plant species *Ranunculus kuepferi* (Ranunculaceae). *International journal of molecular sciences* 21(9), 3318. doi: 10.3390/ijms21093318
- Schinkel, C.C.F., Kirchheimer, B., Dellinger, A.S., Klatt, S., Winkler, M., Dullinger, S., et al. (2016). Correlations of polyploidy and apomixis with elevation and associated environmental gradients in an alpine plant. *AoB Plants* 8.
- Schinkel, C.C.F., Kirchheimer, B., Dullinger, S., Geelen, D., De Storme, N., and Hörandl, E. (2017). Pathways to polyploidy: indications of a female triploid bridge in the alpine species *Ranunculus kuepferi* (Ranunculaceae). *Plant Systematics and Evolution* 303(8), 1093-1108. doi: 10.1007/s00606-017-1435-6.
- Schlüter, P.M., and Harris, S.A. (2006). Analysis of multilocus fingerprinting data sets containing missing data. *Molecular Ecology Notes* 6(2), 569-572. doi: 10.1111/j.1471-8286.2006.01225.x.
- Schmidt, A., Schmid, M.W., and Grossniklaus, U. (2015). Plant germline formation: common concepts and developmental flexibility in sexual and asexual reproduction. *Development* 142(2), 229-241. doi: 10.1242/dev.102103.
- Schmidt, A., Schmid, M.W., Klostermeier, U.C., Qi, W., Guthörl, D., Sailer, C., et al. (2014). Apomictic and sexual germline development differ with respect to cell cycle, transcriptional, hormonal and epigenetic regulation. *PLOS Genetics* 10(7), e1004476. doi: 10.1371/journal.pgen.1004476.
- Schoenfelder, K.P., and Fox, D.T. (2015). The expanding implications of polyploidy. *The Journal of Cell Biology* 209(4), 485-491. doi: 10.1083/jcb.201502016.
- Schreiber, U., and Berry, J.A. (1977). Heat-induced changes of chlorophyll fluorescence in intact leaves correlated with damage of the photosynthetic apparatus. *Planta* 136(3), 233-238. doi: 10.1007/BF00385990
- Selva, J.P., Zappacosta, D., Carballo, J., Rodrigo, J.M., Bellido, A., Gallo, C.A., et al. (2020). Genes Modulating the Increase in Sexuality in the Facultative Diplosporous Grass *Eragrostis curvula* under Water Stress Conditions. *Genes* 11(9), 969. doi: 10.3390/genes11090969.
- Shah, J.N., Kirioukhova, O., Pawar, P., Tayyab, M., Mateo, J.L., and Johnston, A.J. (2016). Depletion of key meiotic genes and transcriptome-wide abiotic stress reprogramming mark early preparatory events ahead of apomeiotic transition. *Frontiers in Plant Science* 7(1539). doi: 10.3389/fpls.2016.01539.
- Soltis, D.E., and Soltis, P.S. (1999). Polyploidy: recurrent formation and genome evolution. *Trends in Ecology & Evolution* 14(9), 348-352. doi: https://doi.org/10.1016/S0169-5347(99)01638-9.
- Soltis, D.E., Visger, C.J., and Soltis, P.S. (2014). The polyploidy revolution then... and now: Stebbins revisited. *American Journal of Botany* 101(7), 1057-1078.
- Soltis, P.S., Marchant, D.B., Van de Peer, Y., and Soltis, D.E. (2015). Polyploidy and genome evolution in plants. *Current opinion in genetics & development* 35, 119-125.
- Soltis, P.S., and Soltis, D.E. (2000). The role of genetic and genomic attributes in the success of polyploids. *Proceedings of the National Academy of Sciences* 97(13), 7051-7057. doi: 10.1073/pnas.97.13.7051.

- Spielman, M., Vinkenoog, R., and Scott, R.J. (2003). Genetic mechanisms of apomixis. *Philosophical Transactions of the Royal Society of London. Series B: Biological Sciences* 358(1434), 1095-1103.
- Stangherlin, A., and Reddy, A.B. (2013). Regulation of circadian clocks by redox homeostasis. *Journal of Biological Chemistry* 288(37), 26505-26511. doi: 10.1074/jbc.R113.457564
- Stirbet, A., Lazár, D., and Kromdijk, J. (2018). Chlorophyll a fluorescence induction: can just a one-second measurement be used to quantify abiotic stress responses? *Photosynthetica* 56(1), 86-104. doi: 10.1007/s11099-018-0770-3.
- Storchová, Z., Breneman, A., Cande, J., Dunn, J., Burbank, K., O'Toole, E., et al. (2006). Genome-wide genetic analysis of polyploidy in yeast. *Nature* 443(7111), 541-547. doi: 10.1038/nature05178.
- Strasser, R.J., Srivastava, A., and Tsimilli-Michael, M. (2000). The fluorescence transient as a tool to characterize and screen photosynthetic samples. *Probing photosynthesis: mechanisms, regulation and adaptation*, 445-483. doi: 10.1016/s0269-7491(03)00094-0
- Strasser, R.J., Tsimilli-Michael, M., and Srivastava, A. (2004). "Analysis of the chlorophyll a fluorescence transient," in *Chlorophyll a fluorescence*. Springer., 321-362.
- Sulpice, R., Flis, A., Ivakov, A.A., Apelt, F., Krohn, N., Encke, B., et al. (2014). *Arabidopsis* coordinates the diurnal regulation of carbon allocation and growth across a wide range of photoperiods. *Molecular Plant* 7(1), 137-155. doi: 10.1093/mp/sst127
- Takahashi, S., and Badger, M.R. (2011). Photoprotection in plants: a new light on photosystem II damage. *Trends in Plant Science* 16(1), 53-60. doi: <https://doi.org/10.1016/j.tplants.2010.10.001>.
- Takahashi, S., and Murata, N. (2008). How do environmental stresses accelerate photoinhibition? *Trends in plant science* 13(4), 178-182. doi: 10.1016/j.tplants.2008.01.005
- Torres, R., Romero, J., and Lagorio, M. (2021). Effects of sub-optimal illumination in plants. Comprehensive chlorophyll fluorescence analysis. *Journal of Photochemistry and Photobiology B: Biology* 218, 112182. doi: 10.1016/j.jphotobiol.2021.112182
- Tucker, M.R., and Koltunow, A.M. (2009). Sexual and asexual (apomictic) seed development in flowering plants: molecular, morphological and evolutionary relationships. *Functional Plant Biology* 36(6), 490-504. doi: 10.1071/FP09078.
- Ulum, F.B., Costa Castro, C., and Hörandl, E. (2020). Ploidy-dependent effects of light stress on the mode of reproduction in the *Ranunculus auricomus* complex (Ranunculaceae). *Frontiers in Plant Science* 11, 104. doi: 10.3389/fpls.2020.00104
- van Baarlen, P., de Jong, H.J., and van Dijk, P.J. (2002). Comparative cyto-embryological investigations of sexual and apomictic dandelions (*Taraxacum*) and their apomictic hybrids. *Sexual Plant Reproduction* 15(1), 31-38. doi: 10.1007/s00497-002-0132-x.
- Van de Peer, Y., Ashman, T.-L., Soltis, P.S., and Soltis, D.E. (2020). Polyploidy: an evolutionary and ecological force in stressful times. *The Plant Cell*, 11-26. doi: 10.1093/plcell/koaa015
- Van de Peer, Y., Maere, S., and Meyer, A. (2009). The evolutionary significance of ancient genome duplications. *Nat Rev Genet* 10(10), 725-732. doi: 10.1038/nrg2600.
- Van de Peer, Y., Mizrachi, E., and Marchal, K. (2017). The evolutionary significance of polyploidy. *Nat Rev Genet* 18(7), 411-424. doi: 10.1038/nrg.2017.26.

- Vass, I. (2012). Molecular mechanisms of photodamage in the Photosystem II complex. *Biochimica et Biophysica Acta (BBA)-Bioenergetics* 1817(1), 209-217. doi: 10.1016/j.bbabi.2011.04.014
- Vinkenoog, R., Bushell, C., Spielman, M., Adams, S., Dickinson, H.G., and Scott, R.J. (2003). Genomic imprinting and endosperm development in flowering plants. *Molecular biotechnology* 25(2), 149-184.
- Walker, D. (1987). *The use of the oxygen electrode and fluorescence probes in simple measurements of photosynthesis*. (p. 212). Sheffield: Research Institute for Photosynthesis, University of Sheffield.
- Warner, D.A., and Edwards, G.E. (1993). Effects of polyploidy on photosynthesis. *Photosynthesis Research* 35(2), 135-147. doi: 10.1007/BF00014744
- Weaver, G., and van Iersel, M.W. (2020). Longer photoperiods with adaptive lighting control can improve growth of greenhouse-grown 'Little Gem' lettuce (*Lactuca sativa*). *HortScience* 55(4), 573-580. doi: 10.21273/HORTSCI14721-19.
- Wei, T., Wang, Y., Xie, Z., Guo, D., Chen, C., Fan, Q., et al. (2019). Enhanced ROS scavenging and sugar accumulation contribute to drought tolerance of naturally occurring autotetraploids in *Poncirus trifoliata*. *Plant Biotechnology Journal* 17(7), 1394-1407. doi: <https://doi.org/10.1111/pbi.13064>.
- Wu, S., Cheng, J., Xu, X., Zhang, Y., Zhao, Y., Li, H., et al. (2019). Polyploidy in invasive *Solidago canadensis* increased plant nitrogen uptake, and abundance and activity of microbes and nematodes in soil. *Soil Biology and Biochemistry* 138, 107594. doi: <https://doi.org/10.1016/j.soilbio.2019.107594>.
- Wu, Z., Skjelvåg, A., and Baadshaug, O. (2004). Quantification of photoperiodic effects on growth of *Phleum pratense*. *Annals of botany* 94(4), 535-543. doi: 10.1093/aob/mch170
- Young, B.A., Sherwood, R.T., and Bashaw, E.C. (1979). Cleared-pistil and thick-sectioning techniques for detecting aposporous apomixis in grasses. *Canadian Journal of Botany* 57(15), 1668-1672. doi: 10.1139/b79-204.
- Yusuf, M.A., Kumar, D., Rajwanshi, R., Strasser, R.J., Tsimilli-Michael, M., and Sarin, N.B. (2010). Overexpression of  $\gamma$ -tocopherol methyl transferase gene in transgenic *Brassica juncea* plants alleviates abiotic stress: physiological and chlorophyll a fluorescence measurements. *Biochimica et Biophysica Acta (BBA)-Bioenergetics* 1797(8), 1428-1438. doi: 10.1016/j.bbabi.2010.02.002.
- Zappacosta, D.C., Ochogavía, A.C., Rodrigo, J.M., Romero, J.R., Meier, M.S., Garbus, I., et al. (2014). Increased apomixis expression concurrent with genetic and epigenetic variation in a newly synthesized *Eragrostis curvula* polyploid. *Scientific Reports* 4, 4423. doi: 10.1038/srep04423.

## List of Publications

**Ulum, F.B., Costa Castro, C., and Hörandl, E.** (2020). Ploidy-dependent effects of light stress on the mode of reproduction in the *Ranunculus auricomus* complex (Ranunculaceae). *Frontiers in Plant Science* 11, 104

**Ulum, F.B., Hadacek, F., and Hörandl, E.** (2021). Ploidy-dependent effects of prolonged photoperiod on photosynthesis of the *Ranunculus auricomus* complex (Ranunculaceae). In prep

## Thesis declarations

Declaration of the author's own contribution to the manuscript with multiple authors

Chapter 2:

**Ulum, F.B., Costa Castro, C., and Hörandl, E.** (2020). Ploidy-dependent effects of light stress on the mode of reproduction in the *Ranunculus auricomus* complex (Ranunculaceae). *Frontiers in Plant Science* 11, 104.

FU and EH designed research. FU performed research, analyzed and interpreted data. CC contributed to FCSS and microsatellite analysis. FU wrote the manuscript with the contributions of EH.

Chapter 3:

**Ulum, F.B., Hadacek, F., and Hörandl, E.** (2021). Ploidy-dependent effects of prolonged photoperiod on photosynthesis of the *Ranunculus auricomus* complex (Ranunculaceae). In prep.

EH and FH conceived and designed the study; FU performed the photosynthesis. FU and FH analyzed data, and FU, EH, and FH wrote and consented to the manuscript

## **Acknowledgment**

I would like to thank Prof. Elvira Hörandl for placing her trust in me to carry out this research, the insightful advice, and the support during the research and writing manuscript.

My thanks to Prof. Dr. Hermann Behling for very supportive of a committee member and reviewing my dissertation.

I further thank Franz Hadacek for his advice in measurement and in data analysis of photosynthesis, and contribution on the metabolite analysis for further publication.

Thank you to Camila Castro for contributing during the work of flow cytometry analysis seed screening and microsatellite analysis. Thank you to Ladislav Hodač and Salvatore Tomasello for helping during my work in molecular Lab.

The work was supported by The German Research Fund “Deutsche Forschungsgemeinschaft” DFG (project Hörandl Ho 4395 4-1) to Prof. Elvira Hörandl and my Scholarship funding was supported by Indonesia endowment fund for education (LPDP).

I express many thanks to the colleague in the Department of Systematics, Biodiversity, and Evolution of Plants, Albrecht-von-Haller Institute for Plant Sciences, University of Göttingen, for warm friendship.

Thank you also to Silvia for taking care of the plant in the climatic chamber.

My special thank you to my parents for their pray and love and to my beloved wife and my sweet kids for all love and full of happiness in accompanying me in Germany.

Finally, I would like to express my gratitude to all people that help me in many ways to complete this work.

## Curriculum vitae

### Fuad Bahrul Ulum

- 3/2017 - 7/2021      Ph.D. Student at Albrecht-von-Haller Institute for Plant Sciences  
Department of Systematics, Biodiversity and Evolution of Plants (with Herbarium), Georg-August-University Göttingen  
Thesis: Ploidy-dependent effect of prolonged photoperiod to the mode of reproduction and photosynthesis of *Ranunculus auricomus* complex (Ranunculaceae)
- 11/2012 – 7/2014      Master Student of Tropical and International Forestry of Faculty of Forest Science and Forest Ecology, Georg-August-University Göttingen  
Thesis: Ploidy levels and reproductive behavior in natural populations of *Centotheca lappacea* from Jambi, Indonesia
- 12/2008 – Present      Lecturer at Biology Department, Faculty of mathematics and science, Jember University, Indonesia
- 8/2003 – 10/2007      Bachelor of Science. Department of Biology. Faculty of Mathematics and Natural Science. Jember University. Indonesia  
Thesis: Production of antibiotic against *Candida albicans* from *Actinomyces* isolates in corn extract media